BIO-C3
Biodiversity changes: causes, consequences and management implications

Deliverable No: **2.1**	Workpackage number and leader: **2.1, Monika Winder, P4**		
Date:	**17.12.2015**	Delivery due date: **31.12.2015**	**24 month**
Title:	**Report on effects of changing drivers on pelagic and benthic species composition and production**		
Lead partner for deliverable:	**Monika Winder (P4)** **Stockholm University**		
Other contributing partners	**P1, P2, P3, P5, P9, P11**		
Authors	**Monika Winder, Luisa Berghoff, Alfred Burian, Catriona Clemmesen-Bockelmann, Jörg Dutz, Dariusz Fey, Anna Golz, Bastian Huwer, Piotr Margonski, Anne Lise Middelboe, Stefan Neuenfeldt, Jens Nielsen, Daniel Oesterwind, Erik Kock Rasmussen, Vincent Siebert, Henrik Skov, Lena Szymanek, Axel Temming, Jonna Tomkiewicz, Thomas Uhrenholdt, Ramunas Zydelis**		
Dissemination level (PU=public, PP=Restricted to other programme participants, including the BONUS Secretariat, CO=confidential)			**PU**
Nature of the Deliverable (RE=Report, OT=Other)			**RE**

Acknowledgements
The research leading to these results is part of the BIO-C3 project and has received funding from BONUS, the joint Baltic Sea research and development programme (Art 185), funded jointly from the European Union's Seventh Programme for research, technological development and demonstration and from national funding institutions.

BIO-C3 overview

The importance of biodiversity for ecosystems on land has long been acknowledged. In contrast, its role for marine ecosystems has gained less research attention. The overarching aim of BIO-C3 is to address biodiversity changes, their causes, consequences and possible management implications for the Baltic Sea. Scientists from 7 European countries and 13 partner institutes are involved. Project coordinator is the GEOMAR Helmholtz Centre for Ocean Research Kiel, Germany, assisted by DTU Aqua, National Institute of Aquatic Resources, Technical University of Denmark.

Why is Biodiversity important?

An estimated 130 animal and plant species go extinct every day. In 1992 the United Nations tried countering this process with the "Biodiversity Convention". It labeled biodiversity as worthy of preservation – at land as well as at sea. Biological variety should not only be preserved for ethical reasons: It also fulfils key ecosystem functions and provides ecosystem services. In the sea this includes healthy fish stocks, clear water without algal blooms but also the absorption of nutrients from agriculture.

Biodiversity and BIO-C3

To assess the role of biodiversity in marine ecosystems, BIO-C3 uses a natural laboratory: the Baltic Sea. The Baltic is perfectly suited since its species composition is very young, with current salt level persisting for only a few thousand years. It is also relatively species poor, and extinctions of residents or invasions of new species is therefore expected to have a more dramatic effect compared to species rich and presumably more stable ecosystems.

Moreover, human impacts on the Baltic ecosystem are larger than in most other sea regions, as this marginal sea is surrounded by densely populated areas. A further BIO-C3 focus is to predict and assess future anthropogenic impacts such as fishing and eutrophication, as well as changes related to global (climate) change using a suite of models.

If talking about biological variety, it is important to consider genetic diversity as well, a largely neglected issue. A central question is whether important organisms such as zooplankton and fish can cope or even adapt on contemporary time scales to changed environmental conditions anticipated under different global change scenarios.

BIO-C3 aims to increase understanding of both temporal changes in biodiversity - on all levels from genetic diversity to ecosystem composition - and of the environmental and anthropogenic pressures driving this change. For this purpose, we are able to exploit numerous long term data sets available from the project partners, including on fish stocks, plankton and benthos organisms as well as abiotic environmental conditions. Data series are extended and expanded through a network of Baltic cruises with the research vessels linked to the consortium, and complemented by extensive experimental, laboratory, and modeling work.

From science to management

The ultimate BIO-C3 goal is to use understanding of what happened in the past to predict what will happen in the future, under different climate projections and management scenarios: essential information for resource managers and politicians to decide on the course of actions to maintain and improve the biodiversity status of the Baltic Sea for future generations.

Executive Summary of BIO-C3 Task 2.1

The Baltic Sea experienced large changes in community composition, yet it is largely unknown how these changes affect ecosystem functioning. The objectives of BIO-C3 Task 2.1 is to improve our understanding on **how biodiversity changes at the base of the food web propagate to higher trophic levels and affect ecosystem functioning**. This overall question was addressed by focusing on processes in benthic, plankton and fish communities.

The flow of carbon and energy from phytoplankton and benthic autotrophs, like macroalgae, seagrasses and microbenthic algae over mussels to top consumers, like ducks is not well described for Baltic coastal waters. Mussels are important food sources for several species of ducks and some fish and benthic vegetation is an important food source for swans. The aim is through a model complex to describe this flow for selected coastal areas and to assess the effect of a change in eutrophication and climate change on the top consumers. So far, a model complex has been set up for Gulf of Riga, which includes nutrients, benthic autotrophs, suspending feeding mussels *(Mytilus & Mya*) and the suspension-depositing feeding mussel *Macoma baltica*. The latter is a new model development, important for describing the carbon – food flow from primary producers to some top consumers (e.g ducks & some fish). The present result indicates that the yearly production of mussels in the Gulf of Riga bordered by the island of Saarmaa is equivalent to about 5% of the primary production. The fraction of mussels consumed by birds is equivalent to about 1.2 % of the primary production.

Phytoplankton are the primary producer of essential biomolecules in aquatic food webs that play a critical role for secondary production. Biochemical composition of phytoplankton differs largely between major taxonomic groups, yet a detailed analysis of several essential biomolecules is lacking. Here we investigate algal fatty and amino acids across major taxonomic groups, which is important because phytoplankton species composition varies greatly over the season. Our findings indicate that major taxonomic groups differ in the concentrations of important biochemical compounds, creating trade-offs for herbivore consumers. These differences in compound concentrations explain why a more diverse nutrition leads to higher production rates of consumers than mono-specific diets. Thus, growth and reproduction of consumers (zooplankton, fish larvae) can be constrained by taxonomic composition or food quality of primary producers.

Zooplankton are a critical link of energy and nutritional transfer from phytoplankton to upper trophic levels. Microzooplankton are an important, but largely understudied group in the Baltic Sea. We investigated whether microzooplankton are able to upgrade food quality using the strength of stoichiometric regulation across different taxonomic groups. Heterotrophic nanoflagellates displayed weak homeostasis, while ciliates and rotifers displayed homeostasis in terms of their internal stoichiometry, similar to copepods. This indicates that microzooplankton have the potential to trophically upgrade poor autotrophic quality for higher trophic levels, and thus are a nutritionally important source for consumers.

An improved understanding of trophic pathways is important for understanding food web dynamics. Compound-specific N and C stable isotope of fatty and amino acids are promising tools for estimating trophic levels and energy source. The application of this novel method was tested in laboratory studied and applied in natural environments of a key zooplankton species (*Acartia* sp.) in the Baltic Sea. Results indicate that *Acartia* feeding differs over the seasonal cycle, which in turn influence consumer biochemical composition, growth and reproduction. Seasonal changes in the nutritional quality of zooplankton as diet resources may therefore propagate to higher trophic level predators in the Baltic Sea and consequently change nutritional flows across aquatic food webs. Outcome of these studies are important to investigate to what extent shift in plankton community composition affect fish larval growth and nutritional prey availability for higher trophic levels.
Further, we show that zooplankton mean size and total abundance (MSTS), a two-dimensional, multi-metric indicator representing a synthetic descriptor of zooplankton community structure is a promising tool to test the temporal dynamics and the present state of the pelagic food web. Its

trends indicate that the investigated pelagic food web structure is or is not optimal for energy transfer from primary producers (phytoplankton) to fish. Pivotal position of zooplankton organisms in the pelagic food web is indicative of both fish feeding conditions (and to some extent the predatory pressure of small pelagic fish on zooplankton) as well as grazing pressure of zooplankton on phytoplankton.

Understanding zooplankton dynamics is important because these organisms are a major prey for larval and juvenile fish. Fish recruitment is largely dependent on hydrological factors, feeding conditions or predator pressure. It is well documented that even if spawning stock biomass of a given fish species is large, the recruitment may be low at high mortality of early life stages. It is therefore essential to evaluate what factors affect the survival of larval and juvenile fish. When analyzing the temperature and zooplankton effect on the growth rate of larval and early-juvenile sprat (*Sprattus sprattus*) it appeared that the bottom-up processes should be considered among the key drivers in the pelagic food web of the southern Baltic Sea. The growth rate of larval sprat in southern Baltic is higher in May-June than in July-August as a result of higher zooplankton biomass, despite much higher temperature in the latest period. The importance of temperature is however observed when geographical differences in growth rate are analyzed within the same time period – higher temperature in Gdansk Basis area, comparing to Bornholm Basin area, resulted in faster growth of larvae collected in Gdansk Basin.

Cod is crucial for the Baltic Sea, with large ecosystem and socio-economic effects. Thus, an improved knowledge about factors affecting cod dynamics is critical. Due to different reasons the status of the Eastern Baltic Cod stock is unclear. This study gives some insights of the dependencies of environmental drivers with respect to all phases of cod life within the important spawning area in the Bornholm Basin. Concerning early life stages, biochemically based estimates of larval nutritional condition and growth showed relationships with prey abundance and stock recruitment and are thus a promising tool to validate bottlenecks for recruitment success and determine “highest survival potential” from time series of zoo- and ichthyoplankton. Within the spawning area it seems that the vertical distribution and condition of adult cod is mainly driven by salinity and oxygen concentration, as well as food availability. The last Major Baltic Inflow led to higher salinity and higher oxygen concentration in the deeper Basin resulting in better living conditions for cod. But it is still unclear if and how the changing condition will influence the status of the Eastern Baltic cod stock in future. On the other hand, this study has shown that the stagnation of inflows from the mid 1980s onwards resulted in decreasing cod condition due to changed availabilities of prey items. The signal created by the inflow stagnation is multi-decadal, and it is hence in questions, if one inflow is sufficient to reverse the observed trend. The results identified some important drivers or rather pressures, which influence the biodiversity of the Baltic.

Results from the ecological model complex developed in Task 2.1 will be applied to tasks 3.4, 4.2 and 4.3 to describe and quantify population growth and survival of key components of the benthic ecosystem in up to two coastal case study areas. Further, the models can be used as a basis for assessments of the impacts of predicted future changes in biodiversity. The studies on plankton food quality, trophic linkages and the role of microzooplankton will support WP4 Task 4.3 in projections of future species composition and food web dynamics. Results from this task will also link to task 3.1 in identifying drivers of biodiversity in the Baltic Sea.

Introduction

Changes in community composition of nearly all trophic levels ranging from plankton to fish and benthos have been described in the Baltic Sea (Ojaveer et al. 2010), but the underlying processes by which these changes impact on coastal and pelagic systems are only partly understood. Improved knowledge on how direct and indirect effects propagate through the entire food web is critical in order to predict ecosystem-wide consequences of changing biodiversity under spatio-temporally varying drivers. The goal of deliverable 2.1 is to investigate bottom-up controlling mechanisms due to drivers of climate and eutrophication, and consequences for transfer efficiency and food quality for higher trophic levels and biodiversity.

Within this task we investigated how shifts in species composition at the base of the benthic and pelagic food web as well as temporal and spatial mismatches between critical trophic linkages influence energy flow and limit overall productivity. In addition, fine-scale benthic ecosystem models (3-D MIKE3 FM) quantify effects of oligo- and eutrophication in relation to the conservation targets of key fish and waterbird species. For the pelagic system, focus was on food quantity and nutritional prey quality using field observations, experiments, compound-specific stable isotopes, quantitative fatty and amino acid analyses. The taxonomic diversity and the functional role of largely understudied but diverse microzooplanktonin 'trophic upgrading' was investigated. These studies are feeding into bioenergetic models in WP4.

Coherent seasonal time series of all trophic levels (phyto-, zooplankton and fish) were established to identify controlling mechanisms and temporal-spatial match/mismatch among key trophic linkages to investigate responses to climate and other drivers. These analyses are linked to larval and adult fish phenology, nutritional status and benthic species composition. Results of these studies support WP4 in projecting future species composition and food web dynamics.

Due to the wealth of new information and detail outputs of the different studies, the key results are highlighted in the core deliverable text and the detailed material and result descriptions are provided as appendices. The outcomes of these studies are inputs to WP3 and WP4.

Core Activities

Focus areas of this task were the Bornholm Basin (BB), Northern Baltic Proper (NBP), SE Baltic coastal areas (SEC) and the Gulf of Finland (GF). Locations of the different studies are highlighted in Fig. 1. Major activities of Task 2.1 'Bottom up control' per partner were as follows:

P9 contributed with benthic ecosystem model and an IBM model for water birds. A hydrodynamic and ecological model (ECOLab/3-D MIKE3 FM) was set up on selected coastal areas. The model aims at describing effects of eutrophication on selected benthic habitats (mussels, clams, eelgrass, macroalgae (e.g., *Fucus vesiculosus, Furcellaria*) and fish species (round goby) and selected benthivorous water birds (e.g. velvet scoter and long-tailed duck).

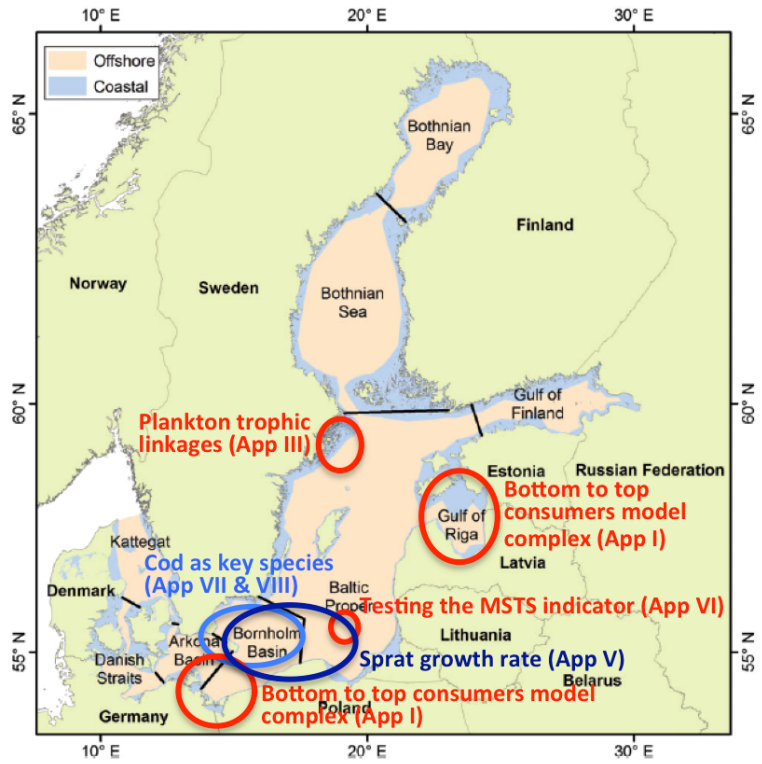

Fig. 1: The Baltic Sea and highlighted focus areas addressed in BIO-C3 Task 2.1. Map source: Andersen et al. (2015).

P4 was responsible for food quality analysis in phytoplankton and energy transfer to consumers, including the functional role of microzooplankton. The goal of the analysis was to investigate if nutritional quality differs between phytoplankton taxonomic groups and to what extent zooplankton buffer imbalances. In addition, the usage of compound-specific stable isotopes of amino and fatty acids was used to trace trophic level and energy source.

P5 was responsible to investigate bottom-up process at the lower trophic levels, based on field data from the southern Baltic Sea. Two analyses were carried out: (i) the zooplankton mean size and total abundance (MSTS) indicator was tested on the Polish monitoring data and (ii) the effects of zooplankton biomass vs. temperature were analysed on the growth rate of larval and early-juvenile sprat.

P1, P3 and P2 were responsible for analyses of phenology in appearance of larval fish and zooplankton as well as the nutritional condition of larval fish over the spawning season and changes in the condition of adult fish. Aim of the analyses was to relate larval fish condition to zooplankton prey fields for an evaluation of match/mismatch scenarios and potential consequences for recruitment. Further aim was to understand the observed changes in adult fish condition

P11 contributed with performing research cruises in the Bornholm Basin with FRV Clupea. During the cruises, requested data and samples, including Ichthyoplankton, Zooplankton and fish stomachs, were taken and delivered to the partner institutes (see Appendix VIII). Beside the expected deliverable, it was possible to analyse adult fish and CTD data as well.

i) Scientific highlights

The benthic to top consumer modelling complex (for details see Appendix I)
To predict and quantify the bottom-up effects of oligo- and eutrophication and climate, and the interaction between these on benthic habitats and in relation to top predators such as fish and water birds, fine-scale benthic ecosystem models (ECO Lab/3-D MIKE3 FM) and bioenergetics models has been developed. The model complex includes hydrodynamics, water quality parameters (nutrients, Chl a, oxygen), common mussels (*Mytilus edulis/ trossulus & Mya a.*) and Baltic clams (*Macoma balthica*) as well as major benthivorous predators; round goby (*Neogobius melanostomus*), Long-tailed Duck (*Clangula hyemalis*) and Velvet Scoter (*Melanitta fusca*). The dynamic mussel model is divided into suspension feeders (*Mytilus & Mya*) and a suspension-deposit feeder *(Macoma b*), which is a major step forward. Modelling *Macoma* has to our knowledge not been done before probably because it also includes modelling *Macoma's* food source, the fluff layer of organic material on top of the sediment.

Nutritional quality of phytoplankton (for details see Appendix II)
The biochemical food quality of algae is a major factor determining ingestion rates, assimilation rates, individual growth rates and mortality of consumers. Thereby, it is not only an important parameter from a community perspective, but also determining the structure of food-webs and the efficiency of energy flows. Aquatic algae consist of a wide array of variable compounds of which many are important or even essential structural components for the growth of consumers (Galloway & Winder 2015). The manifold biochemical requirements of herbivores complicate the quantification of food quality in primary producers and created the notion that the observation of one single compound group is often not sufficient to explain the growth response of consumers. A synopsis of the current state of knowledge and an investigation of several key-parameters of food quality in the most important algae groups helps us to better understand the potential benefits of taxonomically diverse food supply for zooplankton and the multi-dimensional nature of food quality in pelagic primary producers. We conduced a quantitative comparison of key food quality parameters (fatty acids, amino acids and C:N:P ratios) across four major groups of pelagic primary producers (diatoms, cyanobacteria, green algae and haptophytes). Results indicate that major taxonomic groups differ in the concentrations of important biochemical compounds. No algae group has high concentrations for every single compound group, creating trade-offs for herbivore consumers. These differences in compound concentrations explain why a more diverse nutrition leads to higher production rates of consumers than mono-specific diets.

Biochemical markers as tracers for energy transfer (for details see Appendix II)
Compound-specific stable isotopes analysis (CSIA) of amino acids (AA) and fatty acids (FA) are proposed to be promising biomarkers to trace energy flow in aquatic food webs. We investigated the differentiation of algae groups using CSIA. A premise for tracing food web process at a high resolution in aquatic ecosystems is the ability to differentiate base-line source groups, especially major algae groups (Larsen et al. 2009). Recently, different attempts have been undertaken for algae source separation. The most applied method is that of quantitative FA profiles. We tested whether algae can be separated into major groups using a specific biochemical biomarker (CSIA). We found that very promising polar tracer FAs are 18:1n9 and 18:1n7 (present in nearly all algae), which can be used to differentiate haptophytes (enriched in 18:1n7) and diatoms (depleted in 18:1n9), or 18:2n6 and 18:3n6

(differentiation between all groups). The implications of these biomarkers for tracing energy source are currently being analyzed.

The functional role of microzooplankton (for details see Appendix III)
Laboratory experiments were conducted to investigate whether microzooplankton maintain homeostasis (Golz et al. 2015). This is important because microzooplankton are a major component in marine food webs and in comparison to mesozooplankton, less is known about the ability of microzooplankton to maintain stoichiometric balance. Primary producers typically reflect the nutrient ratios of their resource, as their stoichiometric composition can vary widely in conformity to environmental conditions, while consumer C:nutrient ratios are largely constrained within a narrow range (Sterner & Elser 2009). In this study we used laboratory experiments with four different species of microzooplankton, two heterotrophic dinoflagellates (*Gyrodinium dominans* and *Oxyrrhis marina*), a ciliate (*Euplotes* sp.) and a rotifer (*Brachionus plicatilis*) to test the stoichiometric response to five nutrient treatments. We showed that the dependency of microzooplankton C:N:P ratios on C:nutrient ratios of their food source varies between species. Similar to the photoautotroph, the two heterotrophic dinoflagellates were weak stoichiometric regulators. In contrast, the strength of stoichiometric regulation increased to strict homeostasis in both the ciliate and the rotifer, similar to mesozooplankton, suggesting increased homeostasis ability as a result of evolutionary development for increasingly more complex organisms. Our study implies that microzooplankton growth can be constrained by imbalanced resource supply and indicates that these key primary consumers have the potential to trophically upgrade poor stoichiometric autotrophic food quality for higher trophic levels.

Using compound-specific stable isotopes to assess energy transfer between phytoplankton and a key copepod species (for details see Appendix IV)
We used CSIA to assess energy transfer from phytoplankton to a widespread key copepod species (*Acartia* spp.) in the northern Baltic proper with complimentary approach of bulk $\delta^{13}C$ and $\delta^{15}N$ values, $\delta^{13}C$ values of essential amino acids, and quantitative phytoplankton taxonomic data (Nielsen & Winder 2015). Zooplankton seston samples were collected for stable isotope analysis and combined with phytoplankton counts from the monitoring program. Analysis of $\delta^{13}C$ values in essential amino acids have shown great promise in effectively capturing consumer food sources, since essential amino acids are not synthesized by heterotrophic organisms but instead routed directly from dietary sources to consumers, resulting in negligible ^{13}C trophic discrimination (Chikaraishi et al. 2009). We found distinct differences between *Acartia* and seston $\delta^{13}C$ essential amino acid values measured at weekly to monthly sampling intervals, which indicates that *Acartia* preferentially utilized specific dietary resources that comprised only parts of the total phytoplankton composition (i.e. varying from 19.7% to 81.4 % throughout the season). Results also indicated that care should be used when inferring trophic position of consumers relative to seston bulk stable isotope values in cases where consumers are highly selective. Analysis of $\delta^{13}C$ values in essential amino acids showed to be a promising tool to accurately trace consumer resource use in natural systems.
Zooplankton mean size and total abundance (for details see Appendix V)
The zooplankton mean size and total abundance (MSTS), a core HELCOM indicator, is primarily relevant for food webs (EU Marine Strategy Framework Directive (MSFD) criterion 4.3: *abundance/distribution of key trophic groups/species*) and its secondary link is to biodiversity (EU MSFD criterion 1.6: *habitat condition*). The trends indicate whether the

investigated pelagic food web structure is or is not optimal for energy transfer from primary producers (phytoplankton) to fish. Pivotal position of zooplankton organisms in the pelagic food web is indicative of both fish feeding conditions (and to some extent the predatory pressure of small pelagic fish on zooplankton) as well as grazing pressure of zooplankton on phytoplankton. We were testing zooplankton data collected at the P140 station located at the southern slope of the Gotland Basin. Data are the Polish contribution to the HELCOM COMBINE Programme. Considering the temporal changes of the total zooplankton biomass and the mean size of zooplankton organisms as well as conservative approach, i.e. the 'one-out-all-out'-principle (OOAO), starting from 1997, MSTS indicates the sub-GES conditions at the investigated station. The MSTS, a two-dimensional, multi-metric indicator representing a synthetic descriptor of zooplankton community structure is a promising tool to test the temporal dynamics and the present state of the pelagic food web.

Temperature and zooplankton effect on the growth rate of larval and early-juvenile sprat (*Sprattus sprattus*) in the South Baltic Sea (for details see Appendix VI)

Recruitment studies are crucial to investigate the possible link between larval and juvenile fish survival and fish stock size (Houde 1987). Even if spawning stock biomass of a given species is large, the recruitment may be low if high mortality of early life stages occurs as a result of the effect of hydrological factors, feeding conditions or predator pressure. It is therefore essential to evaluate what factors affect the survival of larval and juvenile fish. One of the possible factors influencing survival of larvae and juveniles may be their growth rate as it is assumed that larger and faster growing specimens have higher chance of survival (Anderson 1988). Even if in certain circumstances the faster growing specimens may be the ones that die in higher number, the general assumption about better survival of faster growing larvae seems to be valid to high extend. Therefore, monitoring of the growth rate of larvae and evaluation of factors affecting the growth rate should be considered as an important part of the studies related to ecology of larval fish. The goal of the present work was to describe growth rate of larval sprat in years 2006-2010 and to evaluate the effect of temperature and zooplankton biomass on both the differences among years and the differences between geographical areas (Bornholm Basin and Gdansk Basin). Concluding, the growth rate of larval sprat in southern Baltic is higher in May-June than in July-August as a result of higher zooplankton biomass, despite much higher temperature in the latest period. The importance of temperature is however observed when geographical differences in growth rate are analyzed within the same time period – higher temperature in Gdansk Basis area, comparing to Bornholm Basin area, resulted in faster growth of larvae collected in Gdansk Basin.

Phenology and nutritional conditions of larval and adult fish (for details see Appendix VII)

Larval cod nutritional condition in the Bornholm basin, the major cod spawning area, was analysed for the cohorts in 2006, 2011 and partly 2007. The data set was combined with previously published data from 1994, 1995 & 2007 (Grønkjær et al. 1997, Huwer et al. 2011), which have been re-evaluated in the present context and combined with zooplankton data in order to obtain a more integrated view of the relationship between prey availability, larval Baltic cod condition and growth, and resulting recruitment dynamics of the eastern Baltic cod stock. The proportions of cod larvae with positive growth rates varied between years and months analysed. Best growth and highest numbers of larvae in the plankton samples were found in the summer months correlating to highest production of the relevant zooplankton organisms. A positive correlation between cod larvae nutritional condition and abundance of

the most important food item copepodid C1 stages of *Pseudocalanus spp.* was found, reflecting the importance of adequate food for larval cod growth. Furthermore, years of higher recruitment were correlated with years of cod larvae being in a better nutritional condition. To judge "good condition" the number of larvae showing a positive specific growth rate were compared to all larvae in the sample and reported as percentages. Correlations between larval cod growth rates based on biochemically derived estimates (RNA/DNA ratios) and zooplankton abundance as well as numbers of recruits could be shown, providing support for the "Match-Mismatch" and "Bigger is better" recruitment hypotheses.

Data on individual cod sampled during the Danish part of the Baltic International Bottom Trawl Survey (BITS) ICES Sub-division 25 from 1995-2014 were analysed. The data comprised 55.000 records of individual cod where weight, length, gutted, liver and ovary weight, as well as sex and maturity stage were recorded. Nutritional condition was calculated as Fulton's condition index (K) and hepatosomatic index (HIS). Results show a significant decline in nutritional condition over time both calculated as K and HSI.

Data and samples from six surveys (Nov 2014 and March, June, July, August and September 2015) in Sub-division 25 were collected as part of BIO-C3. It follows the cod reproduction cycle from onset of maturation in November until end of the main spawning season in September, with emphasis on spawning period. The sampling includes app. 300 cod from each cruise, distributed on females and males in different size group. Sampling included records of individual cod where weight, length, gutted, liver and ovary weight, as well as sex and maturity stage were recorded, and liver and ovary samples were obtained for analysis of total lipid and fatty acid composition, as well as histological analysis of maturity stage. Different pelagic and prey types were similarly sampled for total lipid and fatty acid composition. The histological analysis of samples has been performed and provides the basis for sub-sampling of cod for total lipid and fatty acid analysis to be performed in 2016. The results will elucidate both the spawning pattern over the season (size and sex) and the condition changes during the season. Also the lipid and fatty analyses will indicate if cod is limited in specific polyunsaturated fatty acids at present, and data will be compared with data from 2003-4 and 2007-8, where similar analyses were performed for females at specific times of the year, including also information about prey quality. In the present study males as well as females will be included in the analyses.

The onset of the inflow stagnation period since 1983 is reflected in the consumption, and condition of cod <40 cm. Most probably, the absence of sufficient benthic food forces relatively small cod to forage on sprat with relatively low success. The development continued to date. Aggravated by decreasing sprat abundance in the central area of the cod distribution (additional decrease in the mid 90s). Cod >40 cm can compensate by feeding on herring, small cod, and benthic fishes.

Fish distribution and cod condition with respect to environmental changes in the Bornholm Basin (for details see Appendix VIII)

The oxygen concentration and salinity in the Baltic especially in the deeper basins depend on the water inflow from the North Sea. Within the last years, low oxygen concentration and lower salinity become to a problem in the deeper basins for example in the Bornholm Basin because North Sea inflows become rare or to small by volume to fill the deep Baltic basins. Therefore we examined the hydrological conditions in the Bornholm Basin and analysed the possible consequences for the ecosystem with the focus on commercial fish species. Hydrological data suppose a moderate higher salinity and oxygen saturation in 2014 and a substantially higher salinity and oxygen concentration in 2015 in the deeper water layer of

the Bornholm basin compared to the former years (2012 and 2013). This increase was probably caused by smaller inflows of North Sea water in 2013 and a Major Baltic Inflow (MBI) at the end of the year 2014. It seems that the horizontal distribution of herring, sprat and cod and the vertical distribution of herring and sprat were not influenced by those changing conditions. However, the results presume that the vertical distribution of cod is linked to the oxygen and/or salinity concentration due to higher abundance in the deeper water layer with higher salinity and oxygen concentrations in 2014 and 2015. In addition, the data suppose a linkage between the better environmental conditions and the fitness of cod. The status of the gall blatter, which was recorded in 2013, 2014 and 2015, show a better feeding condition of cod in 2014 and 2015 compared to 2013, which is in line with the results of the estimated Fulton's condition factor. The factor shows lowest values in 2013 and highest values in 2015. Assuming that cod condition is somehow driven by environmental factors like oxygen concentration and salinity.

ii) Progress and next steps

Studies and work-tasks were performed according to the workplan and original objectives were obtained. The progress and outstanding next steps are are as follow:

The hydrodynamic models have been completed and calibrated for both study areas. The ecological models including water quality and benthic species have been developed for the Gulf of Riga and the Pomeranian Bay. The Gulf of Riga model is calibrated with respect to most parameters for the period 1970-2008 and final calibration of regional nutrient dynamics are in progress. Due to lack of sufficient data basis, the Pomeranian Bay model is less well developed and need further calibration. The IBM for Gulf of Riga benthivorous predators has been set up and is currently undergoing a calibration process, which includes fine-tuning sub-models and equations describing foraging ecology and bioenergetics, reviews and comparison with literature data. Calibration and validation for the mussel part of the model system is finalised, however, calibration of the nutrients is still in progress. Setting and calibration of model took longer than expected and therefore models outputs are still not ready for testing the effects of selected scenarios. Development of the model has been delayed due to difficulties in getting access to relevant data. However, the recent progress and calibration tasks are ongoing and expected to be finalised in time for scenario runs and analysis in connection with coming deliverables. Model results will be finalized mid 2016 and reported in the following annual report.

Laboratory experiments and sample analysis on the nutritional quality of phytoplankton and biochemical markers of compound-specific stable isotopes as tracers for food resource are completed; data analysis is currently ongoing and two manuscripts will be finalized in 2016. Studies about compound-specific stable isotopes to assess energy transfer in natural systems between phyto- and zooplankton as well as the functional role of microzooplankton are completed and published.

Zooplankton Mean Size and Total Stock (MSTS) has a status of HELCOM core indicator, thus, the concept and the rationale is already sufficiently well developed. In the presented study the MSTS indicator was calculated based on the Polish zooplankton data series that were collected within the HELCOM Combine Monitoring Programme. Further development will focus on technical issues as (i) the unification of the biomass calculation methods over the entire Baltic Sea area, (ii) estimating of the reference periods for chlorophyll *a* EQR and sprat

condition that should be identified based on the sub-regional (i.e. regionally disaggregated) data to reflect the spatial dynamics at the local scale, (iii) coastal vs. offshore areas comparison, (iv) testing methods on how to combine results derived from several data series located in the same assessment unit, and (v) different aspects of confidence variability. The analyses of temperature vs. zooplankton biomass effects on the growth rate of larval and early-juvenile sprat are preliminary. Further work will focus on preparing a manuscript for publication.

Laboratory analyses on (i) detailed stage composition of various zooplankton species and (ii) biochemically based estimates of larval cod condition and growth are completed for a series of years with contrasting environmental conditions and variable cod recruitment success. Furthermore, a series of ichthyoplankton surveys have been conducted during the project period, complementing an existing time-series, and sampling will continue in 2016 to follow the further development of larval abundances after the recent inflow of highly saline, oxygen rich water. The analyses of % cod larvae with positive growth determined with a biochemically derived indicator (RNA/DNA ratios) in relation to zooplankton biomass effects and recruitment are preliminary. Further work will focus on cod larval size group specific analyses for further evaluation of bottlenecks for different larval and zooplankton developmental stages and the preparation of a manuscript for publication.

A study on seasonal changes in cod reproductive parameters and nutritional physiology was originally planned to take place in 2013-2014, however, the timing needed to be changed due to change of research vessel during BITS 1 in March 2014, where the smaller vessel could not accommodate additional staff needed for sampling. Furthermore, the extra BIO-C3 survey conducted by DTU Aqua in September 2015 provided an extraordinary opportunity to sample during the late cod spawning period, a period that is very poorly covered in existing surveys databases.

To get a better knowledge of the possible effects of environmental conditions in the Bornholm Basin with respect to commercial fish (cod), data from other surveys will be merged with the current results and the survey will continue with some minor modifications in 2016. Therefore, data analysis is ongoing and a manuscript about first results will be prepared in spring 2016.

All future outcomes of the task 2.1 will be included in upcoming annual reports.

iii) Methods and results

Major results are highlighted in section (*i*), detailed methods and results for each respective study are described in the Appendices. A list of all attached appendices is given in section (*v*).

iv) Recommendations

The benthic to top consumer modelling will be used to simulate scenarios after finalising the calibration-validation of the model. Discussions of modelling results will follow when models are used in subsequent work packages for assessing impacts of changes in nutrient loads and climate. The model complex will be applied in tasks 3.4, 4.2 and 4.3 to describe and quantify water quality, mussel and clam population growth and survival of key predators in two coastal case study areas.

The study on phytoplankton food quality is useful because quantitative data of various essential biomolecules in algae are scare and a comparison between taxonomic groups is urgently required to understand how shifts in species composition affect the nutritional transfer from primary producers to higher trophic levels. This information is informative to understand to what extend health conditions of organisms at upper trophic levels depends on prey availability. The study on the role of microzooplankton showed that the strength of stoichiometric regulation increases with increasing phylogenetic distance from photoautotrophs. Our study indicates that microzooplankton have the potential to trophically upgrade poor autotrophic quality for higher trophic levels. In the light of increasing eutrophication and the consequent increase of N:P ratios in coastal waters, together with amplified CO_2 emissions predicted for the coming centuries, it is likely that the C:nutrient ratio of autotrophs will increase, which in turn will reduce their quality as food. Microzooplankton may be able to buffer these effects for higher trophic levels to some extent. This information will be useful for BIO-C3 WP4 Task 4.2 and 4.3.

The study on compound-specific C stable isotope of FA and AA showed that these methods are promising tools for estimating consumer trophic levels and energy source, as demonstrated with laboratory studies and applications in natural environments. Feeding on different food sources, as shown for the copepod *Acartia* can also result in switching between prey items of different nutritional quality both in terms of elemental stoichiometry and important macromolecules, which in turn influence consumer biochemical composition, growth and reproduction of consumers. Seasonal changes in the nutritional quality of zooplankton as diet resources may therefore propagate to higher trophic level predators in the Baltic Sea (Möllmann & Koster 2002) and consequently change nutritional flows across aquatic food webs (Winder & Jassby 2011). These studies showed that compound-specific stable isotopes improve our understanding of feeding interactions and will improve Baltic Sea and food web models, which will be informative for Task 4.2.

The zooplankton mean size and total stock (MSTS) indicator appears to be a promising tool to test the condition and the spatio-temporal dynamics of the pelagic food web with the special emphasis on the bottom-up impact(s) at lower food web levels. Based on presented analysis of temperature vs. zooplankton biomass effects on the growth rate of larval and early-juvenile sprat, the bottom-up processes should be considered among the key drivers in the pelagic food web of the southern Baltic Sea. These findings are an important contribution to the ongoing work on identification of the most important driving forces of the pelagic food web (Task 3.1) as well as for the better understanding of the retrospective analyses of biodiversity and ecosystem functioning (Task 4.1).

The BONUS co-financed publication by Eero et al. (2015) describes and summarizes the distress of cod. Due to different reasons, the present stock status of the eastern Baltic cod is unclear. Therefore, data about biology and environmental conditions are essential to expand the knowledge about the actual stock status and to give a scientifically management advice for a sustainable management of the eastern Baltic cod stock. The finding of relationships between nutritional condition and growth of cod larvae, prey abundance (mainly *Pseudocalanus spp.*) and stock recruitment is a promising tool to validate bottlenecks for recruitment success and to determine “highest survival potential” from a time series of ichthyoplankton surveys in the Bornholm Basin. The achieved results give further insights into the complex interaction of the stock with its environmental condition, and are expected to contribute to the development of ecosystem based indicators of reproductive success and management considerations, linking to work to be conducted in WPs 4 & 5. However, more

research is necessary to increase the knowledge of potential abiotic and biotic influences on the eastern cod stock. For example, it is still unclear if and how the Major Baltic Inflow influence the future of the Eastern Baltic stock. Relating the absence of inflows to cod diet and consumption is a promising tool to investigate the foodweb consequences of climate change in the Baltic Sea, and to understand changes in condition and growth of this key commercial species. These findings will form an important contribution to the multispecies modelling in task 4.2, underpinning the implementation of prey dependent growth for cod.

References

Anderson, J. T. (1988). A review of size dependent survival during pre-recruit stages of fishes in relation to recruitment. Journal of Northwest Atlantic Fisheries Science 8, 55-66.

Andersen, J. H. *et al.* (2015) Long-term temporal and spatial trends in eutrophication status of the Baltic Sea. *Biological Reviews*. doi:10.1111/brv.12221

Chikaraishi Y, Ogawa NO, Kashiyama Y, Takano Y, Suga H, Tomitani A, Miyashita H, Kitazato H, Ohkouchi N (2009) Determination of aquatic food-web structure based on compound-specific nitrogen isotopic composition of amino acids. Limnology and Oceanography-Methods 7:740–750

Eero, M. *et al.* (2015) Eastern Baltic cod in distress: biological changes and challenges for stock assessment. *ICES Journal of Marine Science* **72,** 2180–2186.

Galloway AWE, Winder M (2015) Partitioning the Relative Importance of Phylogeny and Environmental Conditions on Phytoplankton Fatty Acids (A Quigg, Ed.). PLoS One 10:e0130053–23

Golz AL, Burian A, Winder M (2015) Stoichiometric regulation in micro- and mesozooplankton. Journal of Plankton Research

HELCOM 2015. Zooplankton Mean Size and Total Stock (MSTS). HELCOM core indicator report. Online. Document viewed on 2015-12-05, http://www.helcom.fi/Core%20Indicators/Zooplankon%20mean%20size%20and%20total%20stock-HELCOM%20core%20indicator%20report%202015-extended%20version.pdf

Houde, E. D. (1987). Fish early life dynamics recruitment variability. American Fisheries Society Symposium 2, 17-29.

Larsen T, Taylor DL, Leigh MB, O'Brien DM (2009) Stable isotope fingerprinting: a novel method for identifying plant, fungal, or bacterial origins of amino acids. Ecology 90:3526–3535

Möllmann C, Koster FW (2002) Population dynamics of calanoid copepods and the implications of their predation by clupeid fish in the Central Baltic Sea. 24:959–977

Nielsen JM, Winder M (2015) Seasonal dynamics of zooplankton resource use revealed by carbon amino acid stable isotope values. Marine Ecology-Progress Series 531:143–154

Ojaveer H, Jaanus A, MacKenzie BR, Martin G, Olenin S, Radziejewska T, Telesh I, Zettler ML, Zaiko A (2010) Status of Biodiversity in the Baltic Sea (Y Ropert-Coudert, Ed.). PLoS One 5:e12467

Sterner RW, Elser JJ (2009) Ecological stoichiometry. In: Levin SA, Carpenter SR, Godfray HCJ, Kinzig AP, Loreau M, Losos JG, Walker B, Wilcove DS (eds) The Princeton Guide to Ecology. Princeton Univeristy Press, p 385

Winder M, Jassby AD (2011) Shifts in zooplankton community structure: Implications for food-web processes in the upper San Francisco Estuary. Estuaries and Coasts 34:675–690; Recommended by Faculty of 1000 Biology

v) Appendices

APPENDIX I: The bottom to top consumer modeling complex (P9)

APPENDIX II: Nutritional quality of phytoplankton and biochemical markers as tracers for energy transfer (P4)

APPENDIX III: Seasonal dynamics of zooplankton resource use revealed by carbon amino acid stable isotope values (P4)

APPENDIX IV: Stoichiometric regulation in micro- and mesozooplankton (P4)

APPENDIX V: Temperature and zooplankton effect on the growth rate of larval and early-juvenile sprat (*Sprattus sprattus*) in the South Baltic Sea (P5)

APPENDIX VI: Testing of the zooplankton mean size and total abundance (MSTS) indicator calculated based on the Polish monitoring data from the southern Baltic Sea. (P5)

APPENDIX VII: Phenology and nutritional conditions of larval and adult fish (P1, P2 and P3)

APPENDIX VIII: Fish distribution and cod condition with respect to environmental changes in the Bornholm Basin including Cruise Report of FRV Clupea Cruise Number 281 & 291 with Metadata (P11)

APPPENDIX I

THE BOTTOM TO TOP CONSUMER MODELLING COMPLEX

Erik Kock Rasmussen, Ramunas Zydelis, Thomas Uhrenholdt, Anne Lise Middelboe, Henrik Skov
DHI

1.1 Method and results

1.1.1 Study area

In order to make comparisons between coastal ecosystems of the Baltic Proper and the northern Baltic, two study areas were chosen; Gulf of Riga (GoR) and Pomeranian Bay (Pom). In both study areas the model grid covers the same depth gradient from the coast (excluding lagoons) to the lower sublittoral. The study areas were chosen based on the presence of large marine Natura 2000 areas designated for the one or several of the modelled target species of predators (water birds).

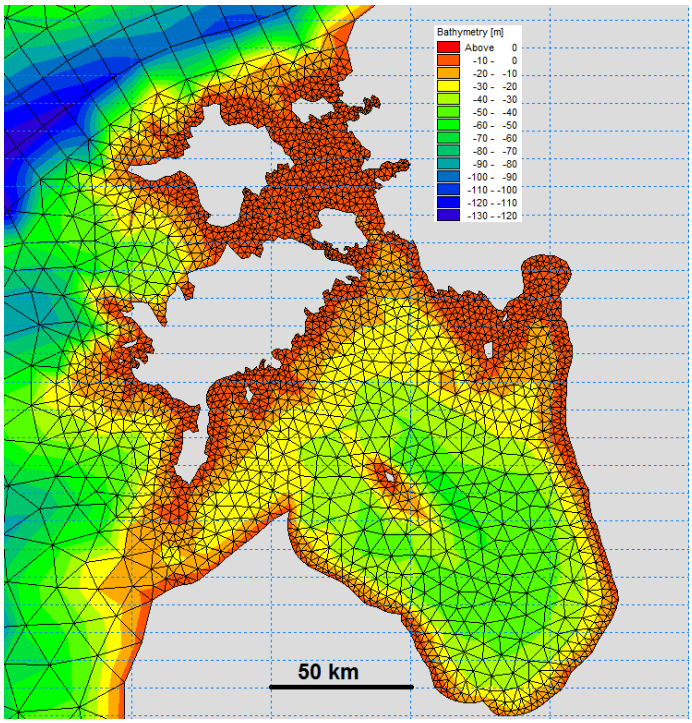

Figure 0-1 **Model grid and bathymetry of the study area "Gulf of Riga".**

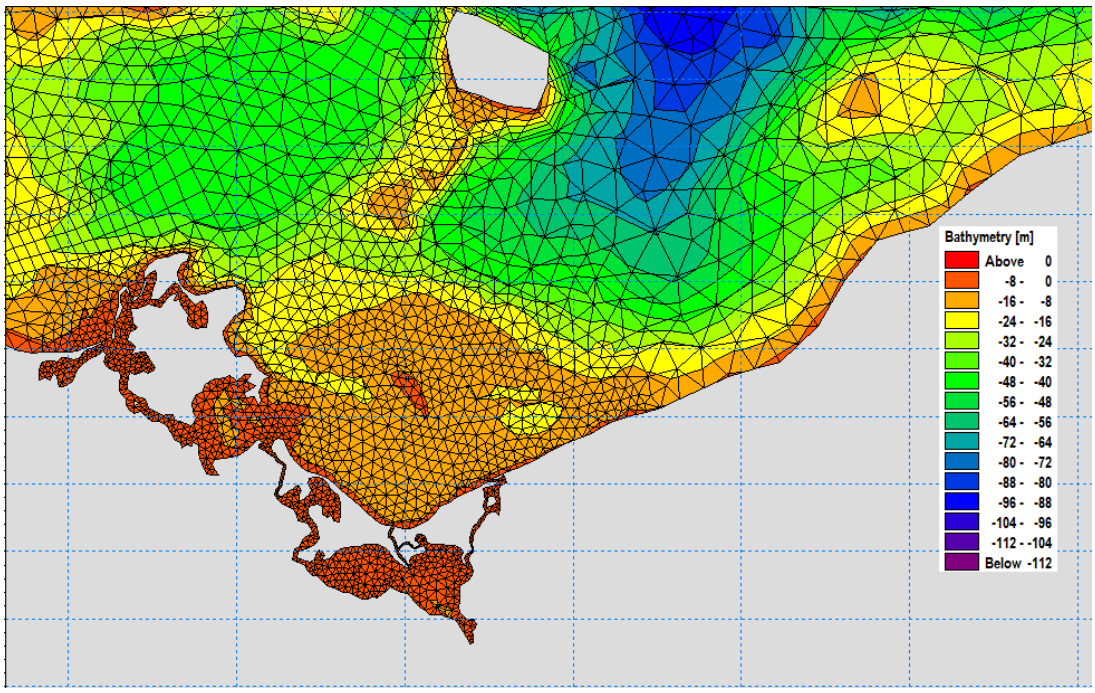

Figure 0-2 **Model grid and bathymetry of the study area "Pomeranian Bay".**

1.1.2 Bottom to top consumer modelling complex

A suite of models has been established which can run separately or as a single integrated model with a high spatial resolution in the coastal areas. The modelling toolbox consisted of:

- Hydrodynamic model (current fields)
- Ecological model (water quality, benthic flora, Blue mussels and Baltic clam)
- Bioenergetic model (water birds and round goby)

This modular approach is advantageous for quantitative and spatial studies. It allows for an assessment of the direct effects on flora, fauna and birds, as well as bottom-up effects due to changes in the supply of food predicted by the Ecological model (e.g. changes in mussels). The overall modelling approach and data flow from Hydrodynamics to Bioenergetic models applied is shown in Figure 0-3.

It is important to highlight that the HD/ Ecological modelling is not a "black-box" model but consists of physically-based deterministic models, which are fully integrated. In other words, physical, chemical and biological processes controlling the scale and magnitude of the effects are built into the models based on equations for the conservation of mass and momentum and biological dose-response relationships.

The fact that the modelling is able to reproduce the observed data in the study areas and has been constructed with an internal logic built on responses to external pressures, makes the modelling system suitable for quantifying changes in bottom-up processes.

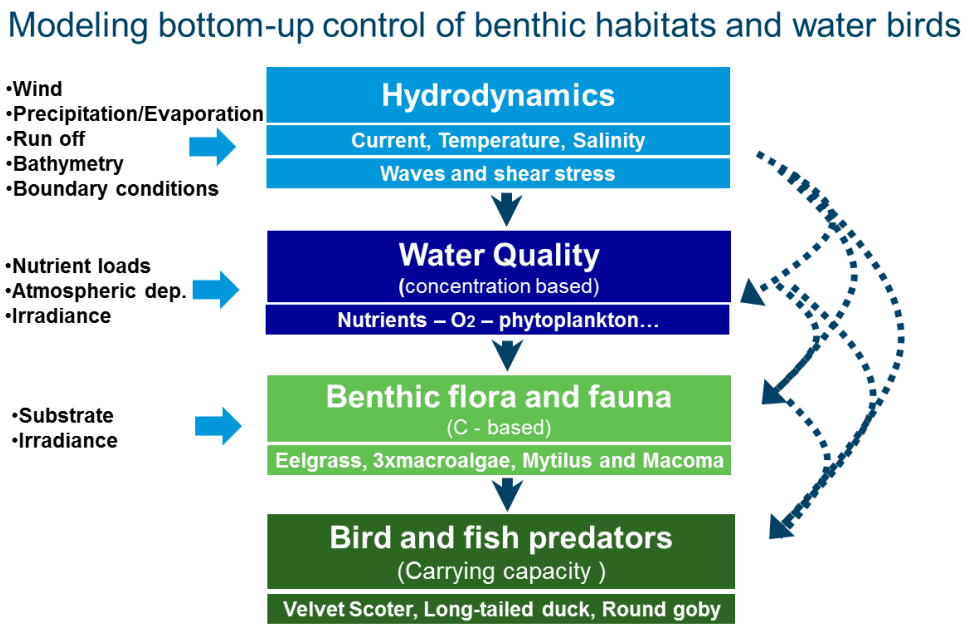

Figure 0-3 **Overall modelling complex used for assessing bottom-up changes in coastal ecosystems.**

1.1.3 Data used for calibration/ validation

Table 0.1 show data used for development and calibration of the different models.

Table 0.1 Overview of data used for developing and calibrating models

Data type	Sources
Bathymetric data and coastline data	Fehmarn Belt Fixed Link Hydrographic Services (FEHY) 500x500m regional bathymetry mainly based on data from Bundesamt für Seeschifffahrt und Hydrographie and Danish Maritime Safety Administration. Baltic Sea Hydrographic Commission, 2013, Baltic Sea Bathymetry Database version 0.9.3. Downloaded from http://data.bshc.pro/ on 04-09-2014
Meteorological data	Meteorological fields (3-hourly; 0.25°x0.25° resolution) 1970-2007 from the Rossby Centre Atmosphere model (RCA) from the BONUS ECOSUPPORT project provided by SMHI for the present project.
Run-off data	Fehmarn Belt Fixed Link Hydrographic Services (FEHY) regional model run-off data set 1970-2007 based on data from IOW (IKZM Oder project) and SMHI (HBV run-off model). Run-off data from the BONUS ECOSUPPORT project and provided by SMHI for the present project.
Hydrodynamic initial and boundary conditions	Fehmarn Belt Fixed Link Hydrographic Services (FEHY) regional model initial and boundary conditions 1970-2007.
Salinity and water temperature in-situ data	Data from the Baltic Environmental Database (BED) from the BONUS ECOSUPPORT project and provided by SMHI for the present project. Fehmarn Belt Fixed Link Hydrographic Services (FEHY) in-situ data 1970-2007 based on data from Danish, German and Swedish institutions and ICES.
Nutrient data	Nutrient data from the Baltic Environmental Database (BED) applied for the BONUS ECOSUPPORT project and provided by SMHI. Measurements received from NMFRI and EMI
Submerged vegetation	Coverage and biomass data received from EMI
Macro zoobenthos	Coverage and biomass data from NMFRI and EMI
Data on sea duck abundance, distribution, diet composition, foraging ecology and bioenergetics	Seaduck abundance and distribution are obtained from the Baltic Sea bird atlases (Durinck et al. 1994, Skov et al. 2011) and reports of EU LIFE project MARMONI. Diet composition of main bird predators, Long-tailed Duck and Velvet Scoter, was taken from published and unpublished sources (e.g., Stempniewicz 1986, 1995, Žydelis 2002, FEBI 2013). Information about foraging ecology and bioenergetics of sea ducks for developing an individual based model extracted from published literature sources, making relevant associations from related species where necessary (e.g., DeLeeuw 1999, Richman and Lovvorn 2004, 2008, Lovvorn et al. 2009, Varennes et al. 2015).
Data on round goby abundance, distribution, diet composition, foraging ecology and bioenergetics	Modelled round goby distribution database shared by J. Kotta. Publications by Bio-C3 members (Ojaveer et al. 2015) and other authors (Azour et al. 2015). Manuscripts prepared by Bio-C3 members (lead authors J. Kotta and K. Nurkse). Other relevant publications on round goby or related fish species.

1.1.4 Hydrodynamic model

The hydrodynamic model is based on the regional model developed by DHI for the Fehmarn Belt Fixed Link EIA (FEHY 2013). For the present purpose, the model was refined in the Gulf of Riga and Bay of Pomerania areas. The model has been executed for the period 1970-2007.

The model is a three-dimensional (3-D) hydrodynamic model based on the MIKE 3 FM modelling system (DHI 2014a). MIKE 3 FM is based on a flexible mesh approach and on the numerical solution of the three-dimensional incompressible Reynolds averaged Navier-Stokes equations invoking the assumptions of Boussinesq and of hydrostatic pressure. Thus, the model consists of continuity, momentum, temperature, salinity and density equations and it is closed by a turbulent closure scheme. The free surface is taken into account using a sigma-coordinate transformation approach.

Model Setup

The hydrodynamic model applies data listed in Table 0.1 for model mesh (bathymetry), model initial and boundary conditions (salinity, temperature, water level, current), model forcings (atmospheric forcing, river inflow) and model calibration data (mainly in-situ temperature and salinity).

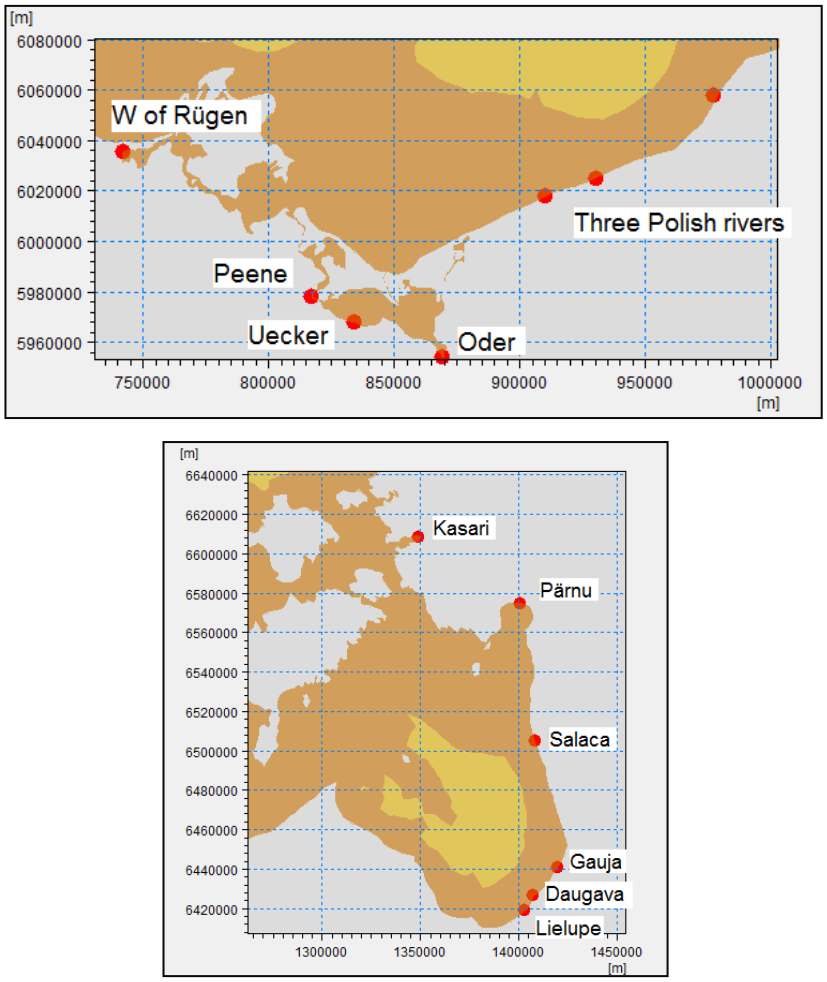

Figure 0-4 **Location of model sources representing local rivers included in the hydrodynamic model**

The concept of the model is that the coarse regional model of the entire Baltic Sea is coupled with more detailed local models at Gulf of Riga and Bay of Pomerania. This is possible due to the flexible mesh approach applied for the modelling. In Figure 0-1 and Figure 0-2 zooms of the two local model meshes are shown.

The model is forced by meteorological data in the form of wind, air pressure and temperature, relative humidity, clearness, precipitation and ice coverage. These data enter the continuity, momentum, temperature and turbulence equations of the model. Specifically in areas with ice, the wind forcing and heat exchange terms are dampened.

Rivers are included in the model as model sources. The river inflow (run-off) to the Bay of Pomerania as provided by FEHY and SMHI is distributed into Oder River (60%), Peene River (10%), west of Rügen (10%), Uecker River (5%) and three Polish rivers (5% each). Similarly the river inflow to the Gulf of Riga is distributed into Daugava River (64%), Lielupe River (14%), Gauja, Salaca and Pärnu rivers (6% each) and Kasari River (4%). The location of the local rivers is shown in Figure 0-4.

Calibration of Hydraulic Model

The regional model has been calibrated against measured salinity and temperature data in a number of stations within the model domain.

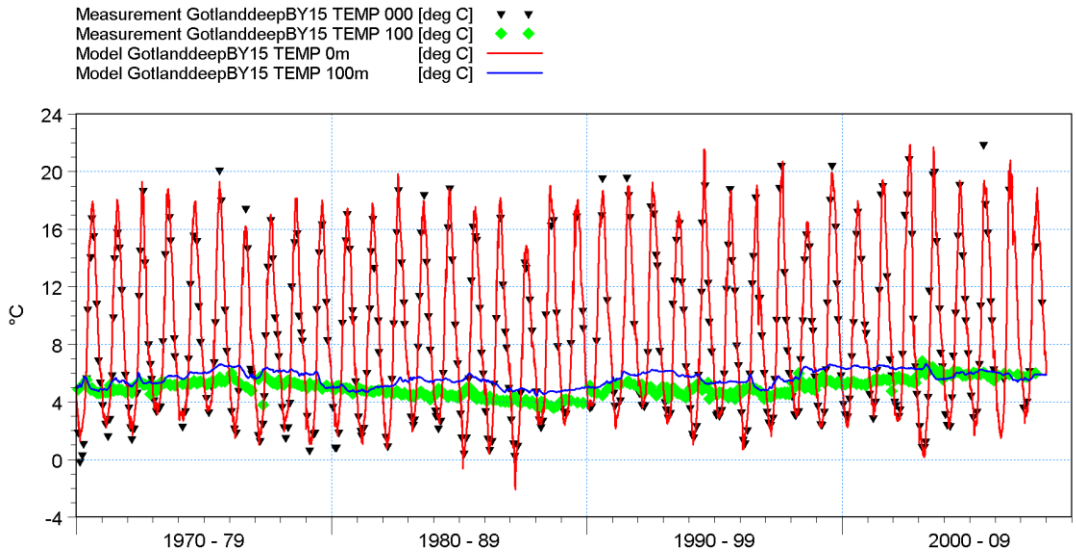

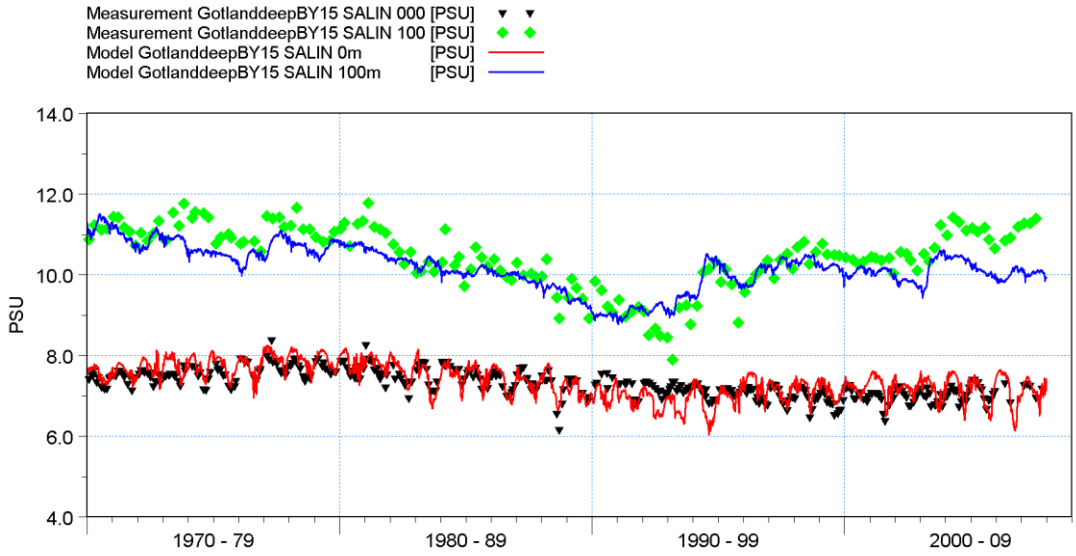

In Figure 0-5 and Figure 0-6 modelled and observed water temperature and salinity at Gotland Deep and Gulf of Riga are compared. The plots show a good agreement between measured and modelled data over the 38-year period. The model is able to reproduce stratification and seasonal and inter-annual variations in the two parameters in both surface and intermediate waters. Based on the comparisons it is concluded that the model is able to reproduce the main transport and mixing conditions in the Baltic Sea in general and in the two local study areas in particular.

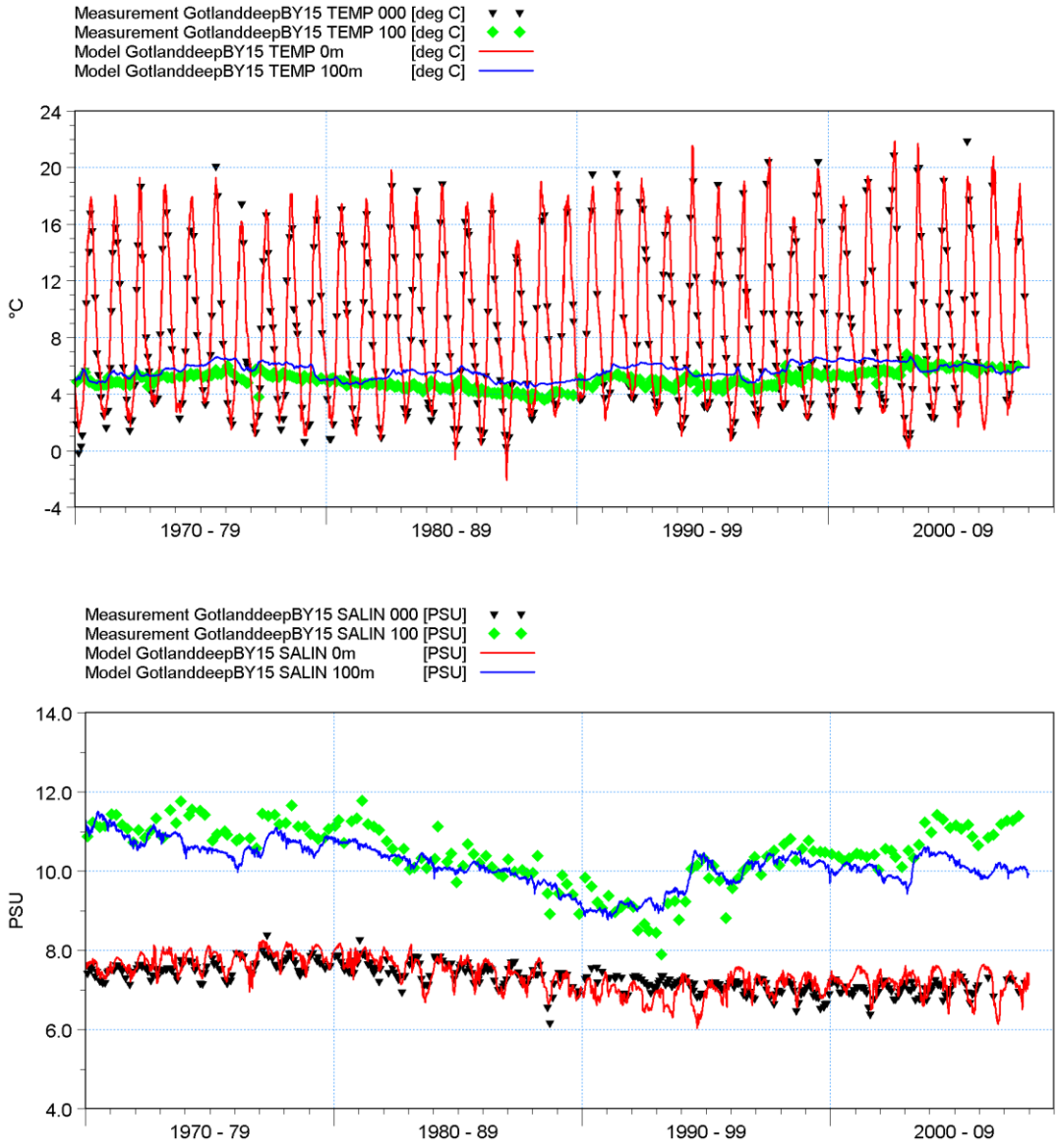

Figure 0-5 **Comparison of measured and modelled water temperature in Gotland Deep in the surface and at 100m depth in the period 1970-2007**

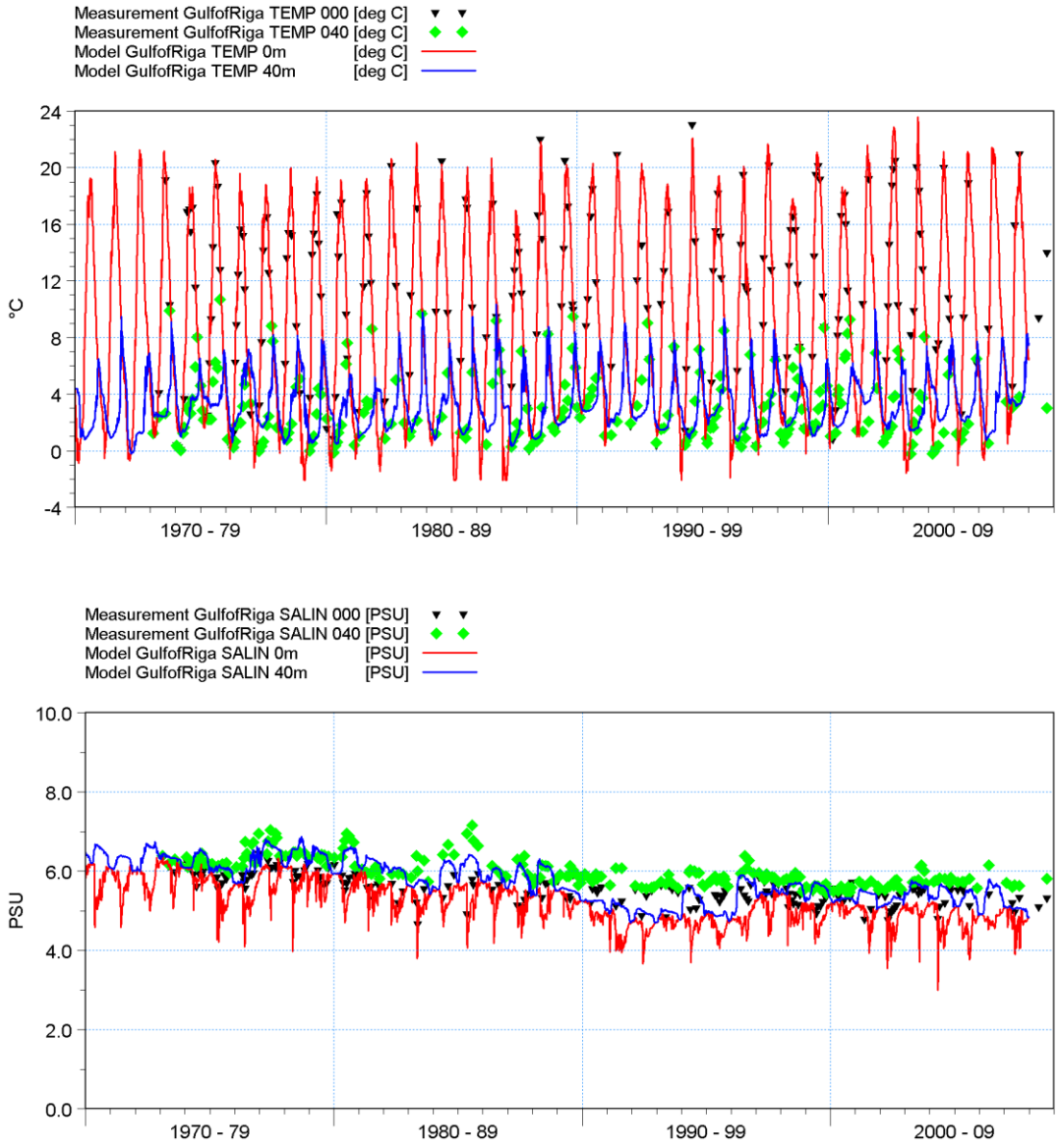

Figure 0-6 **Comparison of measured and modelled water temperature in Gulf of Riga in the surface and at 40m depth in the period 1970-2007**

Examples of model results showing inflow and outflow of the Gulf of Riga and thermal stratification are shown in Figure 0-7 and Figure 0-8.

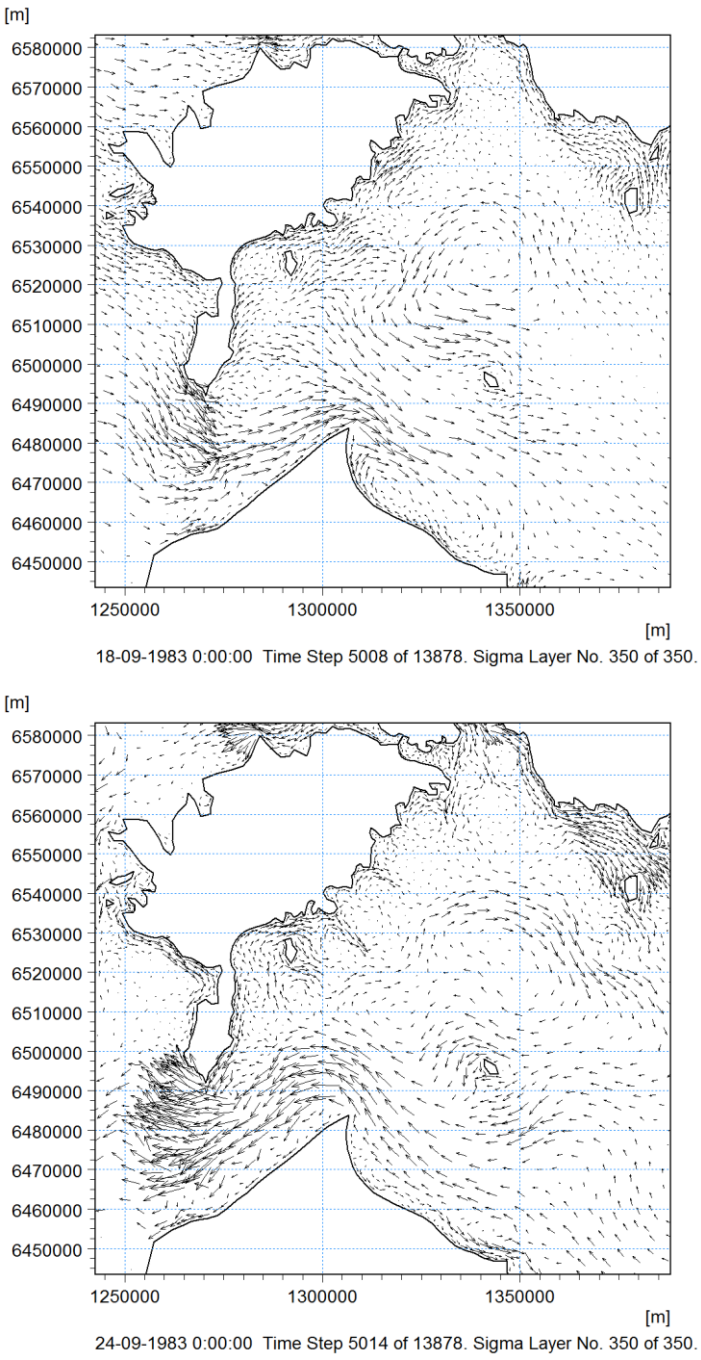

Figure 0-7 **Examples of modelled inflow (upper) and outflow (lower) surface current fields in the Gulf of Riga.**

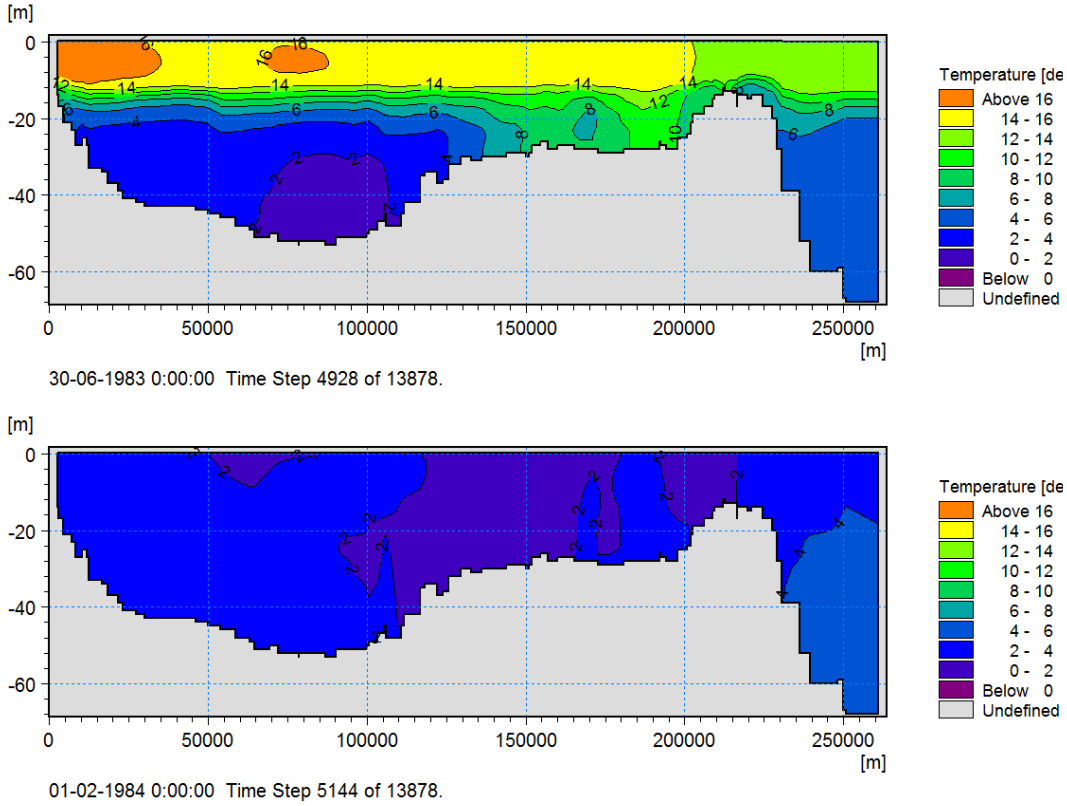

Figure 0-8 **Examples of modelled thermal stratification in summer (upper) and mixed thermal conditions in winter (lower) in a vertical transect starting at the head of Gulf of Riga and ending at the Irbe Strait threshold and the Baltic proper.**

1.1.1 Ecological-biogeochemical model

The ecological-biogeochemical model is based on the ECO Lab modelling system (DHI 2014b).

Model Setup

The ecological-biogeochemical model is coupled to a hydrodynamic model, which together form the basis of the total model complex.

The ecological-biogeochemical model consists of 100+ state variables (see Table 0-2), including the bio-geochemical cycle of C, N and P, 3 phytoplankton groups (diatoms, cyanobacteria and flagellates), eelgrass, tree macroalgae and- microphytobenthos. The benthic fauna is included with population models of the suspension feeders *Mytilus sp. & Mya sp*. and the deposit-suspension feeder *Macoma baltica*. Furthermore, the template includes a description of organic C, N and P in the sediment. The suspension feeding mussels are feeding on suspended organic matter and are especially relying on the availability of phytoplankton. The edibility or quality of the food is determined by the C:N:P ratio. The suspension-deposit feeder population model of *Macoma baltica* is a new development. To be able to simulate the food source, the sediment pool of C, N and P was split into an unconsolidated layer on the sediment surface and a consolidated layer below, see figure 0-9.

Table 0-2 Outline of state variables in the Ecological-biogeochemical model.

	Ecological-biochemical model State variables
Pelagic autotrophs	3 algae groups, Diatom, cyanobacteria, flagellates (C, N, P, Si)
Pelagic nutrients, oxygen, chlorophyll, zooplankton	Nutrients: NO_3, NH_4, PO_4, Si, H_2S, O_2 Part. & dissolved organic matter: DC, DN, DP DSi & DOC, DON, DOP, Zooplankton & chlorophyll
Benthic autotrophs	3 macro algae groups represented by: *Ceramium, Fucellaria, Delesseria*, (C, N, P) Angiosperms: *Zostera*, (C, N, P) Microbenthic algae
Suspension feeders	*Mytilus* & *Mya* population model (C, N, P) 12 size classes
Suspension-deposit feeders	*Macoma baltica* population model (C, N, P) 10 size classes
Sediment	Pools of organic C, N & P, silicate, H_2S Fe-PO_4, sediment H_2S & pore water PO_4, NH_4, NO_3

The unconsolidated layer received the newly settled organic matter, which can be re-suspended and transported by currents. The food sources for *M. baltica* are microbenthic algae and C, N and P from organic matter in the unconsolidated layer. To be able to describe the current and wave generated resuspension the results from the wave model was included as a forcing function.

Resuspension and sedimentation of particulate organic matter are important processes determining the turbidity of the water and thereby the growth condition for the benthic autotrophs. The model is able to describe feed-back mechanisms between suspended organic matter and the biology, such as filtration by mussels clearing the water thereby improving light conditions for the benthic vegetation.

As mentioned the food source to deposit feeding bivalves (*M. baltica*) consists of the uppermost organic enriched sediment layer (fluff layer), which is resuspended, sediment and transported towards the deposition areas. In the Baltic Sea this is deep areas or basins as Arkona-, Bornholm-, Gdansk- and Gotland deep.

The biogeochemical model includes a series of sediment state variables for which initial maps have to be generated by dividing the bottom into erosion, transport and deposition bottoms depending on the yearly frequency of resuspension. The frequency of resuspensions events, are calculated based on hourly simulated current and wave generated shear stress (using the MIKE 3D flow model and 2D wave model). Supported by monitoring data initial maps are defined based on frequency of resuspension. The third step is to run the biogeochemical model a couple of years so the sediment state variables approach a steady state condition.

The net growth of mussels in each size class depends on food supply, temperature, and oxygen conditions. Biomass loss is modelled through a general predation (crab, fish), a bird predation, a starvation mortality, and through release of gametes. A fraction of the released gametes enters the biomass of zooplankton, the remaining biomass of the gametes enters the detritus pools. Recruitments of new mussel to size class 1 are described as spat fall to the bottom, where the biomass is taken from zooplankton. *Macoma* spat settle on soft

bottom, *Mytilus* spat settle on hard surfaces and Mya on sandy to soft sediments. The *Mytilus & Mya* and the *Macoma* sub-model are generic in the sense that spat fall and sediment type, food source and oxygen conditions determine where the mussels can survive and grow.

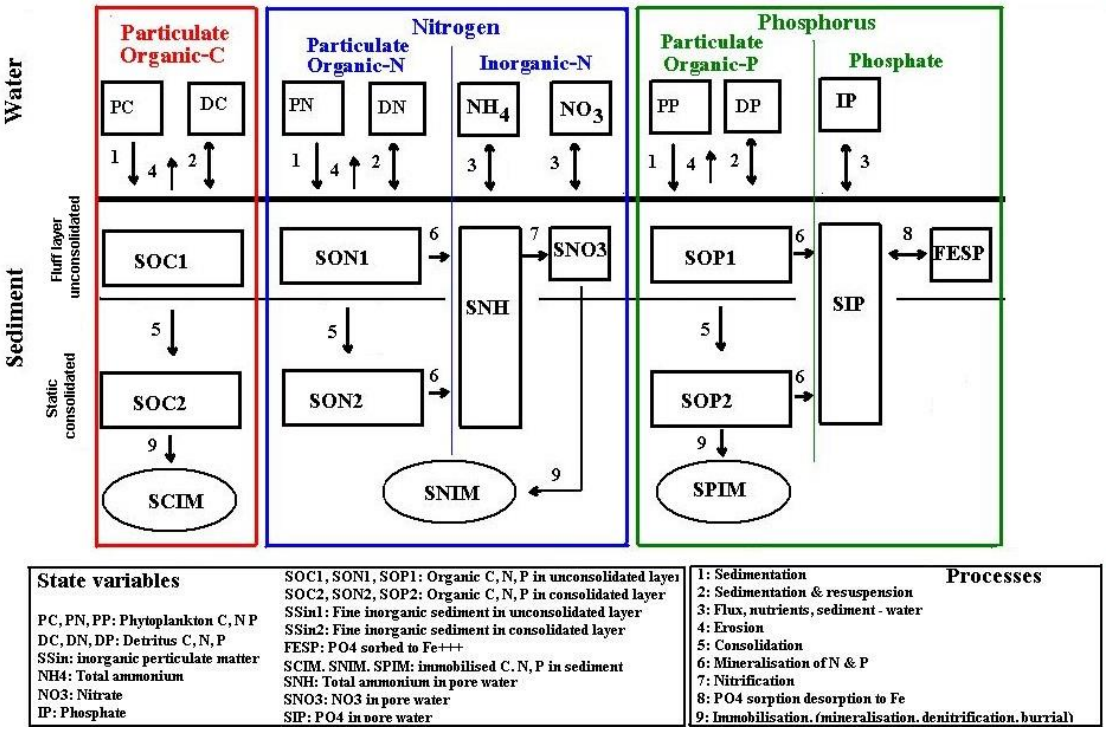

Figure 0-9 **State variables and processes in the sediment part of the biogeochemical model.**

Model Calibration

The general water circulation in the Baltic Sea is counter clockwise. Simulated and measured water chemistry has been compared at stations BY15 (Gotland deep), BY 31 (Landsort deep) and a station in the Golf of Riga.

In Figure 0-10 simulated and measured chlorophyll, oxygen, nitrate and phosphate concentrations at stations BY15 and BY31 are presented for the period 1970-2007. The model is able to mimic the seasonal variation of chlorophyll at the two stations. The only deviations are 3 high chlorophyll concentrations measured during summer blooms at station BY15 (Gotland deep). The simulated dissolved oxygen (DO) in the surface fits well with the measured values. Also DO at 200 m deep at station BY15 (Gotland deep) fits the monitored DO. The model is able to mimic the layer inflow of hypoxic water in late 1970'ties, the mid 1990'ties and mid 2000'ties. However, the model shows a small inflow of hypoxic water in the 1980s that is not seen in the monitored data. The simulated and monitored DO concentrations at 150 m at station BY31 (Landsort deep) are corresponding well, except for a few years in the mid 1990'ties. Also the simulated nitrate concentrations in the surface at station BY15 (Gotland deep) fits well but has a slight tendency for high winter concentrations also seen at station BY31. The modelled NO_3-N concentrations at 200 m in the Gotland deep are too high during hypoxic conditions, the same is the case for the NO_3-N concentrations at Landsort deep. The simulated and monitored concentrations of PO_4-P at station BY15

(Gotland deep) fits well both in the surface and at 200 m. At Landsort deep (BY31) the simulated winter PO_4-P seems to be overestimated so is the PO_4-P concentration at 150 m.

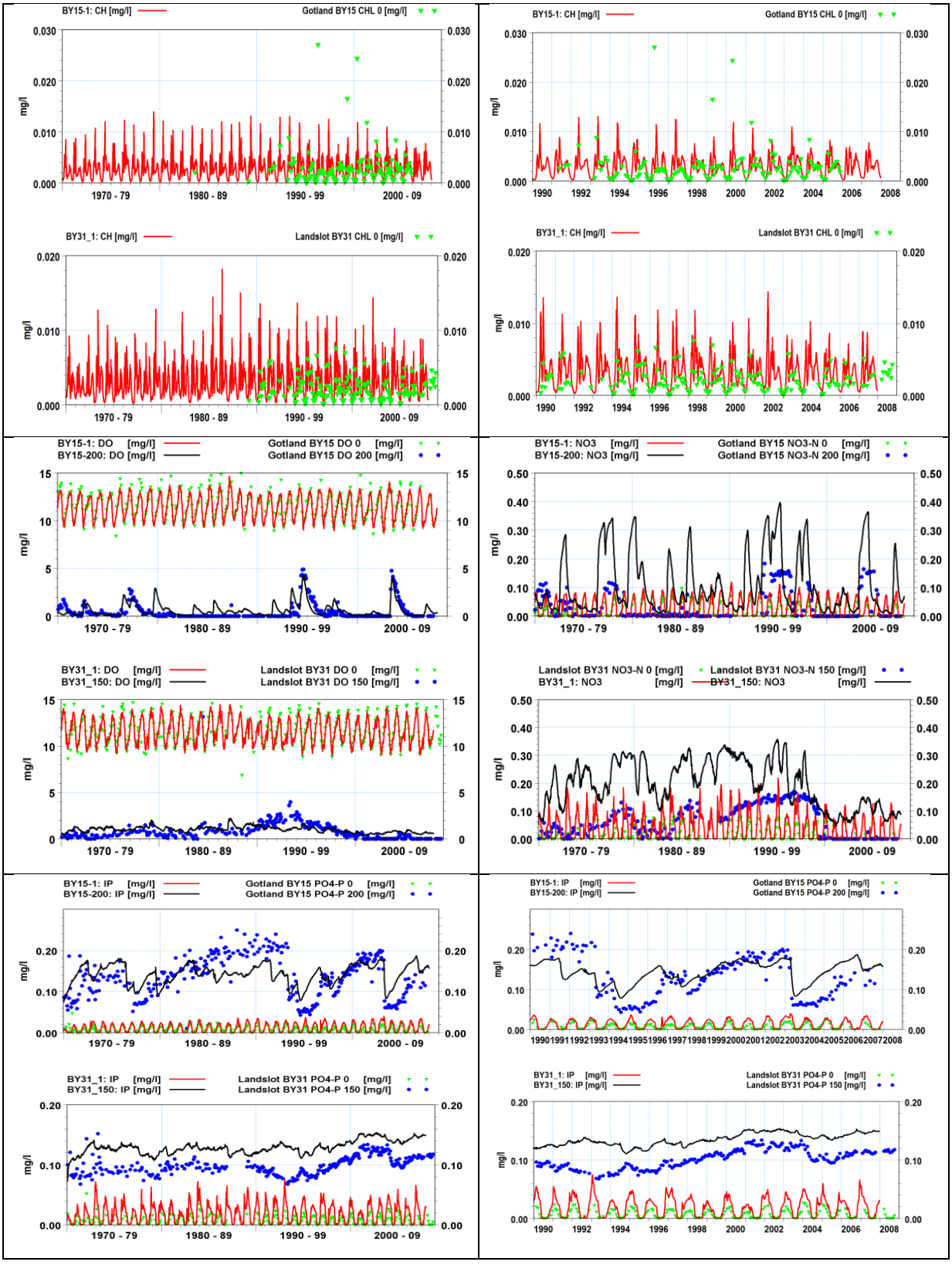

Figure 0-10 **Simulated and measured concentrations at Gotland deep (BY15) and Landsort Deep (By31) of chlorophyll (top), oxygen (mid left), NO_3-N (mid right) and PO_4 (low).**

In Figure 0-11 the water chemistry are presented for the central located station in Gulf of Riga (GoR). The simulated seasonal chlorophyll concentration follows the monitored concentrations. After a high and sharp spring bloom follows a summer level of around 5 µg l^{-1}. The simulated spring bloom is however higher than the monitored values. It might be the model overestimate the spring bloom, but could also be that the sampling is not well representing the actual spring bloom. Seppälä & Balode(1999) measured up to 50 µg l^{-1} in the spring bloom in GoR during a 3 day cruise in April 1994. The simulated concentration of oxygen in the surface and at 40 m depth follows the monitored data. The simulated DO values at the bottom have a tendency not to hit the highest nor the lowest DO concentrations at 40 m depth. The simulated nitrate concentrations during winter are in general overestimated compared with measured NO_3-N. Over time from 1970-2007 there is an increase in both the simulated and the measured winter concentrations which peeks in the beginning of the 1990'ties.

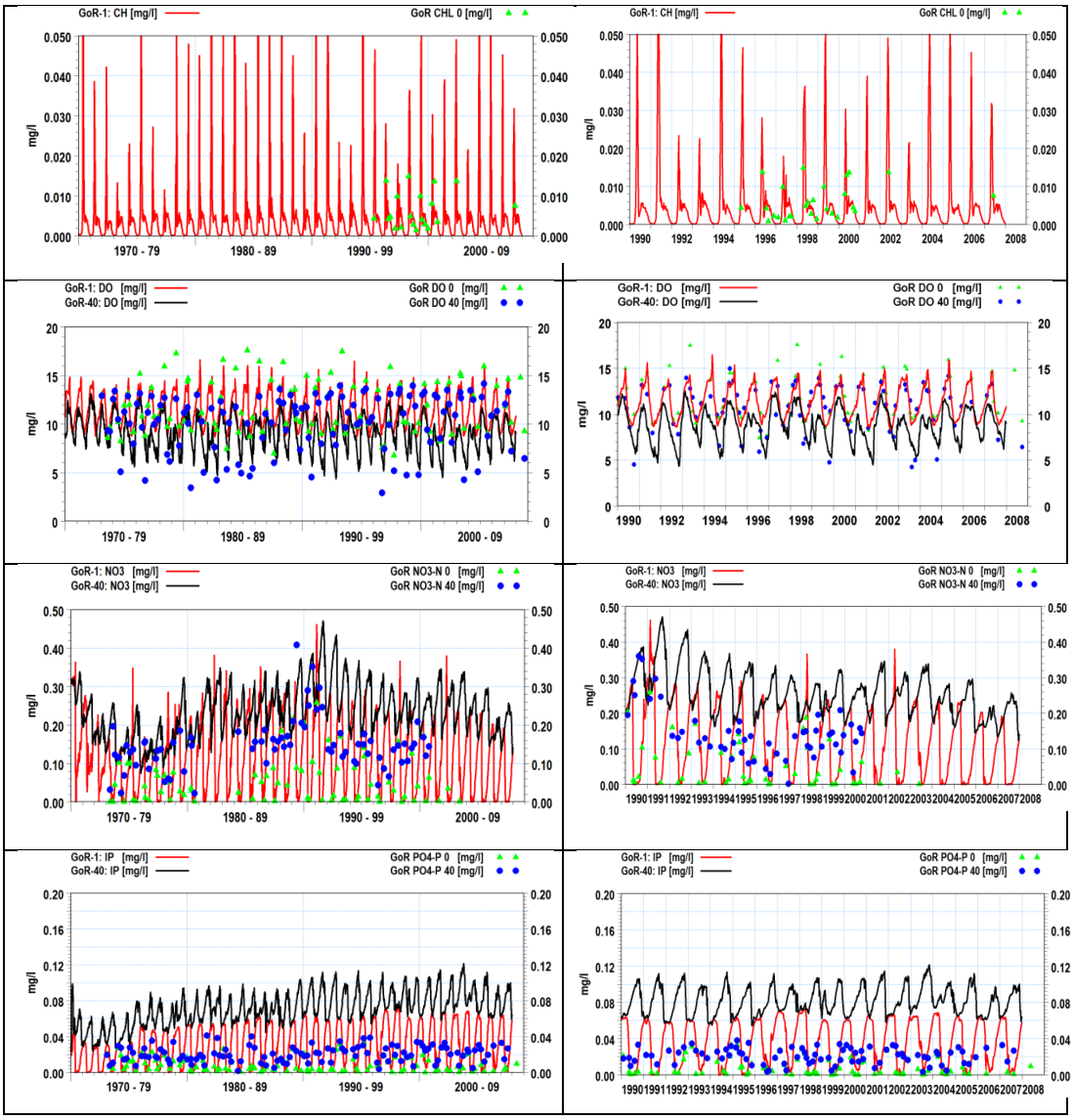

Figure 0-11 **Measured and simulated concentrations of chlorophyll, oxygen, NO_3-N and PO_4-P in Golf or Riga. Left: 1970-2007, right: 1990-2007.**

The simulated winter concentrations of PO_4-P are also too high. In contrast to NO_3-N there is no decline in the concentrations despite reductions in the P- load to GoR from the mid-1990.

The elevated modelled winter concentrations of NO_3-N and especially PO_4-P in GoR has been analyzed further. The concentrations exceed what is simulated at the boundary to the Gulf (BY15), however the Gotland deep station is located far from the boundary of the Gulf. Therefore a mass balance for N and P has been set up for the Gulf and compared with other model results (Savchuk 2002), see Table 0-3 and Table 0-4. A closer examination indicates that the mineralization of the P pool in the sediment is too high. For N the model includes a pool of DON, which for the major part is semi-inert. It need to be photo-oxidized first before it can be mineralized to NH_4 and further nitrified to NO_3. The model N immobilization is lower than found by Savchuk (2002). The nutrient dynamic is therefore still under calibration.

Table 0-3 **P-mass balance for Gulf of Riga 1993-1995. Present model compared with model by (Savchuk. 2002). Red numbers indicate loss of sediment P to water and high P export from Gulf or Riga.**

P mass balance	Model	Savchuk (2002)
Mass	*1993→95*	*Average 1993-95*
Pelagic, 10^3 ton P	31.4→31.8	12.2
Benthic, 10^3 ton P	**171.2→161.9**	146.8
In-Out ,	*10^3 ton P y^{-1}*	*10^3 ton P y^{-1}*
Load land	2.87	2.7
Deposition atmosphere	0.25	0.3
Net export	**4.6**	2.5
Processes	*10^3 ton P y^{-1}*	*10^3 ton P y^{-1}*
Sedimentation to consolidated layer	12.7	19.5
Efflux sediment	23.4	18.7
Burial	1.1	0.8

The simulated biomass of the soft parts in g C m^{-2} of *M. baltica* is presented in Figure 0-12. The highest average biomasses reach 8-9 g C m^{-2} in the Gulf south east of the Saaremaa Island, see Figure 0-12A. The simulated biomasses in each grid is not static in the sense that mortality and spat fall are independent processes and thereby may change the spatial distribution of the biomass, this is seen in figure 0-12B which present the simulated maximum biomasses for each grid cell over the 8 year period. In many areas the biomass exceeds 12 g C m^{-2}. The main location of high biomasses are still south east of the two islands Hiiuma and Saaremaa, however there is also simulated spots with high biomasses west of the islands. The dynamic nature of the simulated biomass is visualized in Figure 0-12 C and D, which are "snap shots" of the standing biomasses in January 2000 and December 2007. In both cases maximum biomass is above 12 g C m^{-2}. The simulated biomasses of *M. baltica* are calibrated against measured biomasses provided by J. Kotta (Figure 0-13). The measured biomasses are point samples in g dw m^{-2} (shell + soft parts) and they are presented by filled circles. The simulated average biomasses has been converted into dry

weight by assuming the ash free dry weight is 18.5% of the dry weight (shell+ soft parts), Rumohr et al. (1987) and the C content is set to 42 % of the ash free dry weight.

Table 0-4 N **Mass balance for Gulf of Riga 1993-1995. Present model compared with model by (Savchuk. 2002). Red numbers indicate loss of sediment N to the water.**

N mass balance	Model 1993-95	Savchuk (2002) 1993-95	Other estimates
Mass	*1993 →95*	*Average*	*Average*
Pelagic, 10^3 ton N	261.9→225.9 - DON: 139.8→116.3	71.8	144
Benthic, 10^3 ton N	**1495.4→1410.9**	568.4	821
In-Out	*10^3 ton N y^{-1}*	*10^3 ton N y^{-1}*	*10^3 ton N y^{-1}*
Load land	85	75.8	111
deposition atmosphere	11.4	14.6	
N-fixation	4.8	12.1	
Net export	50 (21-DON)	19.2	31
Processes	*10^3 ton N y^{-1}*	*10^3 ton N y^{-1}*	*10^3 ton N y^{-1}*
Sedimentation to consolidated layer	135.9	165.8	
Efflux NH_4+NO_3 +DON	67.6	73.1	
Denitrification sediment & water	20.7	74.1	
Burial	24.5	3.2	5

The simulated biomasses are in the same range as the measured biomasses and located in the same areas as the measured biomasses. The simulated average biomasses seem slightly to underestimate the biomasses in the Gulf southeast of Saaremaa between 10-20 m depth. However, from the simulated maximum biomasses it is evident that at some time during the 8 years the model has simulated high biomass in this area. The monitored data represent sampling over a decade, and they are not representing average biomasses. These data collected over time includes low and high biomasses. Samples with high biomasses may visually look more domination than they are, because small circles (biomasses) have a tendency to be hidden in between large circles (biomasses). A more comprehensive analysis between levels of simulated and measured data would be an advantage.
In Figure 0-14 the simulated biomasses (g C m^{-2}) of *Mytilus* and *Mya* are presented. The spatial variation of the simulated biomasses over time is less pronounced for *Mytilus* + *Mya* biomasses relative to the simulated *Macoma* biomasses. This is because *Mytilus* is restricted to hard bottoms and *Mya* to sandy-silty bottoms. Further they are suspension feeders not able to feed on soft bottom sediments. They are therefore restricted to areas where currents or waves creates a continuous water exchange over the bottom. These conditions are confined to the Irbe Väin strait south of the Saaremaa island and on the west costs of Saaremaa and Hiiuma islands.

Simulated and measured biomasses are compared in Figure 0-15. It is assumed that the ash free dry weight of *Mytilus* and *Mya* is 20% of the dry weight Rumohr et al. (1987) and 42% of

the ash free dry weight is C. The largest biomasses are seen in the monitored data for *Mytilus* (range: 0 - 3550 g dw m^{-2}), whereas the biomasses of *Mya* range between 0 and 800 g dw m^{-2}. The simulated average biomasses are in the same range when considering the average and the maximum biomasses. Further, the largest simulated biomasses are located at the same points where monitored *Mytilus* are located.

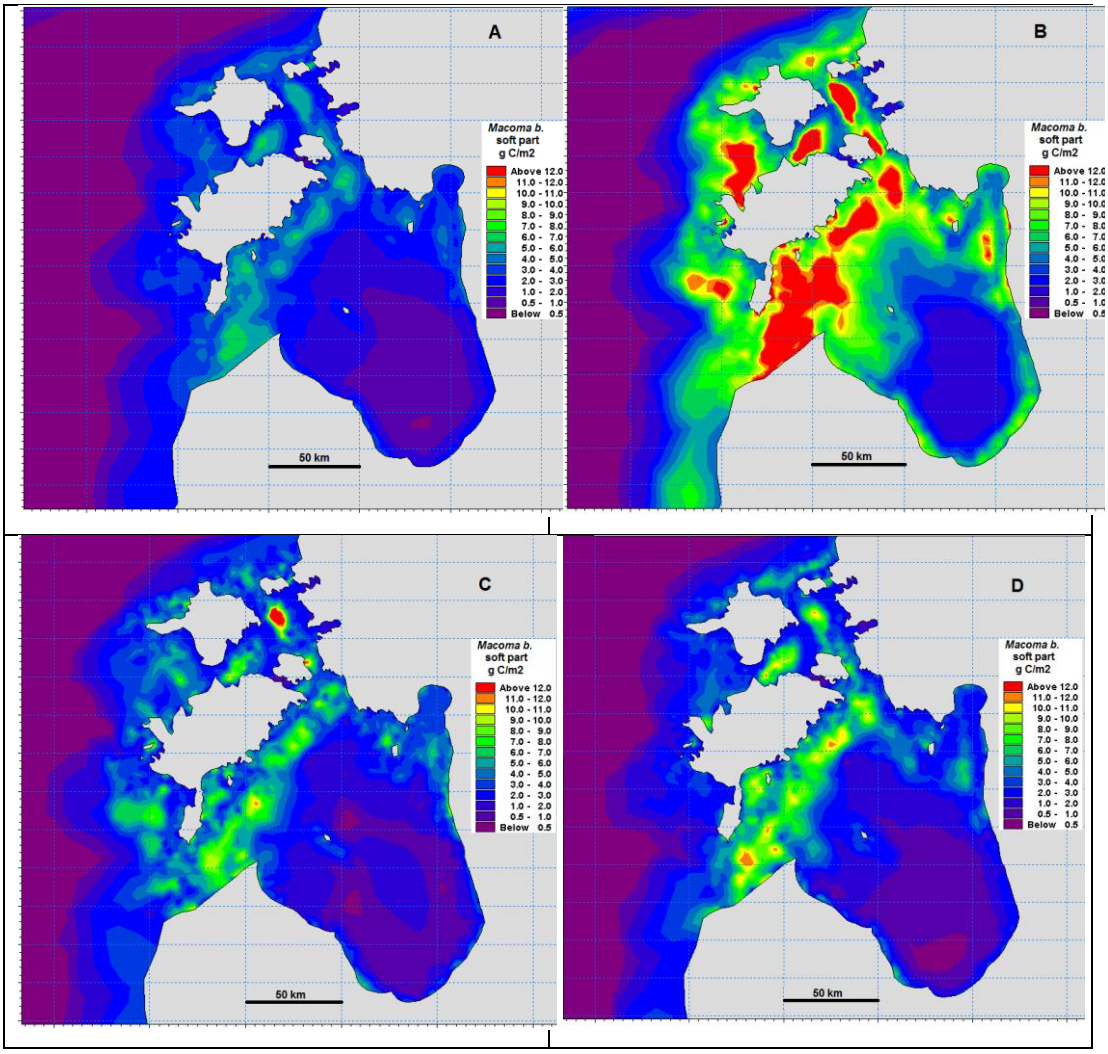

Figure 0-12 **Simulated biomass of *Macoma baltica* (g C m^{-2}) in Golf of Riga. A: mean biomasses, 2000-2007. B: max biomasses, 2000-2007. C Biomass January 2000. D Biomass December 2007.**

Mass budgets for *Macoma* and *Mytilus + Mya* for GoR over the years 1993-95 are presented in Table 0-5 covering the area in Figure 0-15. The productions of *Macoma* and *Mytilus + Mya* are equivalent to 2.0 % and 2.9 % of the primary production in the area. Of the primary production a biomass of mussels equivalent to 0.4% (*Macoma*) and 0.8 % (*Mytilus+Mya*) pr. year is consumed by birds. Mortality other than bird predation accounts for 1.1 % and 1.7 % biomass equivalent of primary production. No data are at present available for verification of these mass considerations.

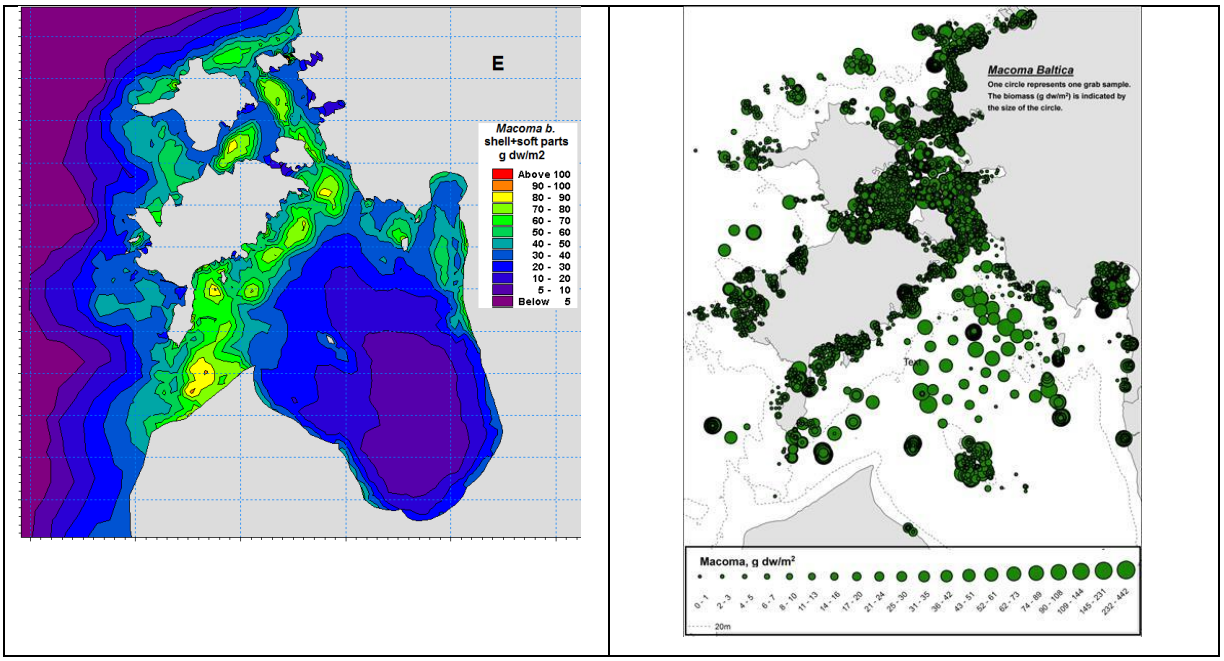

Figure 0-13 **Left: Simulated dry weight (shell+ soft part) of *M. baltica b*. Right: measured *M. baltica* (g dw m^{-2}, data from J. Kotta).**

Table 0-5 **Mass balance for *Macoma* and *Mytilus* plus *Mya* in Gulf of Riga relative to the primary production**

	Macoma			***Mytilus + Mya***	
	***10^3 ton C y^{-1}**	**% of primary production**		***10^3 ton C y^{-1}**	**% of primary production**
Production phytoplankton	4477				
Production benthic autotrophs	154.39				
Change in mass 1993-95	-0.22			3.15	
Production mussel	92.52	2.0		132.93	2.9
Bird predation mussel	17.41	0.4		34.80	0.8
Other mortality mussel	49.36	1.1		79.82	1.7
Spawning loss mussel	25.98	0.6		15.16	0.3

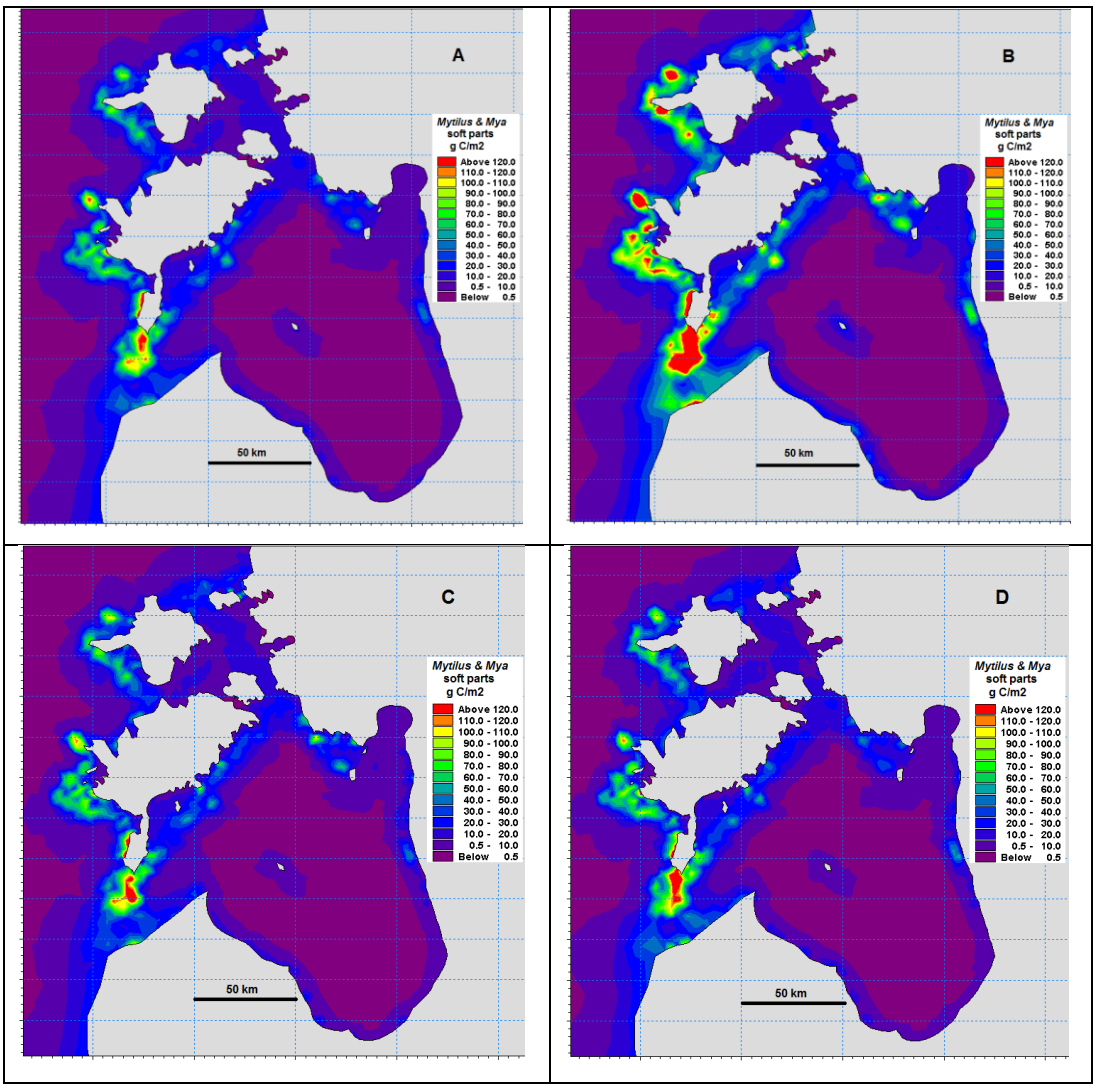

Figure 0-14 **Simulated biomass of *Mytilus + Mya* (g C m^{-2}) in Golf of Riga. A: mean biomasses, year 2000-2007. B: max biomasses, year 2000-2007. C Biomass January 2000. D Biomass December 2007.**

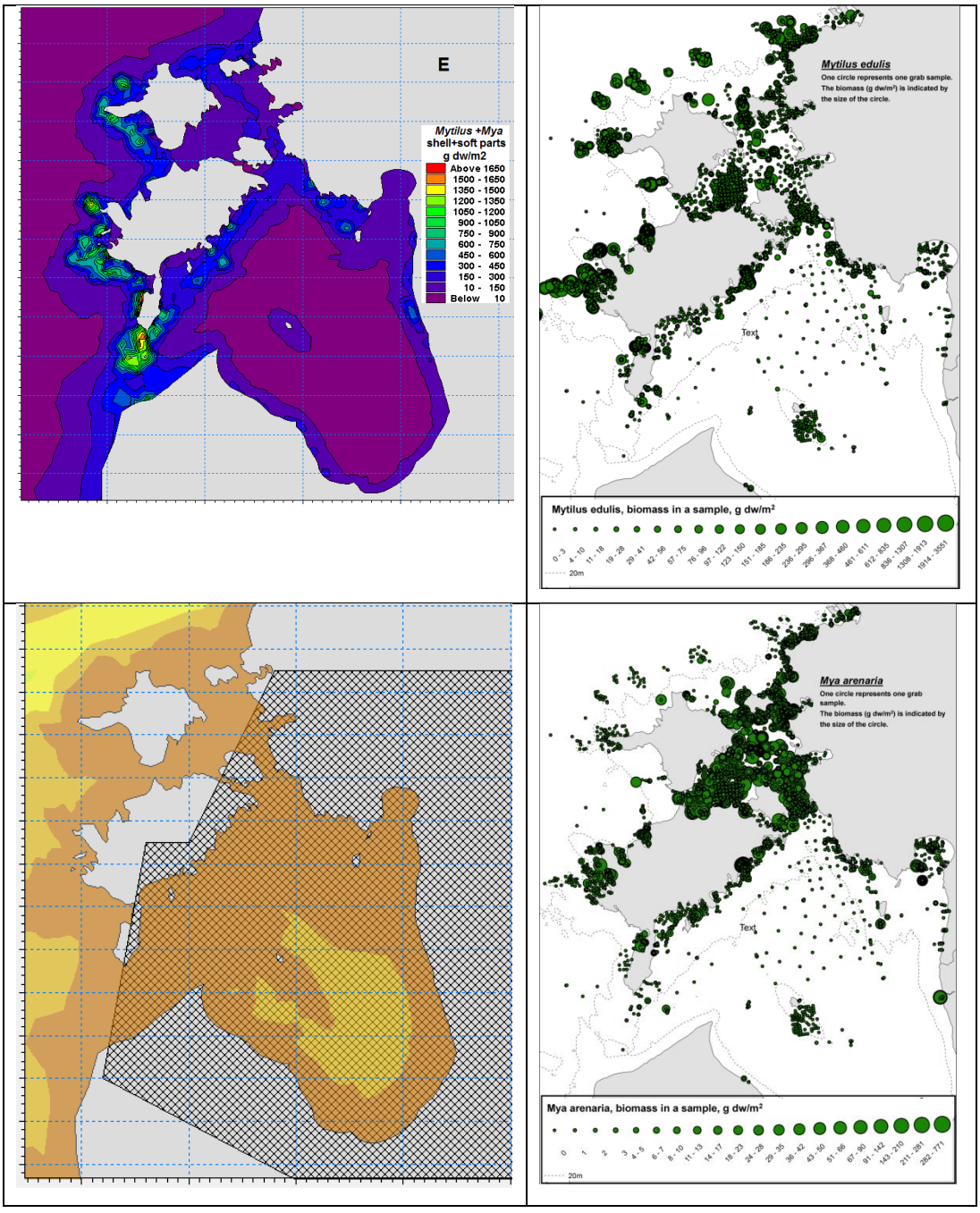

Figure 0-15 **Left: Simulated dry weight (shell+ soft part) of *Mytilus +Mya b*. Right: measured dry weight (g dw m^{-2}) of *Mytilus* and *Mya*, data from J. Kotta. Left low: area included in the mass balance for Gulf or Riga, se tables 3-2, 3-3 and 3-4.**

1.1.2 Sea duck and fish individual-based model

Model Setup

An individual-based model (IBM) for major bivalve predators in the Gulf of Riga has been setup focusing on two most abundant sea ducks species, Long-tailed Duck and Velvet Scoter, and round goby. The IBM is described following a standard protocol for describing individual-based and agent-based models as recommended by Grimm et al. (2006).

Purpose

The overall purpose of the individual-based model is to predict how environmental change might affect carrying capacity of the study area for the analyzed predators when looking at their survival and body condition. The specific objectives were to:

- assess Long-tailed Duck and Velvet Scoter habitat carrying capacity in the Gulf of Riga; and
- predict effects of environmental change scenarios, e.g. climate change, on fitness of wintering Long-tailed Ducks and Velvet Scoters (survival, body condition).

The IBM relates individual behaviors such as feeding activity, rate of food intake or inter-specific competition to environmental factors and food availability and provides detailed insight into aspects which constrain species fitness and numbers of birds using certain resources.

State variables and scales

The Gulf of Riga IBM runs at discrete time steps of a fixed duration (1 hour). Space is represented by discrete patches with fixed location. In our model patches are defined as a variable grid with cells of 2 x 2 km in shallow waters and 4 x 4 km in waters deeper than 20 m (Figure 0-16). This grid is used for model development and calibration, and the grid resolution will be increased once the desired model performance is achieved.

The model is being constructed using package MORPH as a platform Stillman (2008) and has the following predefined 5 entities.

- *Global environment* - State variables which apply throughout the modelled system.
- *Patches* – Locations, which are characterised by local patch variables and containing resources and foragers.
- *Resources* - The food consumed by foragers. Collections of several resources are termed diets.
- *Components* - Elements within resources which foragers assimilate into their bodies.
- *Foragers* - Animals which move within the system attempting to maximise their survival and body condition.

The global state variables are the major driving forces in the model system (e.g., time step, day length, water temperature, etc.). Patches are smaller entities, they depend on global variables, and are characterized by patch variables (e.g., patch coordinates, area, depth, etc.). Patches contain resources (e.g., bivalves), which consist of components (e.g., bivalve meat contents, amount of shell). Foragers, which in our case are birds and fish, consume resources in combinations called diets. From diets foragers assimilate components and metabolize them. Foragers can make choices and, attempting to maximize their fitness,

move between patches, consume diets or emigrate from the model system. Consequences of forager decisions are expressed as fitness (e.g., probability of survival, body condition).

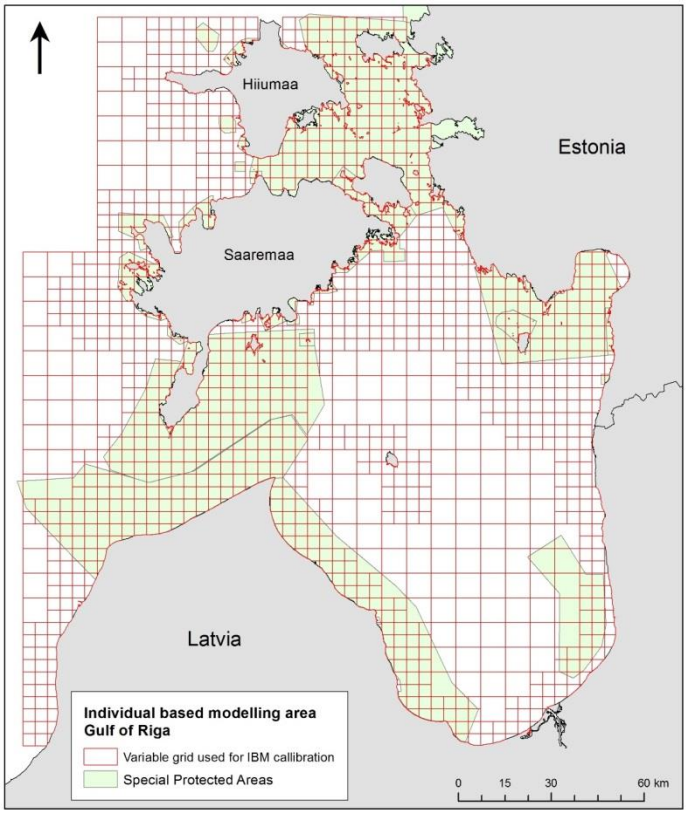

Figure 0-16 The map showing Gulf of Riga individual based model (IBM) grid.

Process overview and scheduling

Process overview and scheduling define environmental and individual processes that are built into the model.

The constructed IBM defines the following processes (Grimm et al. 2006, Stillman 2008):

- *Change in resource density*. Changes in the density of a resource on a patch caused by consumption by the foragers and / or other factors.
- *Change in component density*. Changes in the density of a component in a resource.
- *Forager immigration*. The movement of foragers into the system.
- *Forager decision making*. The optimal patch and diet selection of foragers and decisions to emigrate from the system.
- *Forager emigration*. The movement of foragers from the model system.
- *Forager movement between patches*. Movement of foragers between patches.
- *Forager diet consumption*. The transfer of resource components into foragers when diets are consumed.
- *Forager physiology*. Change in the size of a forager's component reserve due to the balance of consumption and metabolism.
- *Forager mortality.* Death of foragers.

In the IBM design time is represented using discrete time steps of constant duration. During each time step global events are processed first, followed by patch events and then forager events. Finally, results are displayed and saved.

Design concepts

The design concepts provide a common framework for designing and communicating IBMs.

Emergence. Emergence defines which system-level phenomena emerge from individual traits, and which phenomena are imposed.

The following phenomena emerge from the interaction between individual forager traits and global and patch variables, resource and component densities, and forager constants and variables.

- *Resource depletion*. The amount of each resource consumed by foragers from each patch during each time step.
- *Forager distribution and diet selection*. The location of each forager and its diet during each time step.
- *Proportions of time foragers spend feeding*. Proportion of each time step each forager spends feeding.
- *Forager component reserve size*. The amount of each component within each forager's reserves during each time step.
- *Forager mortality and emigration*. The number of foragers remaining in the system after a given number of time steps.

Adaptation. Adaptation describes whether the model individuals have adaptive traits which directly or indirectly can improve their potential fitness, in response to changes in themselves or their environment.

Foragers' adaptive traits are their location and diet selection. During each time step, foragers select the patch / diet combination which maximizes their perceived fitness.

Fitness. This concept defines whether fitness-seeking is modelled explicitly or implicitly. If explicitly, what is the fitness measure of modelled individuals?

Individual fitness is assumed to equal the probability of surviving to the end of a time step. Survival probability is influenced by a number of mortality sources (causes of death). The forager selects the patch and diet combination which maximizes its perceived survival. Once the forager has selected a patch and diet, the consequences of this decision are determined by true probability of survival.

Prediction. Prediction defines how individuals predict the future conditions they will experience and whether this influences their decisions.

Foragers remember their foraging success during a defined number of previous time steps. This memory is used to calculate average state variables over previous time steps. The model does not allow foragers to know the future values of any state variables.

Sensing. Sensing describes the internal and environmental state variables, which model individuals are assumed to "know" and consider in their adaptive decisions.

The amount of knowledge foragers have can be varied. This can range from perfect knowledge of the complete system during the current time step, through complete knowledge of local patches, to no knowledge at all. Similarly, the amount of knowledge a

forager has of its own state, both during the current time step and previous time steps, can be varied. Foragers base their decisions on the perceived survival probability associated with different patches and diets (or no diet). Foragers tend to avoid patches and diets with low perceived survival probabilities.

Interaction. This concept identifies interactions among individuals in the model system.

Foragers interact within patches through the consumption of a shared resource (depletion competition). The number of other foragers within a patch can also affect any of a forager's state variables, and hence perceived and true survival probabilities. These effects can be either positive or negative, depending on the submodels used. Foragers can only interact within patches.

Stochasticity. Stochasticity is part of IBMs and the amount of stochasticity can be varied. Any of state variables, except for patch size and location, and forager species can be stochastic. The probability of a forager dying during a time step is a stochastic event unless the probability is zero or one.

Collectives. Collectives describe whether individuals are grouped into some kind of collective, e.g. a social group.

Collectives are not represented as social groups. We use "super-individuals" in our model design so that each forager represents more than one individual (super-individual). The number of individuals within a forager is set at the start of a simulation, but can decrease through time as some individuals within the forager die. In contrast, all individuals within a forager simultaneously immigrate to or emigrate from the system.

Observation. Observation describes how data are collected from the IBM for testing, understanding, and analyzing. All state variables can be displayed and saved during each time step.

Initialization

Initialization deals with questions as: How are the environment and the individuals created at the start of a simulation run? Is initialization always the same, or was it varied among simulations? Were the initial values chosen arbitrarily or based on data?

In IBMs created using MORPH platform, the initial values of state variables are either read from a parameter file, created using random numbers, or calculated from state variables defined earlier in the parameter file. The sequence of random numbers is itself randomized at the start of each simulation so that replicate simulations using the same set of parameters will produce slightly different predictions. All global and patch variables are initialized at the start of the simulation. Forager state variables are initialized once the forager has immigrated into the system.

Input

The particular data used to parameterize the model depend on the particular system to which it is applied. Table 0.6 lists parameters, which were used to parameterize the Gulf of Riga seaduck and goby IBM. Parameters are either single values, values for each time step read in from a file, or an equation (sub-model) to calculate values during each time step.

Table 0.6 **Description and values of the baseline individual-based model parameter file developed for Long-tailed Duck and Velvet Scoter in the Gulf of Riga. [*Round goby sub-model is still in development phase, therefor not presented in this table*.]**

Entity/ State variable	Value	Variable description
Global environment		
Day	Day 1 = October 1, Day 182 = March 31	Represents duration of bird wintering season
Time	01 – 24 hours per day	Simulation is conducted at 1 h time steps
Day length	Daily day length	Calculated based on central position of the Gulf of Riga and date
Daylight	0 or 1 depending upon above	Based on sunset and sunrise times
Water temperature	Mean daily water surface temperature	Extracted from DHI hydrodynamic model
Patches		
Number	1271	The number of grid cells. Each grid cell represents a discrete patch.
Location	Central coordinates of each patch	Measured in UTM32N
Size	4-16 km^2 or less if patch includes land	Size of each patch measured in GIS. If a grid cell (patch) includes both marine and land areas, then land area was excluded.
Patch variable1: Water depth	Mean water depth of a patch	Calculated in GIS using DHI bathymetry raster of 50 m resolution
PV2: Land	Distance to land	Calculated mean value for each patch using 'path distance' to land (50 m resolution)
PV3: Shipping	Distance to main shipping lanes	Euclidean distance of each patch to a shipping lanes defined using shipping AIS data (HELCOM).
PV4: Wind farm	Distance to estuaries	Currently unused variable, reserved for later inclusion if deemed necessary
PV5: Included	0 or 1	Used to include/exclude patches from different model runs.
Resources		
Number	2 – number of resources	A simplified model constructed using 2 major bivalve resources – Blue Mussels and Clams
Name	Resource name: MusselsAll ClamsAll	Principal prey types
Initial density	Initial density of bivalves on each patch, numbers/m^2	Resource density obtained using Mytilus and Macoma biomasses modelled for the Gulf of Riga and accepting a simplified assumption that bivalves of all sizes are available to birds and converting total biomass into a number of 12 mm long specimens
Change in density	Change in resource density in time considering all other factors except bird and round goby consumption: MusselsAllDens*POWER(0.9982,(1/24)) ClamsAllDens*POWER(0.9982,(1/24))	Proportional daily decline in numerical abundance of bivalves due to natural mortality and predations by other predators not accounted in the IBM
Components		
Number	1	Number of resource components
Name	Flesh dry mass	0.0078 g AFDW (12 mm Mytilus)
Component density	Grams of flesh dry mass per prey item Grams of shell dry mass per prey item	Values calculated using allometric equations for 12 mm size Mytilus and Macoma
Foragers		
Number of forager types	Number of forager types: 2	Long-tailed Duck Velvet Scoter
Number of foragers	200 300 400	This is a number of super-individuals, where each consists of 1,000 individuals resulting in a population of 200,000 (or more) Long-tailed Ducks and the same number of Velvet Scoters. Super-individuals are used to reduce noise between

Entity/ State variable	Value	Variable description
		replicates and ensure faster model processing.
Individuals per forager	1,000	Number of individuals per forager (super-individual)
Forager constants	C1: Foraging efficiency normal(1,0.125,0,1000)	A value drawn at random from a normal distribution with mean of 1, standard deviation of 0.125, and max of 1000.
	C2: Dominance uniform(0,1)	A value drawn at random from a uniform distribution with a min of 0 and max of 1
	C3: Arrival day int(uniform(1,30))	Long-tailed Duck: a value drawn at random from a uniform distribution starting from day 31 until day 60 (throughout November) Velvet Scoter: a value drawn at random from a uniform distribution starting from day 1 until day 30 (throughout October)
	C4: Departure day int(uniform(153,182))	A value drawn at random from a uniform distribution starting from day 153 until day 182 (throughout March)
	C5: Maximum species density: 0.005	A rule was set that maximum species density shall not exceed 5,000 birds/km^2
Forager variables	Underwater time per dive (hours): [*equation*]	Basic relationship between water depth and diving activity: empirically developed sub-model (*in development*)
	Travel time per dive (hours): ((WaterDepth/1.15)+(WaterDepth/1.4))/3600	Travel time calculated according to: speed of descent 1.15 m/s, speed of ascent 1.4 m/s , (Heath et al. 2006, 2007)
	Surface time per dive (hours): [*equation*]	Basic relationship between water depth and diving activity: empirically developed sub-model (*in development*)
	Forage (bottom) time per dive (hours): if((UWTPDive-TravTPDive)>0, UWTPDive-TravTPDive,0)	Value derived by subtraction of time spent travelling to and from bottom from total time spent underwater
	Disturbance by proximity to land: if(Land>200,1,0)	A simplistic assumption was made that all birds are excluded from patches within 200 m to land.
	Disturbance from shipping: [*equation*]	An equation based on empirical data and literature defining species-specific distances to ships (*in development*)
Diet consumption rate	Bivalves eaten per second of the bottom time, as a function of numerical abundance of prey (bivalves/m^2). *Mytilus*: if((CountLtDuck / PatchSize <=MaxLtDuckDens), Daylight*Eff*3600* (ForTPDive/ (UWTPDive+SurfTPDive))* ((46.664*MusselDietDensity/(23.994+ MusselDietDensity))/60),0) Clams: (*in development*)	Functional response of seaduck intake rate of benthic bivalves based on equation provided by Richman and Lovvorn (2003) and Varennes et al. (2015). (*in development*)
Maximum diet consumption rate	Maximum number of bivalves that can be eaten per second of the bottom time: (ForTPDive/(UWTPDive+SurfTPDive))*2*3600	Set rule that birds cannot eat more than 2 mussels per second of bottom time.
Component assimilation rate	Flesh dry mass: 0.73*(22.46/33.4)	Derived from literature: energy assimilation rate from flesh was assumed to be 0.73 (Hockey 1984); 1 g of mussel ash free dry weight contains 22.46 kJ (Rumohr et al. 1987); energy density of body reserves 33.4 kJ/g (Kersten & Piersma 1987)
Component metabolic rate while feeding	Long-tailed Duck: ((((16*0.796*(TravTPDive/2)+11*0.796*ForTPDive+ 15.4*(TravTPDive/2))+(16*0.796*(TravTPDive/2)+ 11*0.796*ForTPDive+15.4*(TravTPDive/2))*0.27)+ ((((16*0.796*(TravTPDive/2)+11*0.796* ForTPDive+ 15.4*(TravTPDive/2))+(16*0.796*(TravTPDive/2)+ 11*0.796* ForTPDive+15.4*(TravTPDive/2))*0.27))* 0.97)+((((5.48-0.09*WaterTemp)*0.796*0.74)+	Sub-model compiled using literature data about energetic cost of different Long-tailed Duck activities while foraging. Velvet Scoter: (*in development*)

Entity/ State variable	Value	Variable description
	((0.7*12.2*0.796)*0.26))*SurfTPDive)+((93*0.796)*(9.6*60/24/3600)))*3600/1000)/33.4/0.6 Velvet Scoter: (*in development*)	
Component metabolic rate while resting	Long-tailed Duck: ((((5.48-0.09*WaterTemp)*0.796* 0.74)+((0.7*12.2*0.796)*0.26)+((93*0.796)*(15*60/24/3600)))*3600/1000)/33.4/0.6 Velvet Scoter: (*in development*)	Sub-model compiled using literature data about energetic cost of Long-tailed Duck metabolic costs while resting. Velvet Scoter: (*in development*)
Component metabolic rate while moving	Long-tailed Duck: ((93*0.796)*3600/1000/33.4/0.6)*(15*60/24/3600) Velvet Scoter: ((93*1.6)*3600/1000/33.4/0.6)*(10*60/24/3600)	Equally distributed flights cost per day, assuming that Long-tailed Duck flies 15 minutes per day and Velvet Scoter 10 minutes per day (Pelletier et al. 2008), and flight costs 93 W/kg (Lovvorn et al. 2009)
Initial size of reserve store	Long-tailed Duck: 557+172 Velvet Scoter: [*1120 + 480*]	796 g is the average Long-tailed Duck body mass at the beginning of wintering season (own unpublished data from eastern Baltic). Starvation body mass is assumed being about 30% lower than average individual weight, i.e. 557 g. Velvet Scoter: (*in development*)
Target size of reserve store	Long-tailed Duck: 557+(172+0.5*Day) Velvet Scoter: (*in development*)	Mean weight of Long-tailed Ducks in the eastern Baltic in March was measured as 820 g. To reach that body weight birds need to gain 0.5 g per day during wintering season. Velvet Scoter: (*in development*)
Fitness components	Starvation	

Survival probability	Long-tailed Duck:
	if(FleshDryMassFinalStore>557,1,0)
	Velvet Scot8888er:
	if(FleshDryMassFinalStore>1120,1,0)
		Bird dies if body weight falls below the starvation weight

Emigration probability	if(Day=DepartureDay,1,0)	Birds are not allowed to leave the model system, until the departure day as identified above

Model Calibration

The IBM for Gulf of Riga benthivorous predators has been set up and is currently undergoing a calibration process, which includes fine-tuning sub-models and equations describing foraging ecology and bioenergetics, reviews and comparison with literature data. Initially, separate IBMs are constructed for different predators (Figure 0-17), sea ducks and round goby, so that model performance could be assessed and calibrated preventing additional noise from concurrently acting other predators. Once species models are calibrated, all considered predators will be merged into a single model system. Further, model spatial resolution will be increased for waters shallower than 15 meters in order to better resolve spatial resource utilization.

The final model will be subject to sensitivity testing of multiple parameters and the same IBM setup will be used for running scenarios representing environmental change.

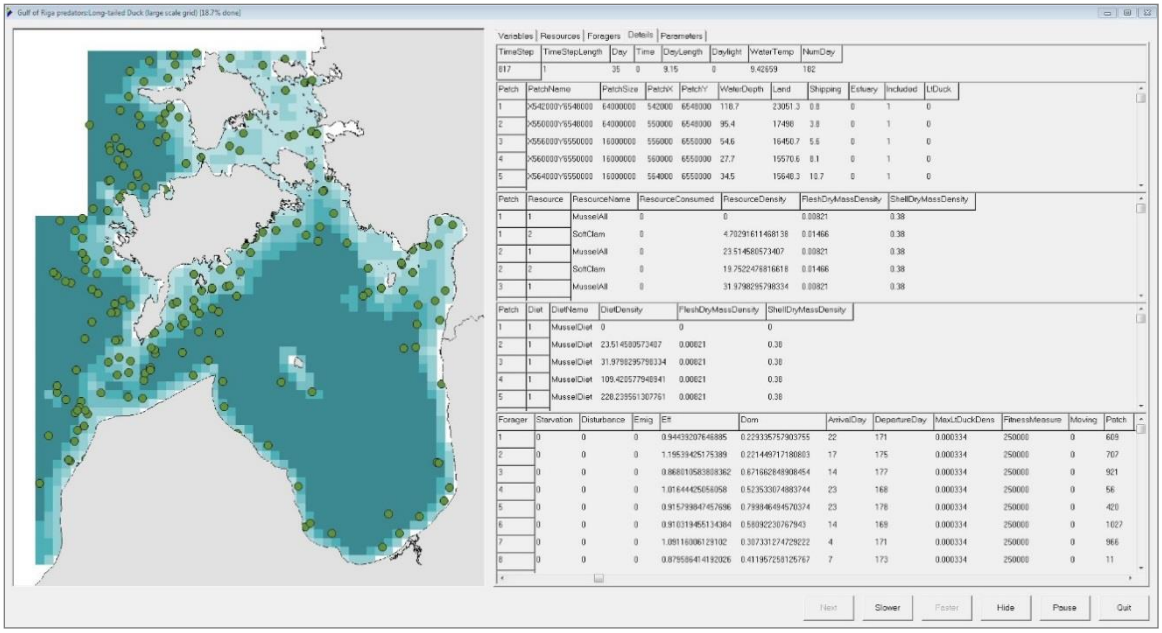

Figure 0-17 Screenshot of IBM simulation in MORPH environment.

1.1.3 References

Azour F., van Deurs M., Behrens J., Carl H., Hüssy K., Greisen K., Ebert R., Møller P.R. 2015. Invasion rate and population characteristics of the round goby *Neogobius melanostomus*: effects of density and invasion history. Aquatic Biology 24: 41-52.

Durinck, J., Skov, H., Jensen, F.P. and Pihl, S. 1994. Important marine areas for wintering birds in the Baltic Sea. EU DG XI research contract no. 2242/90-09-01. Ornis Consult report.

Ojaveer H., Galil B.S., Lehtiniemi M., Christoffersen M., Clink S., Florin A.-M., Gruszka P., Puntila R., Behrens J.W. 2015. Twenty five years of invasion: management of the round goby *Neogobius melanostomus* in the Baltic Sea. Management of Biological Invasions 6: in press.

De Leeuw, J.J. 1999. Food intake rates and habitat segregation of Tufted Duck Aythya fuligula and Scaup Aythya marila exploiting Zebra Mussels Dreissena polymorpha. Ardea, 87, 15-31.

DHI 2014a. MIKE 21 & MIKE 3 FLOW MODEL FM, Hydrodynamic and Transport Module, Scientific Documentation. MIKE by DHI 2014.

DHI 2014b. ECO LAB, Short Scientific Description. MIKE BY DHI 2014.

FEBI 2013. Fehmarnbelt Fixed Link EIA. Bird Investigations in Fehmarnbelt – Baseline. Volume II. Waterbirds in Fehmarnbelt. Report No. E3TR0011.

FEHY 2013. Fehmarnbelt Fixed Link. Marine Water - Baseline. Hydrography, Water Quality and Plankton of the Baltic Sea. Report No. E1TR0057 - Volume I

Grimm, V., Berger, U., Bastiansen, F., Eliassen, S., Ginot, V., Giske, J., Goss-Custard, J.D., Grand, T., Heinz, S., Huse, G., Huth, A., Jepsen, J.U., Jørgensen, C., Mooij, W.M., Müller, B., Pe'er, G., Piou, C., Railsback, S.F., Robbins, A.M., Robbins, M.M., Rossmanith, E., Rüger, N., Strand, E., Souissi, S., Stillman, R.A., Vabø, R., Visser, U. and DeAngelis, D.L. 2006. A standard protocol for describing individual-based and agent-based models. Ecological Modelling, 198, 115-126.

Heat J.P., Gilchrist H.G., Ydenberg R.C. 2007. Can dive cycle models predict patterns of foraging behaviour? Diving by common eiders in an Arctic polynya. Animal Behaviour 73: 877-884.

Heath, J.P., Montevecchi, W.A. and Robertson, G.J. 2008. Allocating foraging effort across multiple time scales: behavioral responses to environmental conditions by Harlequin Ducks wintering at Cape St. Mary's, Newfoundland. Waterbirds, 31, 71-80.

Hockey, P.A.R. 1984. Growth energetics of the African Black Oystercatcher, *Haematopus moquini*. Ardea, 72, 111-117.

Kersten, M. and Piersma, T. 1987. High levels of energy expenditure in shorebirds; metabolic adaptations to an energetically expensive way of life. Ardea, 75, 175-187.

Lovvorn, J.R., Grebmeier, J.M., Cooper, L.W., Bump, J.K. and Richman, S.E. 2009. Modeling marine protected areas for threatened eiders in a climatically changing Bering Sea. Ecological Applications, 19, 1596-1613.

Pelletier, D., Guillemette, M., Grandbois, J.M. and Butler, P.J. 2008. To fly or not to fly: high flight costs in a large sea duck do not imply an expensive lifestyle. Proc. R. Soc. B, 275, 2117-2124.

Richman, S.E. and Lovvorn, J.R. 2004. Relative foraging value to Lesser Scaup ducks of native and exotic clams from San Francisco Bay. Ecological Application 14: 1217-1231.

Richman, S.E. and Lovvorn, J.R. 2008. Costs of diving by wing and foot propulsion in a sea duck, the White-winged Scoter. J. Comp. Physiol. B, 178, 321-332.

Rumohr H., T. Brey, S. Ankar. 1987. A compilation of biometric conversion factors for benthic invertebrates of the Baltic Sea. The Baltic Marine Biologists Publication No. 9. 19987. ISSN 0282-8839

Savchuk O.P. 2002. Nutrient biochemical cycles in the Gulf of Riga: scaling up field studies with a mathematical model. Journal of Marine Systems 32 (2002) 253-280.

Seppälä J., M. Balode 1999. Spatial distribution of phytoplanktonin the Gulf of Riga during spring and summer stages. Journal of Marine Systems 23 (1999) P 51-67

Skov, H., Heinänen, S., Žydelis, R., Bellebaum, J., Bzoma, S., Dagys, M., Durinck, J., Garthe, S., Grishanov, G., Hario, M., Kieckbusch, J. J., Kube, J., Kuresoo, A., Larsson, K., Luigujoe, L., Meissner, W., Nehls, H. W., Nilsson, L., Petersen, I.K., Roos, M. M., Pihl, S., Sonntag, N., Stock, A., Stipniece, A., Wahl., J. 2011. Waterbird populations and pressures in the Baltic Sea. TemaNord 2011:550, Nordic Council of Ministers, Copenhagen.

Stempniewicz, L. 1986. The food intake of two Scoters *Melanitta fusca* and *M. nigra* wintering in the Gulf of Gdańsk, Polish Baltic coast. Vår Fågelv. Suppl., 11, 211-214.

Stempniewicz, L. 1995. Feeding ecology of the Long-tailed Duck *Clangula hyemalis* wintering in the Gulf of Gdańsk (southern Baltic Sea). Ornis Svecica, 5, 133-142.

Stillman, R.A. 2008. MORPH – An individual-based model to predict the effect of environmental change on foraging animal populations. Ecological modelling, 216, 265-276.

Varennes E., Hanssen S.A., Bonardelli J.C., Guillemette M. 2015. Functional response curves of avian molluscivores: high intake rates maintained even at low prey density. Marine Ecology Progress Series 526: 207-212.

Žydelis, R. 2002. Habitat selection of waterbirds wintering in Lithuanian coastal zone of the Baltic Sea. PhD thesis, University of Vilnius, Lithuania.

APPENDIX II

Nutritional quality of phytoplankton and biochemical markers as tracers for energy transfer

Monika Winder, Alfred Burian and Jens Nielsen
Stockholm University

Methods and results

4-10 algae species of each of the taxonomic groups (total 30 different species) were cultured under optimal growth conditions (no nutrient or light limitation leading to exponential growth) at 18 °C, filtered on precombusted GF/F filters and frozen at -80 °C until further analysis. Chemical analysis of amino acids, C:N:P ratios and fatty acids were quantified according to standard protocols. For both amino and fatty acids, the relative (% expressed relative to total biomass of compound group) and absolute concentration (weight per unit algae biovolume) of individual compounds was determined. Fatty acids are split in neutral (mostly storage) and polar (functional compounds) fractions and for each fraction the ratio and absolute amount of single FA was investigated separately.

In addition, CSIA of δ^{15}N AA, δ^{13}C AA, and δ^{13}C FA as well as of bulk stable isotopes are conducted according to standard protocols. A premise for successful separation is that algae groups deviate significantly in biomarker composition, and further that larger variation exists between than within groups. Our main target in this study was to compare and combine different approaches as well as explores new possibilities for algae group-separation (CSIA FA, CSIA AA). The analysis of trade-offs between different methods will yield a clearer picture of the potential of different methods and of their practical application.

First results indicate that major taxonomic groups differ in the concentrations of important biochemical compounds. No algae group has high concentrations for every single compound group, creating trade-offs for herbivore consumers. These differences in compound concentrations explain why a more diverse nutrition leads to higher production rates of consumers than mono-specific diets. Furthermore, food quality is important both in terms of relative and absolute amounts. Whereas absolute amounts impact production rates, relative ratios will determine how efficiently available resource can be utilised. Insight into both these aspects in algae groups provide increased insight into diet quality.

CSIA of δ^{13}C FA indicated several new and interesting patterns: we demonstrate that cyanobacteria, whose taxonomic diversity has not been well represented in previous FA research, are very heterogeneous in their FA composition. Whereas they are generally considered as very poor food sources (seen also in several of our species), a number of strains in our analysis showed high concentrations of PUFAs (e.g.

18:3n3, 18:4n3). Therefore, the FA food quality of these strains was practically identical with fresh-water chlorophytes. Further, our analysis of haptophytes revealed 18:5n3 as a reliable group specific tracer, which is neither found in diatoms, green algae or cyanobacteria. Moreover, several quantitative differences in FA between taxonomic groups were noticeable, which we still have to explore further.

In our current data set (species n=30), clear group-specific differences between isotopic values of single FAs were noticeable, and isotope-based separation of algae classes seems very promising. Further, we saw clear differences between isotopic ratios of the same FA in polar and total FA fractions, which can be attributed to enzyme selectivity during FA esterification (Fig. 1). This means that both polar and total fractions can be used complementarily as diet tracers. Very promising polar tracer FAs are 18:1n9 and 18:1n7 (present in nearly all algae) (Fig. 2), which can be used to differentiate haptophytes (enriched in 18:1n7) and diatoms (depleted in 18:1n9), or 18:2n6 and 18:3n6 (differentiation between all groups). Also some PUFAs (e.g. 16:4n3 and EPA) show significant inter-group differences.

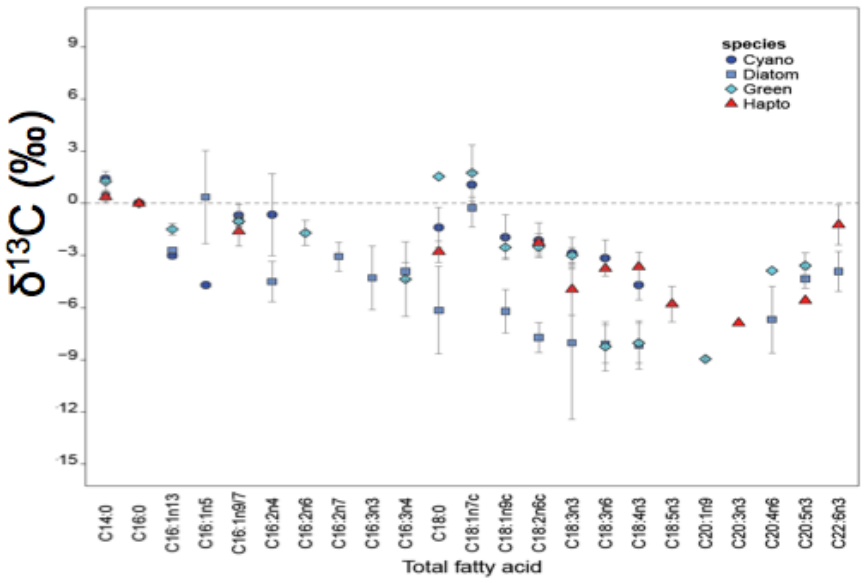

Fig. 1: Isotopic ratios of individual total fatty acids standardised to the isotopic ratio of C16:0. Relative ratios of total fatty acids are displayed. Note that values are means and that not necessarily all species within a group produce the same set of individual FAs.

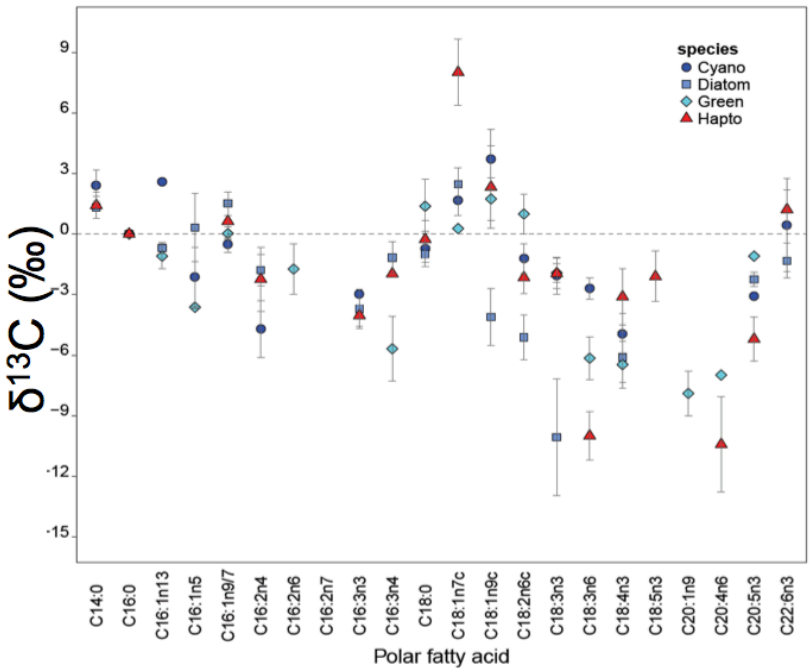

Fig. 2: Isotopic ratios of individual polar fatty acids standardised to the isotopic ratio of C16:0. Relative ratios of total fatty acids are displayed.

APPENDIX III

Seasonal dynamics of zooplankton resource use revealed by carbon amino acid stable isotope values

Monika Winder, Jens M. Nielsen
Stockholm University

This study is published in:
Nielsen JM, Winder M (2015) Seasonal dynamics of zooplankton resource use revealed by carbon amino acid stable isotope values. Mar Ecol Prog Ser 531:143-154

Methods and Results:

Methods

We sampled zooplankton and seston at weekly to monthly intervals between March and December 2012 at a coastal station in the northern Baltic proper. *Acartia* and seston samples of bulk $\delta^{13}C$ and $\delta^{15}N$ values, and $\delta^{13}C$ values of the E-AAs Isoleucine (Ile), Leucine (Leu), Lysine (Lys), Phenylalanine (Phe) and Valine (Val), were analysed at the UC Davis stable isotope facility. $\delta^{13}C$ AA-CSIA was analysed using GC-C-IRMS and stable isotope ratios are described as:

$$\delta(‰) = [(R_{sample} / R_{standard}) -1] \times 1000$$

where R = ^{13}C / ^{12}C or ^{15}N / ^{14}N of AA or bulk tissue. The $R_{standard}$ is an international standard of atmospheric N_2 for N or Pee Dee belemnite for C.
Correlation coefficients of C and N bulk isotope values of *Acartia* and seston were calculated using nonparametric Spearman rank correlations. Dynamic factor analysis (DFA) was used to assess seasonal variation in $\delta^{13}C$ E-AAs values for *Acartia* and seston (separately) Zuur et al. (2013).

Results

Bulk $\delta^{13}C$ and $\delta^{15}N$ values and phytoplankton community composition

Low *Acartia* $\delta^{13}C$ bulk values (-26.1‰) were present in early summer followed by a late summer increase (-20.8‰) before declining again in fall (Fig. 1a). Bulk C isotope composition of seston showed a similar cycle to *Acartia* $\delta^{13}C$ values peaking in summer with values of -22.9‰ before declining to values of -26.9±0.06‰ in fall (Fig. 1a). *Acartia* $\delta^{13}C$ values correlated significantly with seston $\delta^{13}C$ values at lag zero (spearman's rho=0.52, $p<0.01$, df:15). Differences between *Acartia* and seston $\delta^{13}C$ values varied between -1.7 to 3.9 (Fig. 1c), indicating that *Acartia* does not assimilate diet components broadly represented in the seston $\delta^{13}C$ values.
Acartia bulk $\delta^{15}N$ values varied between 5.5-10‰ changing at similar times but in opposite direction to $\delta^{13}C$ bulk values, with lowest values in late summer (Fig. 1b). Similar seasonal fluctuations were present in seston N isotope composition varying from 2.3‰ to 6.4‰ (Fig. 1b). Seston and *Acartia* $\delta^{15}N$ significantly correlated (spearman's rho=0.62 , $p<0.01$, df:15)

with relative differences between $\delta^{15}N$ values of *Acartia* and seston varying between 1.7 and 4.7, increasing from day 161 to late fall (Fig. 1c). The increasing difference between *Acartia* and seston N isotope composition could indicate either increasing trophic position or a greater mismatch between *Acartia* diet uptake and seston.
The phytoplankton taxonomic composition expressed as percent C varied temporally during the season, with diatoms abundant in spring followed by an increase of the photosynthetic ciliate *Mesodinium rubrum* and dinoflagellates (Table 2). In summer a bloom of cyanobacteria, mainly *Nodularia spumegina* and *Aphanizomenon* spp. was followed by a second increase of dinoflagellates. In autumn dinoflagellates decreased while prymnesiophyceae and *M. rubrum* increased. Throughout the annual cycle a mixture of chlorophytes, chrysophytes, euglenophytes and unidentified species persisted (grouped as other algae), contributing between 2.85 and 25.66 % of total phytoplankton.

Seasonal changes in AA-CSIA

Acartia $\delta^{13}C$ E-AA values separated into three significant seasonal clusters (PERMANOVA, model F: 28.99, $p<0.01$,df =18): early summer (dates 116-172), late summer (dates 186-256) and fall (dates 270-340, Table 1). In contrast, no significant seasonal clusters were observed for seston $\delta^{13}C$ E-AA values (PERMANOVA, model F: 2.37, p=ns, df = 17).
Difference in absolute values between individual *Acartia* E-AAs $\delta^{13}C$ values and seston E-AAs $\delta^{13}C$ values of Ile (ranging from -4.38 to 4.68‰), Leu (-3.97 to 4.00‰) and Val (-11.31 to 0.24‰) showed three seasonal phases, with high values in early summer, lower values in late summer and increased values in fall (Fig. 2), similar to the cluster analysis. Differences in *Acartia* and seston $\delta^{13}C$ Phe values (-6.49 to 4.37‰,) were relatively constant around -5‰ until an increase from Julian day 270. The three seasonal phases were caused primarily by the Acartia $\delta^{13}C$ E-AA values, while seston $\delta^{13}C$ E-AA values instead showed a more or less continuous seasonal increase (data not shown).

DFA of $\delta^{13}C$ *Acartia* and seston E-AA values

Acartia and seston DFA models showed distinct differences in seasonal patterns. The most parsimonious *Acartia* DFA model included two common trends and a diagonal and unequal covariance matrix (AICc: 188.34, Fig. 3a-b). All time series of the $\delta^{13}C$ AA values were explained well by the final *Acartia* DFA model (r^2=0.73-0.99). The first trend showed three clear phases during the seasonal cycle, with positive values in early summer (dates 116-172), followed by negative values in late summer (dates 186-256) and again high values in fall (dates 186-256). The first trend was driven positively by factor loadings of the Ile, Leu, Phe and Val $\delta^{13}C$ values. The second trend, showing a continuous seasonal increase, was driven mainly by Lys and Phe. *Acartia* DFA results were not affected by the removal of the $\delta^{13}C$ Lys values time series (and thus directly comparable to the seston DFA). The most parsimonious seston DFA model included one common trend and a diagonal and unequal covariance matrix (AICc: 194.68, Fig. 3c). The common seston trend increased positively, except with a slight decrease from day 210 to day 285 with positive factor loadings of Ile, Leu and Phe. $\delta^{13}C$ values of Ile, Leu and Phe all fitted well with the final seston DFA model (r^2=0.50-0.99). Contrarily, Val only showed a weak relationship with the common trend (r^2=0.01), indicating that variation in the isotope composition of Val was poorly described by the seston DFA model. The inclusion of a diagonal and unequal covariance matrix, present for both *Acartia* and seston models, indicated that observational (i.e. analytical) error differs between $\delta^{13}C$ E-AA values.

Linking AA-CSIA to phytoplankton composition

The most parsimonious RDA model used to associate variation in phytoplankton composition with the E-AA $\delta^{13}C$ values showed a strong fit, with the phytoplankton explaining 74.6% of the total variance of the *Acartia* E-AA $\delta^{13}C$ values (adj. r^2= 0.64, $F_{(1,18)}$=7.26, p<0.01, Fig. 4a). The first and second RDA axes significantly explained 59.4% and 12.3% of the constrained variance, respectively (p<0.01). The *Acartia* RDA model separated the data in the same three distinct groups as partitioned by the Hierarchal cluster analysis. The final model included 5 phytoplankton groups as predictor variables with dinoflagellates explaining 35% of the constrained variance (adj. r^2:0.30, p<0.01), while 13% of the variance was explained by diatoms (adj. r^2:0.12, p=0.01), 9.5% by cryptophytes (adj. r^2:0.08, p=0.01), 8.4% by prasinophyceae (adj. r^2:0.07, p=0.03) and 7.5% by cyanobacteria (adj. r^2:0.06, p=0.04). The five significant phytoplankton dietary sources comprised seasonally between 19.7% and 81.4 % of the total phytoplankton composition (Table 2). The unconstrained component of the model (i.e. variation not explained by the phytoplankton composition) accounted for only 26.4% of the total variance.

The final RDA model for the seston E-AA $\delta^{13}C$ values and phytoplankton composition included groups of cyanobacteria, cryptophytes and prasinophyceae and explained only 35% of the total variance (adj. r^2:0.21, $F=2.47_{(1,17)}$, p=0.04 , Fig. 4b), with a significant first RDA axis explaining 23.4% of the variance (p=0.01). Even though the three phytoplankton groups were included in the most parsimonious model, no individual phytoplankton group significantly explained enough variance of the constrained component for seston (9.7%-13.3%, r^2: 0.06-0.08, p=0.08-0.15). These three phytoplankton groups comprised only between 3.1 and 47.1 % of the total phytoplankton composition throughout the year (Table 2). Instead the unconstrained component in the RDA model explained the majority of the total variance (65%), indicating that the majority of the variance in the seston E-AA $\delta^{13}C$ values is accredited to other factors than the phytoplankton composition.

Conclusion and future perspectives

The high temporal sampling frequency employed successfully captured rapid changes in both seston and zooplankton isotope composition. *Acartia* $\delta^{13}C$ E-AA values seemed to encode seasonal variation from a range of putative dietary sources, supporting application of $\delta^{13}C$ E-AA values as a sound method to study consumer resource assimilation. Selective feeding by consumers, as shown here for *Acartia* stresses the importance of critically evaluating isotope baseline information prior to inferring organismal trophic position. The seasonal increase in differences between *Acartia* and seston $\delta^{15}N$ values could indicate elevated zooplankton trophic position, for example through increased feeding on protists (Stoecker & Egloff 1987, Mitra et al. 2013). However, the preferential feeding pattern apparent in the $\delta^{13}C$ E-AA values indicate that using seston to infer isotope baseline information may be misleading, something also noted in bulk isotope studies of other preferential zooplankton feeders

.

Feeding on prey items of different nutritional quality also influences the biochemical composition of consumers themselves. In turn, seasonal changes in the nutritional quality of zooplankton propagate to higher trophic level predators (Möllmann et al. 2004) and consequently change nutritional flows across aquatic food webs (Winder & Jassby 2011). Realizing that energy flows across the phytoplankton-zooplankton interface are not

temporally or spatially static should motivate future work on measuring zooplankton resource assimilation in order to retrieve accurate information on ecosystem energy dynamics.

References

Möllmann C, Kornilovs G, Fetter M, Köster F (2004) Feeding ecology of central Baltic Sea herring and sprat. Journal of fish biology 65:1563-1581

Winder M, Jassby AD (2011) Shifts in zooplankton community structure: implications for food web processes in the upper San Francisco Estuary. Estuaries and Coasts 34:675-690

Zuur AF, Fryer R, Jolliffe I, Dekker R, Beukema J (2003) Estimating common trends in multivariate time series using dynamic factor analysis. Environmetrics 14:665-685

Table legends

Table 1 *Acartia* and seston essential amino acid $\delta^{13}C$ values of, Isoleucine, Leucine, Lysine (only *Acartia*). Julian date note the number of days since the start of the year 2012. *Acartia* clusters, denote significantly different clusters as partitioned by the Hierarchical cluster analysis (PERMANOVA, model F: 28.99, $p<0.01$,df =18).

	Acartia	*Acartia* essential amino acid $\delta^{13}C$ values					Seston essential amino acid $\delta^{13}C$ values			
Julian date	clusters	Ile	Leu	Lys	Phe	Val	Ile	Leu	Phe	Val
116	1	-25.58	-35.73	-27.25	-31.78	-31.14	-30.26	-37.30	-28.29	-31.17
137	1	-26.27	-34.25	-25.30	-32.26	-29.31	-27.52	-36.06	-25.11	-30.06
145	1	-24.72	-31.98	-24.95	-31.91	-29.07	-26.02	-35.03	-26.11	-29.16
150	1	-24.45	-33.91	-25.36	-33.88	-29.13	-27.90	-36.54	-26.77	-33.50
161	1	-26.68	-32.53	-28.11	-32.20	-28.64	-27.54	-35.72	-27.00	-23.86
172	1	-23.45	-30.34	-27.92	-33.32	-29.84	-26.32	-34.25	-25.68	-30.52
186	2	-27.23	-35.00	-21.44	-31.97	-31.46	-26.99	-34.39	-26.83	-35.63
199	2	-26.41	-32.67	-21.87	-31.70	-33.09	-27.42	-33.84	-24.41	-33.45
214	2	-27.99	-34.43	-24.60	-32.56	-35.10	-25.28	-33.46	-26.24	-31.23
228	2	-29.65	-36.20	-23.26	-35.86	-36.43	-26.24	-32.24	-24.54	-29.94
242	2	-25.96	-33.04	-22.60	-30.95	-33.76	-25.12	-33.38	-26.01	-30.44
248	2	-28.40	-35.72	-25.57	-31.47	-34.19	-24.02	-33.32	-26.20	-29.86
256	2	-28.42	-35.73	-24.00	-33.14	-34.99	-26.42	-34.60	-26.07	-31.36
270	3	-21.76	-29.42	-21.36	-25.47	-26.22	-24.83	-33.42	-25.71	-30.28
285	3	-24.67	-32.31	-21.22	-28.24	-27.48	-28.13	-35.46	-26.87	-30.84
298	3	-21.84	-29.65	-20.93	-25.77	-26.82	-25.87	-33.32	-25.51	-30.99
312	3	-23.90	-31.58	-20.63	-26.41	-26.26	-27.18	-32.99	-25.76	-30.11
318	3	-22.45	-30.53	-21.48	-25.10	-26.81	-25.21	-31.88	-24.76	-27.89
340	3	-22.04	-30.21	-18.45	-26.89	-26.85	-25.97	-33.71	-	-30.29

Table 2 Phytoplankton taxa in percent carbon composition (% calculated from relative C ng /l) throughout the stable isotope sampling period, abbreviated as Cryp (cryptophytes), Cyan (cyanobacteria), Diat (diatoms), Dino (dinoflagellates), Meso (mesodinium), Pras

(prasinophyceae), Prym (prymnesiophyceae) and Other (comprised of chlorophytes, chrysophytes, euglenophytes and unidentified species). Julian date note the number of days of the year.

Phytoplankton percent carbon composition (%)								
Julian date	Cryp	Cyan	Diat	Dino	Meso	Pras	Prym	Other
116	5.58	0.00	10.68	43.60	14.64	21.49	0.04	3.97
137	1.23	1.22	1.69	16.79	64.13	0.60	0.03	14.30
145	2.95	0.18	1.23	26.57	47.57	8.39	0.16	12.95
150	1.96	0.53	0.70	25.17	33.18	6.63	19.80	12.02
161	0.98	0.89	0.17	23.77	18.79	4.87	39.44	11.10
172	1.17	13.15	0.21	27.08	11.43	1.56	40.64	4.76
186	1.91	40.76	0.35	33.59	14.05	4.39	1.58	3.38
199	10.83	10.42	0.00	55.18	4.29	4.95	5.56	8.77
214	6.77	17.65	0.85	36.71	3.72	3.05	20.17	11.08
228	7.41	27.48	1.15	19.56	5.57	12.22	22.64	3.98
242	20.49	2.82	1.96	37.41	9.96	6.50	12.13	8.72
248	22.30	1.55	1.43	39.38	11.91	8.13	6.22	9.07
256	24.11	0.28	0.90	41.34	13.87	9.77	0.31	9.42
270	17.15	0.26	14.59	16.71	20.29	4.24	1.10	25.66
285	21.71	0.13	1.53	14.74	13.13	6.82	35.86	6.08
298	14.30	1.81	15.78	14.48	17.64	6.40	26.95	2.64
312	13.10	0.91	9.41	8.25	34.97	4.58	16.96	11.82
318	11.91	0.00	3.04	2.02	52.31	2.75	6.97	21.01
340	26.05	0.30	3.93	15.18	31.18	1.46	6.82	15.09

Figure legends

Fig. 1 Seasonal dynamics of a) *Acartia* and seston $\delta^{13}C$ bulk values, b) $\delta^{15}N$ bulk values and c) and $\Delta^{13}C$ and $\Delta^{15}N$ (differences between C and N isotope composition of *Acartia* and seston). Julian date denote time of the year.

Fig. 2 Differences between *Acartia* and seston $\delta^{13}C$ E-AA values of Isoleucine (black), Leucine (red), Phenylalanine (blue) and Valine (green) for each Julian date.

Fig. 3 Dynamic factor analysis (DFA) estimated common trends for *Acartia* $\delta^{13}C$ E-AA values, a) the 1st trend, b) the 2nd trend, and c) the 1st and only trend estimated from the seston $\delta^{13}C$ E-AA values. Factor loadings in each plot denote the fit of individual $\delta^{13}C$ E-AA values relative to the common trend. DFA models of *Acartia* and seston were estimated from $\delta^{13}C$ values of Isoleucine, Leucine, Phenylalanine and Valine. Additionally for *Acartia* $\delta^{13}C$ Lysine values were also included. Julian date denotes the time of the year.

Fig. 4 Redundancy analysis (RDA) using $\delta^{13}C$ E-AA values for each Julian date as response variables and phytoplankton composition as predictor variables for a) *Acartia* and b) seston. Colours in both *Acartia* and seston plots denote seasonal groups of early summer (green),

late summer (red) and fall (blue), as partitioned from the *Acartia* hierarchal cluster analysis (PERMANOVA, model F: 28.99, $p<0.01$,df =18). Predictor variables of phytoplankton groups included in the final model are denoted by grey arrows, while scores for each E-AAs $\delta^{13}C$ values are shown in black.

Fig. 1

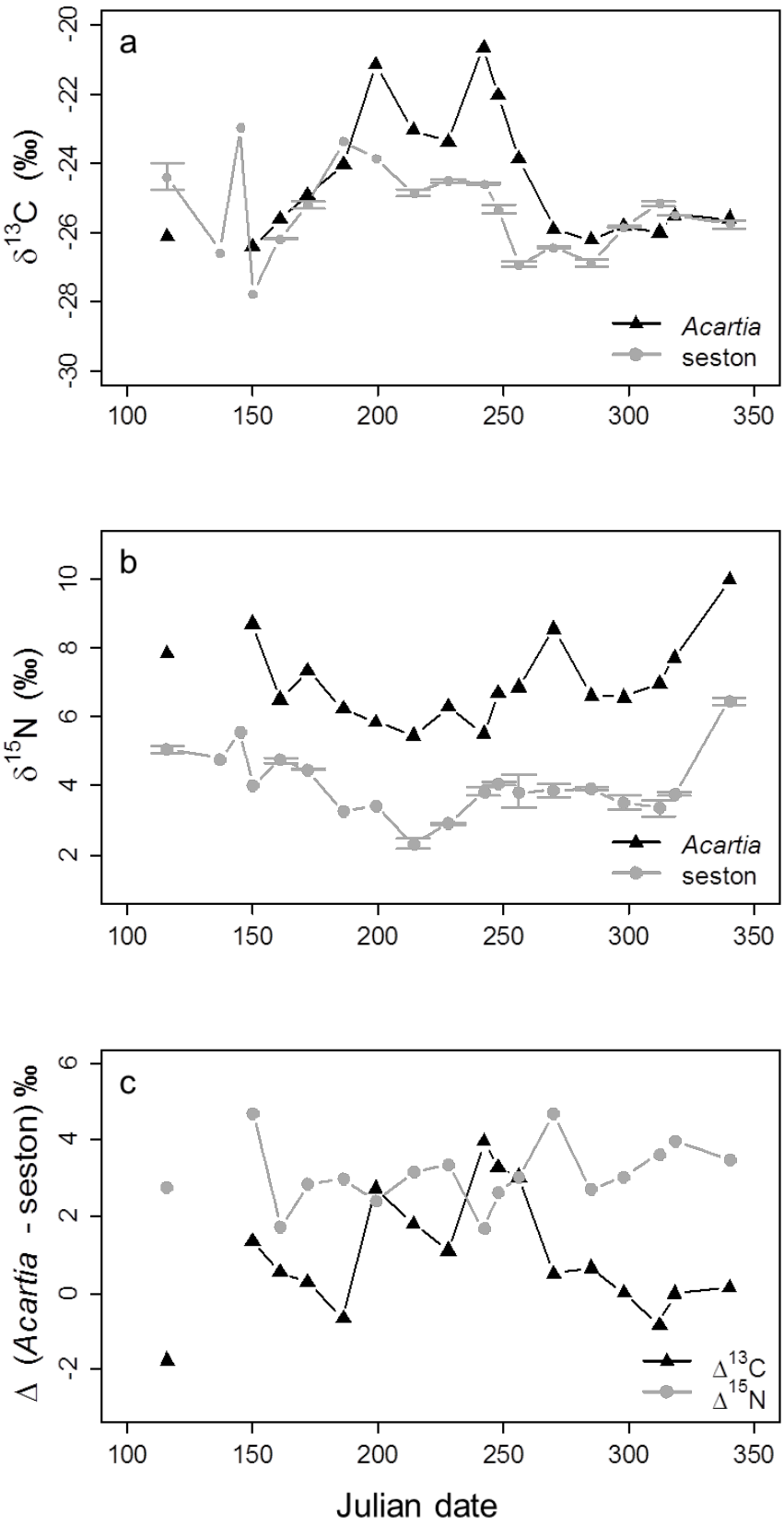
a
b
c
$\delta^{13}C$ (‰)
$\delta^{15}N$ (‰)
Δ (*Acartia* - seston) ‰
Acartia
seston
$\Delta^{13}C$
$\Delta^{15}N$
Julian date

Fig. 2

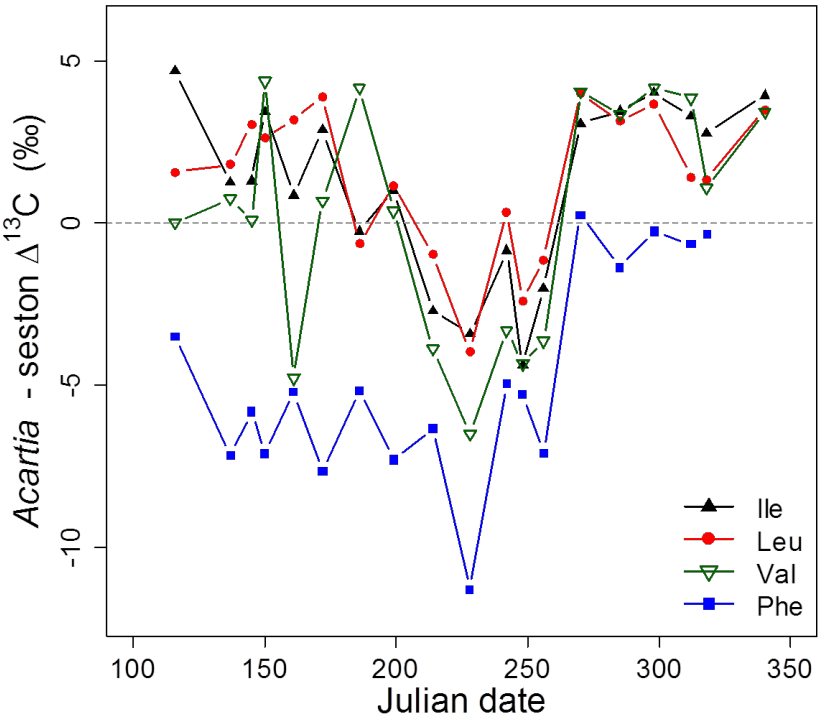
Acartia - seston Δ13C (‰)
5
0
-5
-10
100
150
200
250
300
350
Julian date
Ile
Leu
Val
Phe

Fig. 3

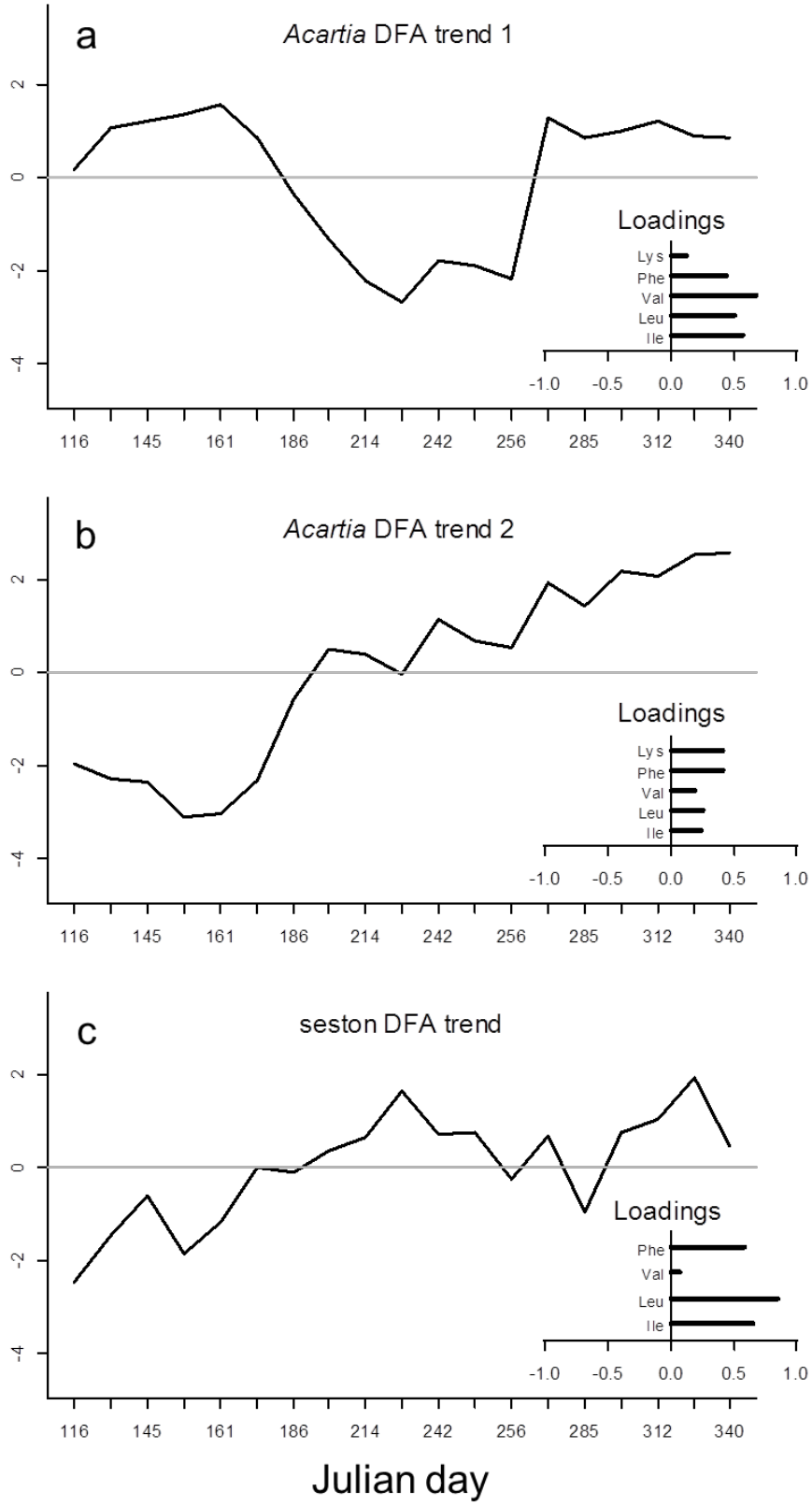
a
Acartia DFA trend 1
Loadings
Lys
Phe
Val
Leu
Ile
-1.0
-0.5
0.0
0.5
1.0
2
0
-2
-4
116
145
161
186
214
242
256
285
312
340
b
Acartia DFA trend 2
Loadings
c
seston DFA trend
Julian day

Fig. 4

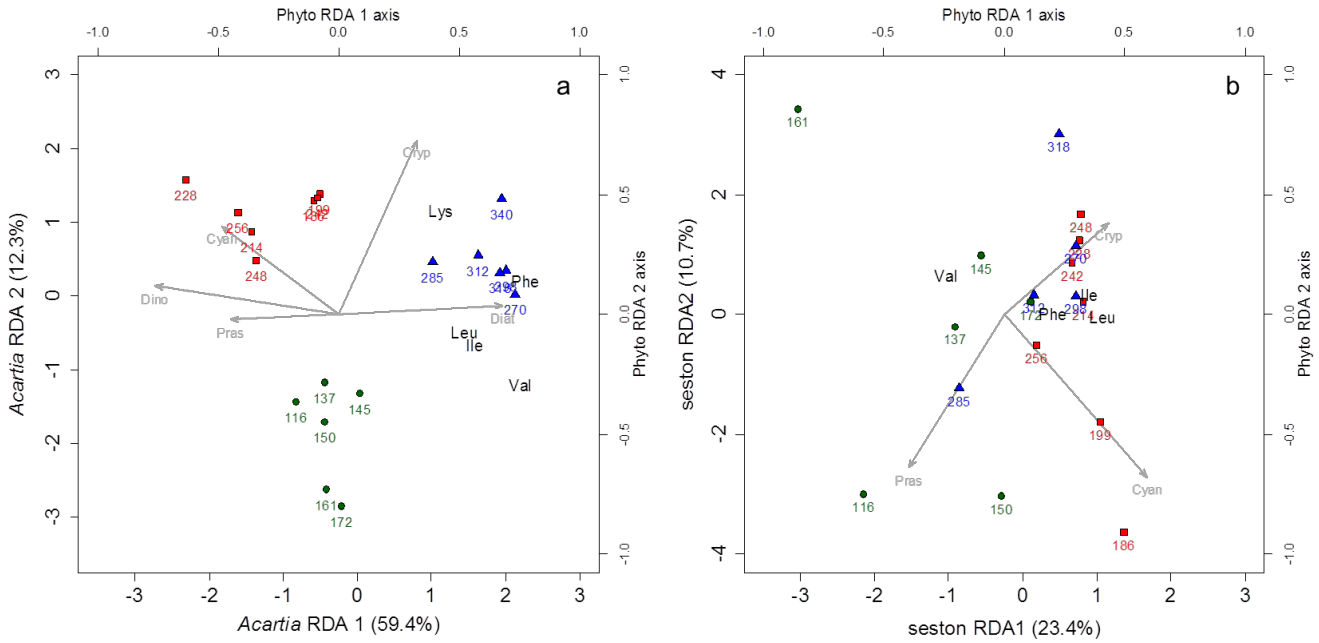
a
Phyto RDA 1 axis
Phyto RDA 2 axis
Acartia RDA 2 (12.3%)
Acartia RDA 1 (59.4%)
Cryp
Lys
Cyan
Dino
Pras
Diat
Phe
Leu
Ile
Val
b
seston RDA2 (10.7%)
seston RDA1 (23.4%)

Fig. 5

APPENDIX IV

JPR Advance Access published January 8, 2015

Journal of
Plankton Research

plankt.oxfordjournals.org

J. Plankton Res. (2015) 0(0): 1–13. doi:10.1093/plankt/fbu109

Stoichiometric regulation in micro- and mesozooplankton

ANNA-LEA GOLZ, ALFRED BURIAN AND MONIKA WINDER*
DEPARTMENT OF ECOLOGY, ENVIRONMENT AND PLANT SCIENCES, STOCKHOLM UNIVERSITY, 10691 STOCKHOLM, SWEDEN

*CORRESPONDING AUTHOR: monika.winder@su.se

Received September 3, 2014; accepted December 14, 2014

Corresponding editor: Roger Harris

Aquatic ecosystems experience large natural variation in elemental composition of carbon (C), nitrogen (N) and phosphorus (P), which is further enhanced by human activities. Primary producers typically reflect the nutrient ratios of their resource, whose stoichiometric composition can vary widely in conformity to environmental conditions. In contrast, C to nutrient ratios in consumers are largely constrained within a narrow range, termed homeostasis. In comparison to crustacean zooplankton, less is known about the ability of protozoan grazers and rotifer species to maintain stoichiometric balance. In this study, we used laboratory experiments with a primary producer (*Nannochloropsis* sp.), three different species of protozoan grazers and one mesozooplankton species: two heterotrophic dinoflagellates (*Gyrodinium dominans* and *Oxyrrhis marina*), a ciliate (*Euplotes* sp.) and a rotifer (*Brachionus plicatilis*) to test the stoichiometric response to five nutrient treatments. We showed that the dependency of zooplankton C:N:P ratios on C: nutrient ratios of their food source varies among species. Similar to the photoautotroph, the two heterotrophic dinoflagellates weakly regulated their internal stoichiometry. In contrast, the strength of stoichiometric regulation increased to strict homeostasis in both the ciliate and the rotifer, similar to crustacean zooplankton. Our study further shows that ciliate and rotifer growth can be constrained by imbalanced resource supply. It also indicates that these key primary consumers have the potential to trophically upgrade poor stoichiometric autotrophic food quality for higher trophic levels.

KEYWORDS: homeostasis; nutrient limitation; heterotrophic dinoflagellate; ciliate; rotifer

INTRODUCTION

Aquatic ecosystems experience large variability in the amount of available nutrients, such as carbon (C), nitrogen (N) and phosphorus (P) on account of natural environmental factors and human activities (Gruber and Galloway, 2008; Taylor and Townsend, 2010). Variation in C:N:P stoichiometry consequently affects the C-to-nutrient ratio available for primary producers. Autotrophic organisms, such as phytoplankton and vascular plants have relatively weak stoichiometric homeostasis regulation capacity and typically reflect the elemental

available online at www.plankt.oxfordjournals.org

ratios of their resource (Sterner *et al.*, 1992; Persson *et al.*, 2010). Thus, their elemental composition can vary considerably among ecosystems, depending on mineral nutrients availability as well as CO_2 and solar radiation (Sterner *et al.*, 1992; Meunier *et al.*, 2014). Additionally, the stoichiometric match of the nutrient supply ratio and primary producer depends on the state of the growth phase, with weak regulation capacity at low growth rate and less stoichiometric variation within a narrower range at high growth rate (Ågren, 2008; Hillebrand *et al.*, 2013; Meunier *et al.*, 2014). The physiological plasticity in elemental composition of primary producers affects their quality as a food resource for heterotrophic herbivores, which require uptake of macronutrients from their prey for metabolic growth. In contrast to primary producers, elemental ratios of heterotrophs are generally more constrained within a relatively narrow taxon- and stage-specific range (Sterner and Elser, 2002; Persson *et al.*, 2010). While this generalized framework holds across many autotrophic and heterotrophic organisms, the degree of homeostasis varies widely as a function of species composition and environmental conditions (Hessen *et al.*, 2013). Regulation of elemental composition and nutrient cycling has been well demonstrated for crustacean zooplankton, particularly for cladocerans and copepods (Kiørboe *et al.*, 1985; Sterner, 1993). However, comparatively little is known about whether microbe zooplankton (protozoa and rotifers), which play a key function in pelagic food web processes (Landry and Calbet, 2004), maintain stoichiometric balance similar to crustacean plankton.

The degree of maintaining constant elemental ratios has important consequences for consumer–resource interactions, the supply of elemental composition to upper trophic levels and for nutrient recycling. While C is an important element of organic macromolecules, N and P are important compounds for specific macromolecules. P is an essential building block for RNA, phospholipids and DNA, and N for proteins (amino acids) and nucleic acids (Sterner and Elser, 2002; Hessen and Anderson, 2008). Consumers have developed physiological mechanisms to maintain homeostasis (Frost *et al.*, 2005), such as adjusting net assimilation or excretion of elements to match metabolic and somatic requirements. Even though the benefits of homeostasis are not clearly understood, it is thought to be more common in heterotrophs due to their high energetic requirements for nutrient storage (Persson *et al.*, 2010). Heterotrophic organisms have to build N and P into complex macromolecules such as amino acids, proteins or polyphosphates, which require high amounts of C as a structural component (Persson *et al.*, 2010). Therefore, accumulation of N and P in heterotrophic organisms might be constrained when C is limited, which in turn would keep their body C:N and C:P ratios relatively constant (Persson *et al.*, 2010).

The degree of mismatch between the C:nutrient ratios of consumers and their prey will further determine internal nutrient recycling and the elemental nutrient quality for higher trophic levels, which is a key determinant for trophic efficiency. Deviations in the elemental food resource ratio from a consumer requirement may constrain growth fitness of herbivores, which may propagate up the food chain (Hessen *et al.*, 2013). However, homeostasis in food chains also means that food quality effects are buffered in primary consumers and not transferred to higher trophic levels (Saikia and Nandi, 2010), and thus dampen the effect of nutritional imbalances on primary producers. For example, protists have the potential to transfer bacterial C into a better quality food resource for zooplankton and may fuel higher trophic levels through trophic upgrading and repacking within the microbial loop (Faithfull *et al.*, 2011). Utilization of bacteria by protozoans can further substitute potentially limiting nutrients, particularly P, that are often several orders of magnitude more concentrated in bacteria than in the dissolved phase (Faithfull *et al.*, 2011). While the role of heterotrophic microbes for trophic upgrading biochemical compounds is highly species-specific, their elemental composition may be less variable as a consumer's demand for N relative to P is generally homeostatic (Sterner and Elser, 2002).

Microbial zooplankton such as heterotrophic nanoflagellates, ciliates and rotifers are a primary link of carbon and nutrient transfer from bacteria and small-sized primary producers to mesozooplankton (Stoecker and Capuzzo, 1990). Due to their high metabolic rates and short generation times, microbial zooplankton play a central role in the pelagic food web for grazing, secondary production and likely nutrient regeneration (Landry and Calbet, 2004). The goal of our study is to investigate the homeostatic ability in terms of C:N:P ratios of microbial zooplankton (protozoa and rotifers) and inter-taxonomic variability. We cultured two heterotrophic dinoflagellates, one ciliate and one rotifer species under varying nutrient ratios (i.e., different food quality regimes) and compared our results of homeostasis regulation with published literature on micro- and mesozooplankton species.

METHOD

Experimental design and nutrient manipulation

The marine Eustigmatophyte, *Nannochloropsis* sp., was cultured as food source under five different nutrient regimes from low N (4:1 N:P; N_{Low}) to medium N (10:1 N:P;

N_{Med}) and replete (20:1 N:P ratio; $NP_{Repl.}$) as well as low and medium P (P_{Low}: 205:1; P_{Med}: 102:1 N:P) levels, respectively (for concentrations see Table I). This primary producer was chosen as food source because of its relatively high food quality and small size to facilitate separation from the consumer. *Nannochloropsis* sp. was grown in artificial seawater (salinity of 20) enriched with f/2 medium following Guillard and Ryther (1962) and Guillard (1975), while the N and P concentrations were doubled following the original f medium (Guillard and Ryther, 1962). To ensure a stable nutrient regime, the algae were cultured in continuous flow through systems (chemostats). The dilution rate for the nutrient-limited treatments was set to 0.15 d^{-1} and to 0.36 d^{-1} in the replete (control) treatment to account for higher growth rates. The density and stability of the chemostat cultures was assessed by daily measurements of carbon concentrations based on photometric light extinctions (at 750, 664, 647, 630 nm) using carbon-extinction equations determined from dilution series. Four zooplankton species were chosen as grazers due to their common occurrence in natural systems and for use in aquaculture: two heterotrophic dinoflagellates *Gyrodinium dominans* and *Oxyrrhis marina* Dujardin 1841 (SCCAP K-175), the ciliate *Euplotes* sp., and the rotifer *Brachionus plicatilis* (L-strain). Stock cultures were reared under replete conditions at 18°C and a 12:12 light:dark cycle.

The experiment was carried out in glass culturing flasks filled with 500 mL of the nutritionally manipulated artificial seawater. Prior to transferring the heterotrophic organisms into the experimental containers, they were washed through plankton-nets with a mesh size of 10 μm for the heterotrophic dinoflagellates and 20 μm for the ciliate and the rotifer. The separation procedure worked well since the algae were 3 μm and the heterotrophic dinoflagellates 14–20 μm, the ciliate 98 μm, and the rotifer 260 μm in size. Zooplankton were fed with chemostat-grown food algae at a target value of 1 mg C L^{-1} and at the same temperature and light regimes as the stock cultures. The experiment was designed as a full-factorial design, where each treatment was set up in triplicate over 6 d. The food concentrations were kept constant by measuring the carbon content of aliquots every 24 h using the photometric light extinction described above, and by inoculating each replicate with fresh medium and food.

Table I: Nitrogen to phosphorus (N:P) molar supply ratios and N and P concentration in the culture medium used to grow Nannochloropsis *sp. for the different nutrient treatments*

Treatments	N:P supply ratio	N (μmol L^{-1})	P (μmol L^{-1})
N_{Low}	4	297	72
N_{Med}	10	742	72
$NP_{Repl.}$	20	1484	72
P_{Med}	102	1484	14
P_{Low}	205	1484	7

Low and Med refers to low and medium N and P limitation, respectively, Repl. refers to replete NP nutrient concentration.

At the end of the experiment, the zooplankton were washed with artificial seawater through plankton-nets and kept in food and media-free artificial seawater for at least 1 h to ensure food vacuole/gut clearance. While we assume that most of the food should have been digested during this time, we cannot exclude the possibility that this procedure has not fully cleared all food particles in the vacuoles or gut. Thus, our results resemble natural field conditions, as consumers typically do not differentiate between the organisms and particles left in the digestive track. Food algae and zooplankton of each treatment were filtered onto pre-combusted Whatman GF/F filters for elemental analysis. Particulate C and N were measured using a CHN Analyzer (LECO CHNS-932). Particulate P was analyzed by combusting the samples at 500°C in the presence of $MgSO_4$ and KNO_3 followed by a digestion in an acid persulfate solution ($K_2S_2O_8$). The amount of phosphate was determined by Segmented Flow Analysis (ALPKEM O. I. Analytical Flow Solution IV, modified method # 319528). All nutrient ratios are reported as molar elemental ratios.

Population growth rates were calculated for *Euplotes* sp. and *B. plicatilis* under replete and nutrient-limited conditions by taking subsamples at the first and last (sixth) day of each experiment. Population density of both species and lorica length and width of *B. plicatilis* were measured by microscopic counts, using an inverted microscope following Utermöhl (1958). Population growth rates were calculated as $\ln(T_6 - T_1)$/time, where T_1 and T_6 are the abundances at Days 1 and 6, respectively, and time is the experimental duration of 6 days.

Cell and vacuole biovolume of *Euplotes* sp. for nutrient-limited treatments were calculated from cell length and width as well as vacuole diameter measurements from photographs of preserved specimen using ImageJ (Rasband 1997–2014). The geometric form of a rational ellipsoid was used for cell and a sphere for vacuole biovolume following Olenina *et al.* (Olenina *et al.*, 2006). Biovolumes for *Euplotes* sp. grown under replete conditions were not measured because vacuoles were either absent or not prominent enough. Lorica biovolume (v) of *B. plicatilis* was calculated as $v = 0.52 \times a \times b \times c$; where 0.52 is a constant; a, b and c, are length, width and depth ($c = 0.4 \times a$), respectively (McCauley, 1984), which takes into account that cell dimensions change disproportionately during growth according to Kennari *et al.*

(Kennari *et al.*, 2008). The geometric shape of a sphere was used to calculate egg biovolume.

Data analysis

One-way analysis of variance (ANOVA) and Tukey's HSD post hoc tests were used to assess differences in stoichiometric, growth rate and biovolume responses among experimental treatments. Data were either log- or square root transformed to satisfy equal variance and normality assumptions.

To describe the relationship between the nutrient ratios of the resource and the consumers we applied a homeostatic regulation coefficient model using a linear relationship between the consumer and resource stoichiometry. A slope equal to or >1 indicates poor homeostasis, while a slope approaching 0 indicates homeostatic regulation. The homeostatic regulation coefficient H is calculated as 1/slope. The stoichiometric regulation is proportional to H, as an increasing value indicates stronger stoichiometric regulation of internal elemental composition (Sterner and Elser, 2002). The culture medium was used for *Nannochloropsis* sp.'s resource stoichiometry while *Nannochloropsis* sp. was the resource for the zooplankton species. Statistical analyses were performed using the R software environment 2.14.1 (R Core Team, 2012).

RESULTS

Elemental composition

N:P ratios of *Nannochloropsis* sp. mirrored N:P ratios of its resource, the nutrient manipulated media (Fig. 1, Table I).

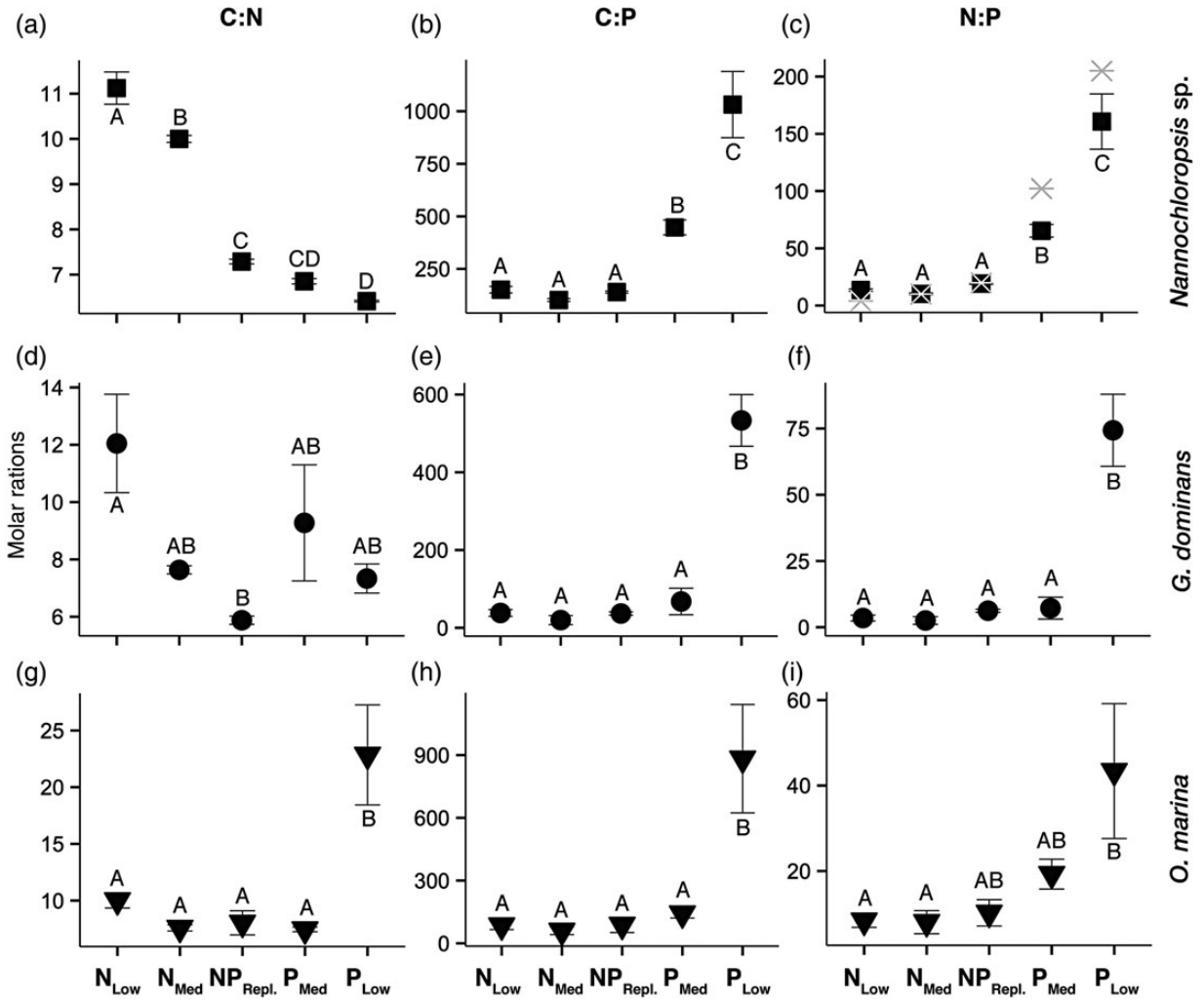

Fig. 1. Mean molar (μmol) C:N, C:P and N:P ratios (±SE) of the algae *Nannochloropsis* sp. (**a**–**c**), and the dinoflagellates *Gyrodinium dominans* (**d**–**f**) and *Oxyrrhis marina* (**g**–**i**) across the five nutrient treatments (Low and Med refers to low and medium N and P limitation, respectively, Repl. refers to replete NP nutrient concentration). Letters from A–D indicate significant differences among treatments and the grey crosses in c indicate the medium supply ratios.

The replete C:N molar ratio of *Nannochloropsis* sp. was 7.3 and increased significantly to 10 and 11 at N_{Med} and N_{Low}, respectively, and decreased slightly at P_{Med} and P_{Low} (Fig. 1). The replete C:P ratio was 140 and was not affected by N limitation, and increased up to 3.3 times at P_{med} and 7.4 times at P_{Low}. *Nannochloropsis* sp. reached a N:P ratio of 19 under replete nutrient levels, which was slightly lower in the N-limited treatments and increased to 65 and 161 at P_{Med} and P_{Low}, respectively. Similar trends between nutrient treatments were observed in the absolute elemental composition, with lowest average nutrient concentrations (N and P) in the corresponding nutrient-limited treatments (Table II).

C:N ratios of the heterotrophic dinoflagellate *G. dominans* reared on N_{Low} algae increased from the $NP_{Repl.}$ treatment of 5.9−12 and were not affected by P_{Med} and N limitation (Fig. 1d). Similar to the food resource, C:P ratios of *G. dominans* were not affected by N limitation with an average C:P value of 35, but C:P increased from 37 in the $NP_{Repl.}$ to 68 and 533 at P_{Med} and P_{Low}, respectively. The N:P ratio of *G. dominans* reflected their higher sensitivity to P limitation, which increased from 6 to 7 and 74 at $NP_{Repl.}$, P_{Med} and P_{Low}, respectively (Fig. 1f). Similar to their food resource, average absolute elemental concentrations of N and P were lowest when *G. dominans* was reared on N and P limited algae, respectively (Table II). Similar to *G. dominans*, nutrient ratios of the heterotrophic dinoflagellate *O. marina* were most strongly affected by P limitation (Fig. 1g−i) and their N:P ratio increased 2- and 4-fold at P_{Med} and P_{Low} from 10.2 at $NP_{Repl.}$. Surprisingly, their C:N ratio quadrupled at P_{Low} compared with the other nutrient treatments. A comparable pattern was observed in the absolute nutrient concentrations, and the P_{Low} treatment had the lowest average N concentration (Table II).

Elemental ratios of the ciliate *Euplotes* sp. were not affected by the stoichiometric ratios of their food (Fig. 2a−c). Both C:N and C:P ratios tended to be higher in the nutrient-limited treatments compared with the control, although differences were not significant. Similarly, the rotifer *B. plicatilis* was marginally affected by the stoichiometric ratios of their food (Fig. 2d−f). C:N ratios increased when reared on N_{low} and P_{low} algae within a narrow range (from 5 to 5.5 and 5.4, respectively), and both C:P and N:P ratios of *B. plicatilis* were higher at N_{Med} compared with all other treatments, which was however not significantly different (Table III).

Homeostatic regulation

The relationship between the nutrient ratios of the resource (nutrient manipulated media and food algae) and the corresponding consumers (algae and zooplankton) was satisfactorily explained by the homeostatic regulation coefficient model. *Nannochloropsis* sp. weakly regulated its internal N:P ratio over varying resource ratios, indicated by the low $H_{N:P}$ coefficient ($H = 1.5$, Table IV, Fig. 3). Similarly, H indicated weak internal stoichiometric regulation for the heterotrophic dinoflagellates, *G. dominans* and *O. marina*, with coefficient values <1.8 (Table IV). In contrast, both the ciliate, *Euplotes* sp. and the rotifer, *B. plicatilis* strongly regulated their internal stoichiometry as indicated by their higher $H_{N:P}$ values of 4.8 and 69, respectively (Fig. 3, Table IV). H coefficients showed that both *Euplotes* sp. and *B. plicatilis* regulated N more strongly compared with P ($H_{C:N} = 53$ and 23.5; $H_{C:P} = 3.4$ and

Table II: Algae and zooplankton stoichiometric composition in the replete (Repl.), low (Low) and medium (Med) nitrogen (N) and phosphorus (P) treatments

Treatment	Nutrient	*Nannochloropsis* sp. (ng μg DW^{-1})	*G. dominans* (ng μg DW^{-1})	*O. marina* (ng μg DW^{-1})	*Euplotes* sp. (ng μg DW^{-1})	*B. plicatilis* (ng μg DW^{-1})
N_{Low}	C	76.62 ± 9.34	41.42 ± 2.56	86.07 ± 4.89	136.55 ± 43.37	239.07 ± 40.08
	N	8.00 ± 0.79	4.15 ± 0.54	10.04 ± 0.33	28.27 ± 8.69	50.30 ± 8.24
	P	1.30 ± 0.03	3.22 ± 0.92	2.85 ± 0.52	6.52 ± 0.73	8.97 ± 0.63
N_{Med}	C	123.34 ± 5.55	35.85 ± 6.72	35.14 ± 4.07	258.10 ± 37.40	395.49 ± 9.06
	N	14.39 ± 0.74	5.51 ± 1.08	5.46 ± 0.83	52.20 ± 6.83	91.24 ± 2.98
	P	3.14 ± 0.08	9.95 ± 4.71	1.68 ± 0.28	10.06 ± 2.05	8.83 ± 0.30
$NP_{Repl.}$	C	168.66 ± 6.88	37.96 ± 14.80	55.71 ± 5.25	207.72 ± 43.41	276.58 ± 18.19
	N	26.97 ± 0.94	7.69 ± 3.17	8.29 ± 1.09	44.83 ± 8.28	64.32 ± 4.59
	P	3.11 ± 0.04	2.91 ± 1.29	2.28 ± 0.79	23.84 ± 9.44	16.34 ± 6.77
P_{Med}	C	339.88 ± 21.91	16.98 ± 3.48	18.12 ± 7.81	262.51 ± 11.14	346.43 ± 85.13
	N	57.83 ± 3.74	2.20 ± 0.42	2.80 ± 1.16	54.03 ± 2.97	77.65 ± 18.72
	P	1.97 ± 0.10	1.63 ± 1.06	0.35 ± 0.16	7.06 ± 1.61	10.01 ± 2.67
P_{Low}	C	161.52 ± 12.42	54.06 ± 2.46	87.95 ± 14.22	131.15 ± 34.85	204.91 ± 62.05
	N	29.37 ± 2.23	8.66 ± 0.62	4.64 ± 0.53	26.83 ± 7.24	44.60 ± 13.78
	P	0.42 ± 0.06	0.27 ± 0.03	0.32 ± 0.12	5.87 ± 3.28	6.19 ± 1.45

Mean C, N and P concentrations per dry weight were calculated at the end of the experiment ($n = 3$, SE < 0.01).

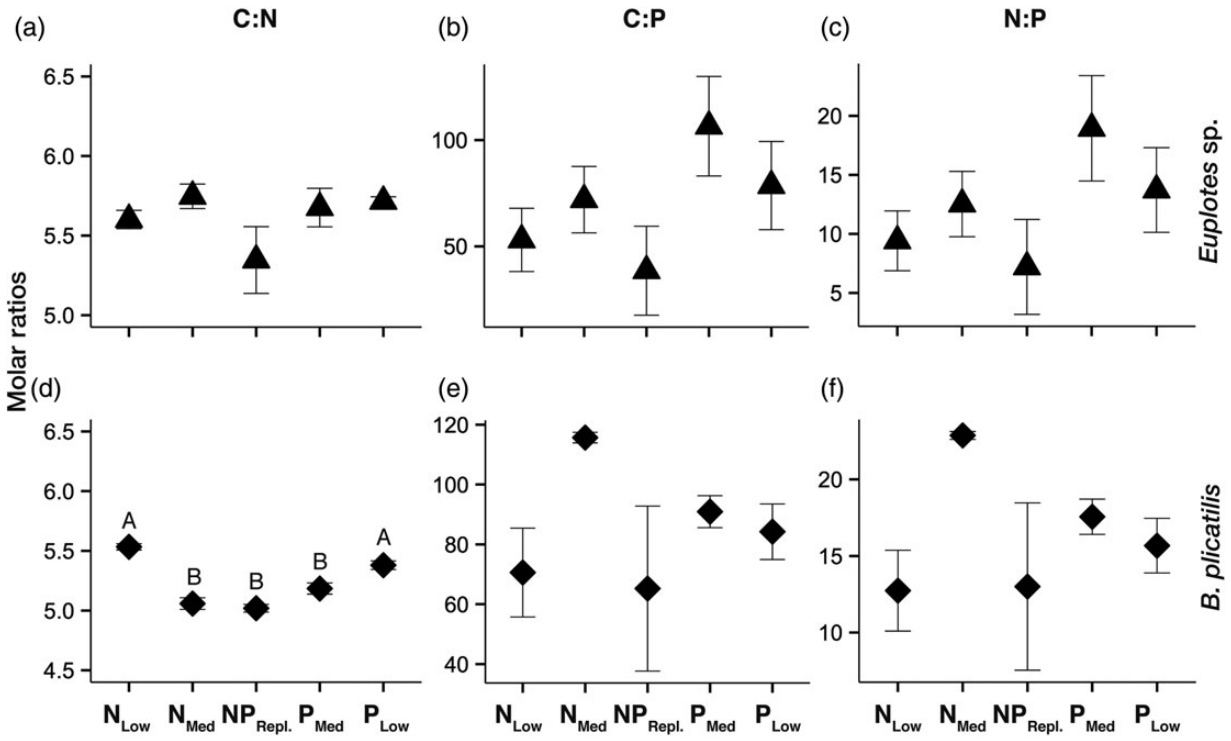

Fig. 2. Mean molar (μmol) C:N, C:P and N:P ratios (±SE) of the ciliate *Euplotes* sp. (**a**–**c**) and the rotifer *Brachionus plicatilis* (**d**–**f**) across the five nutrient treatments. For abbreviations see legend Fig. 1. Letters from A–B indicate significant differences among treatments.

Table III: Overview of published zooplankton and prey phytoplankton C:N, C:P and N:P molar ratios under varying experimental nutrient conditions

	Microzooplankton				Food				
Treatment	Species	C:N	C:P	N:P	Food type	C:N	C:P	N:P	Reference
N_{Low}	*O. marina*	8.5	217	25	*Rhodomonas salina*	13.4	278.5	18.8	Malzahn *et al.* (2010)
P_{Low}	*O. marina*	7.3	385	52	*R. salina*	8.7	847.9	98.9	Malzahn *et al.* (2010)
$NP_{Repl.}$	*O. marina*	7	180	25	*R. salina*	8.8	368.0	38.5	Malzahn *et al.* (2010)
N_{Low}	*B. calyciflorus*	5.6	121	21.7	*Selenastrum capricornutum*	16.3	76	4.7	Jensen *et al.* (2006)
P_{Low}	*B. calyciflorus*	7	105	15.1	*S. capricornutum*	12.9	484	38.1	Jensen *et al.* (2006)
$NP_{Repl.}$	*B. calyciflorus*	5.6	70	12.6	*S. capricornutum*	7.6	66	8.8	Jensen *et al.* (2006)
N_{Low}	*Acartia tonsa*	5.7	177.6	32.5	*R. salina*	13.4	278.5	18.8	Malzahn *et al.* (2010)
P_{Low}	*A. tonsa*	5.8	186.5	33.0	*R. salina*	8.7	847.9	98.9	Malzahn *et al.* (2010)
$NP_{Repl.}$	*A. tonsa*	5.1	245.3	46.9	*R. salina*	8.8	368.0	38.5	Malzahn *et al.* (2010)

For treatment abbreviations see legend of Table I.

20, respectively), which was more pronounced in *Euplotes* sp. Our results are consistent with published data for *O. marina* with low *H* coefficient values (Table IV). Similar to *B. plicatilis*, the conspecies *Brachionus calyciflorus* showed strong internal stoichiometric regulation, however P regulation ($H_{C:P} = 11.9$) was greater than N regulation ($H_{C:N} = 1.2$) in *B. calyciflorus* (Table IV). *H* literature values for copepods also indicate strong internal regulation and are in the same range as the ciliate and rotifer species (Table IV).

Population growth rates and cell biovolumes

Euplotes sp. population growth rates were significantly higher in the replete and P_{Low} treatment compared with N_{Low} ($N_{Low} = 2.16$; $NP_{Repl.} = 2.27$; $P_{Low} = 2.19$) (Fig. 4a). For *B. plicatilis* population growth rates did not differ significantly ($F_{2,6} = 5.03$, $P = 0.06$) between nutrient treatments, but showed tendencies toward higher growth rates at P-limited conditions ($N_{Low} = 1.62$; $NP_{Repl.} = 1.59$; $P_{Low} = 1.65$) (Fig. 4b).

Cell biovolume of *Euplotes* sp. was significantly smaller at P_{Low} with a mean biovolume of 136×10^3 μm^3, compared with $>161 \times 10^3$ μm^3 at N_{Low}, N_{Med} and P_{Med} (Fig. 5a). Contractile vacuoles were largest in the nutrient-limited treatments (~500 μm^3) and decreased to half the volume at P_{Med} (Fig. 6). This resulted in a significantly higher vacuole-to-cell ratio at P_{Low}, with the vacuole contributing to 0.34% of the cell biovolume (Fig. 5c and e). Mean *B. plicatilis* biovolume was lowest in both N and P limited treatments ($<4709 \times 10^3$ μm^3), and almost a third larger at P_{Med} (Fig. 5b). Egg biovolume was not significantly different between treatments and showed a tendency of bigger eggs at N_{Low}. The egg-to-biovolume ratio was highest at N_{Low} and P_{Low} and lowest at P_{Med}, although not significantly different from the replete treatment (Fig. 5d and f).

Table IV: Regression equations of the resource and consumer nutrient ratios and the homeostatic regulation coefficient H *for zooplankton species from our study and the literature*

Species	Ratios	Regression equation	*H* (1/slope)
Nannochloropsis sp.	NP	$y = 0.67x + 0.51$	1.49
G. dominans	CN	$y = 0.62x + 0.35$	1.62
G. dominans	CP	$y = 1.28x - 1.35$	0.78
G. dominans	NP	$y = 1.09x - 0.81$	0.92
O. marina	CN	$y = -0.71x + 1.64$	1.41
O. marina	CP	$y = 1.04x - 0.39$	0.96
O. marina	NP	$y = 0.58x + 0.25$	1.72
O. marina[a]	CN	$y = 0.36x + 0.53$	2.78
O. marina[a]	CP	$y = 0.58x + 0.86$	1.72
O. marina[a]	NP	$y = 0.46x + 0.77$	1.72
Euplotes sp.	CN	$y = 0.02x + 0.73$	4.80
Euplotes sp.	CP	$y = 0.29x + 1.06$	3.42
Euplotes sp.	NP	$y = 0.21x + 0.70$	52.94
B. plicatilis	CN	$y = 0.04x + 0.68$	23.50
B. plicatilis	CP	$y = 0.05x + 1.78$	20.47
B. plicatilis	NP	$y = 0.02x + 1.16$	68.47
B. calyciflorus[b]	CN	$y = 0.81x + 0.25$	1.23
B. calyciflorus[b]	CP	$y = 0.08x + 1.80$	11.92
B. calyciflorus[b]	NP	$y = 0.12x + 1.33$	8.29
A. tonsa[a]	CN	$y = 0.11x + 0.64$	9.39
A. tonsa[a]	CP	$y = \lvert -0.04x \rvert + 2.41$	23.97
A. tonsa[a]	NP	$y = \lvert -0.01x \rvert + 1.59$	88.30

H is calculated as 1/slope.
[a]Malzahn *et al.* (2010).
[b]Jensen *et al.* (2006).

DISCUSSION

The regulation of elemental composition and nutrient cycling has been well demonstrated for heterotrophic organisms, and especially for crustacean mesozooplankton (Sterner *et al.*, 1992; Sterner and Elser, 2002). In comparison, little is known about whether protozoans and rotifers maintain stoichiometric balance. Our study indicates that the regulatory strength of internal stoichiometry in zooplankton species increases from unicellular osmotrophs to mesozooplankton. The two heterotrophic dinoflagellates, *G. dominans* and *O. marina* displayed weak homeostasis regulation, whereas the ciliate *Euplotes* sp. and rotifer *Brachionus* spp. regulated their internal stoichiometry over a large stoichiometric range in their resource.

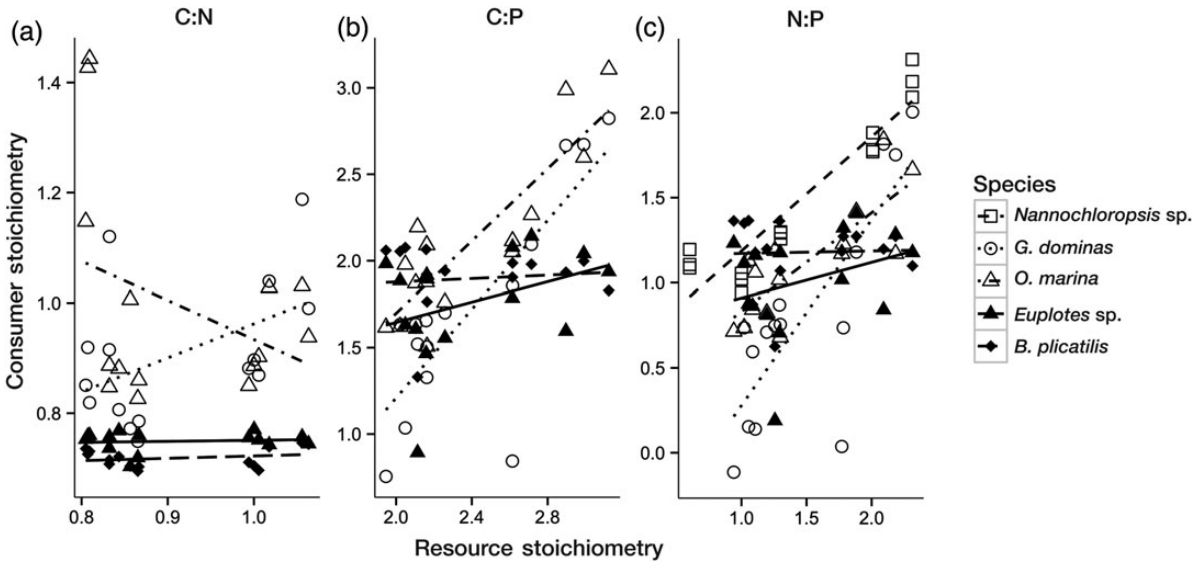

Fig. 3. Primary producer (N:P) and consumer stoichiometry (C:N:P) as a linear function of resource stoichiometry for mean values of log-transformed (**a**) C:N (**b**) C:P and (**c**) N:P ratios (in μmol) used to calculate the strength of homeostasis regulation. Regression coefficients are shown in Table IV. The resource stoichiometry of *Nannochloropsis* sp. was the culture medium and *Nannochloropsis* sp. was the food source for zooplankton species.

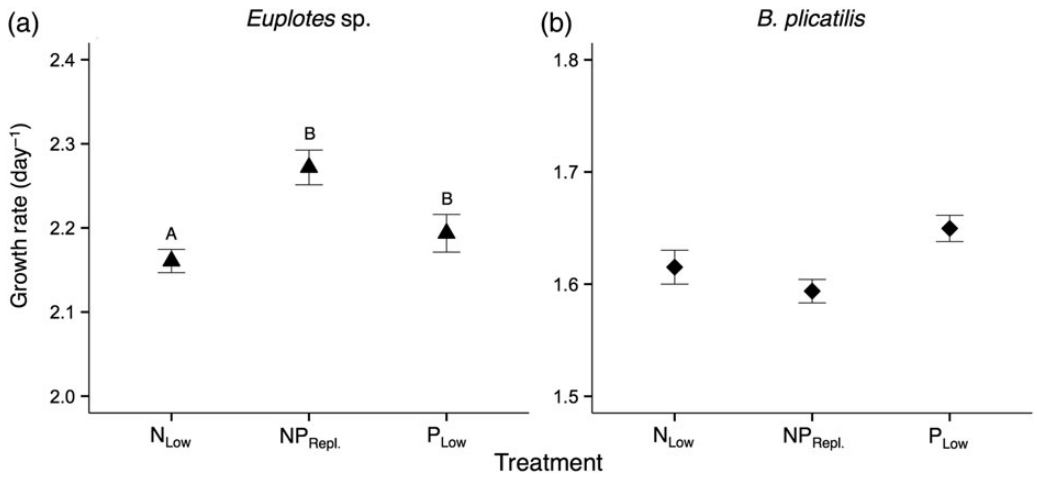

Fig. 4. Growth rates of *Euplotes* sp. (**a**) and *B. plicatilis* (**b**) calculated as mean $\ln(T_6 - T_1)$/time per treatment ($\pm$SE). For treatment abbreviations see legend Fig. 1. Letters from A–B indicate significant ($P < 0.05$) differences among treatments.

These metabolic mechanisms are supported by both the nutrient ratios as well as the homeostasis regulation coefficients.

The primary producer, *Nannochloropsis* sp., showed significant differences in its elemental composition depending on the nutrient supply of the culture media. The N:P ratio ranged from 10 to 161, the C:P from 100 to 1032 and C:N from 11 to 6 under nutrient limitation, and approached Redfield ratios of C_{106}:N_{16}:P_1 under nutrient-replete conditions. The weak internal stoichiometric regulation in *Nannochloropsis* sp. and high elemental cell plasticity over a wide elemental range is consistent with other studies (Geider and La Roche, 2002; Malzahn *et al.*, 2010) and the general assumption of weak homeostatic regulatory capacity in autotrophs (Sterner and Elser, 2002; Hillebrand *et al.*, 2013). It has been shown, however, that the degree of homeostasis in autotrophs can vary depending on species composition, growth phase and environmental conditions (Ågren, 2008; Hessen *et al.*, 2013). Further, the range of C:N and N:P ratios of *Nannochloropsis* sp. observed in our experiment is comparable with observed ratios of marine particulate matter, which in their extremes span can range from 5 to 316 for N:P and from 27 to 1702 for C:P ratios at the global scale (Martiny *et al.*, 2013), with the majority of pelagic systems having C:P ratios from 100 to 500 (Martiny *et al.*, 2013). Thus, our experiments were within realistic resource stoichiometric ratios experienced by herbivores.

The two heterotrophic dinoflagellates *O. marina* and *G. dominans* used in our experiments were not able to completely reduce the stoichiometric imbalance of their food source and the elemental nutrient patterns of their prey were traced in these consumers. This is further supported by the lower homeostasis coefficient, similar to the phytoplankton species. Our findings are comparable to other studies indicating that heterotrophic dinoflagellates are rather poor stoichiometric regulators for N and P (Goldman *et al.*, 1987; Malzahn *et al.*, 2010). A flexible cell stoichiometry may be of advantage for heterotrophic dinoflagellates, as they are often exposed to variation in food quality and quantity in their natural habitat (Meunier *et al.*, 2012). Both species can accumulate elements through luxury consumption when they are available in excess (Hantzsche and Boersma, 2010; Meunier *et al.*, 2012) and use these stores later to supplement growth, instead of using energy to dispose of excess material (Persson *et al.*, 2010). It may therefore be more energetically efficient to maintain a rather flexible cell stoichiometry when exposed to varying elemental food quality. Both dinoflagellates seemed to be better adapted to internal N regulation compared with P regulation, as suggested by the 8–10 times higher N:P and C:P ratios at P-limited compared with N-limited conditions. A more variable P content than N is consistent with other autotroph and consumer studies, which is in part linked to growth metabolism and the high amount of P in RNA (Sterner *et al.*, 1992).

Both heterotrophic flagellates had to cope with the excess C they ingested under nutrient limitation. Previous studies have shown that *O. marina* displayed higher respiration rates when reared on both N- and P-limited algae compared with replete food (Hantzsche and Boersma, 2010; Meunier *et al.*, 2012), suggesting that *O. marina* regulates its excess C via higher respiration and thus release of CO_2. However, respiration rates of *O. marina* are higher when fed with N-limited algae compared with P-limited algae (Meunier *et al.*, 2012), which is

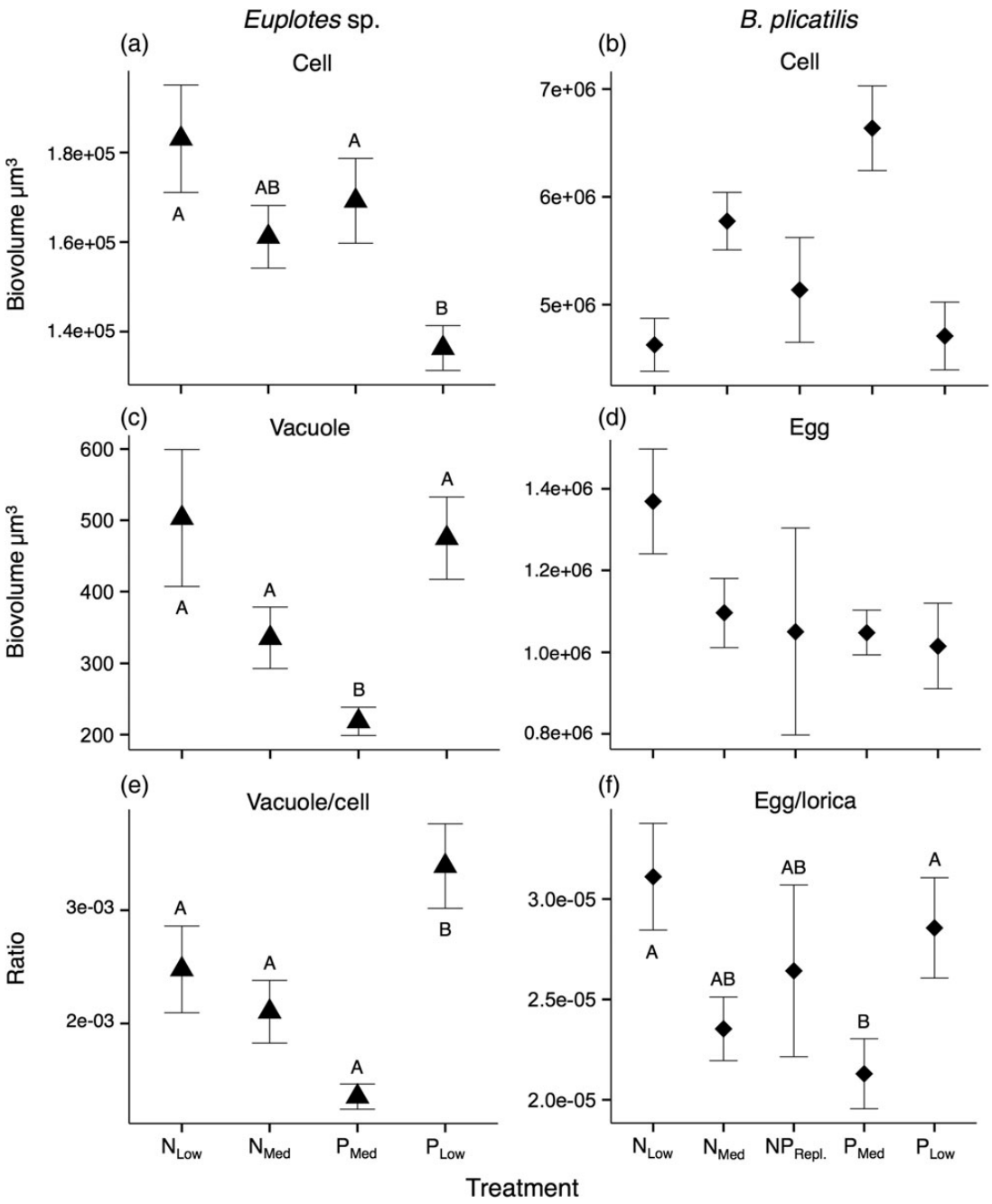

Fig. 5. Physiological response of *Euplotes* sp. and *B. plicatilis* to nutrient-limited treatments. Cell and vacuole biovolume and cell-to-vacuole biovolume ratio (**a**–**c**, respectively) for *Euplotes* sp. at low and med N and P treatments, respectively. Lorica biovolume, egg biovolume and egg-to-lorica biovolume ratio for *B. plicatilis* (**d**–**f**). Letters from A–B indicate significant differences ($P < 0.05$) among treatments.

likely due to the metabolizing of different macromolecules such as N-rich proteins. Proteins have a higher respiration quotient than lipids, as the amount of CO_2 eliminated per oxygen consumed is higher for lipids (Sakami and Harrington, 1963). Therefore, organisms that are metabolizing proteins have lower oxygen consumption, and thus lower respiration rates than those metabolizing P-rich lipids (Lusk, 1924; Weir, 1949). If nutrient limitation results in different substrates being metabolized during respiration, it will affect nutrient remineralization differently and therefore impact phytoplankton communities and nutrient cycling.

In comparison to dinoflagellates, the ciliate *Euplotes* sp. and rotifer *Brachionus* spp. showed higher regulation of

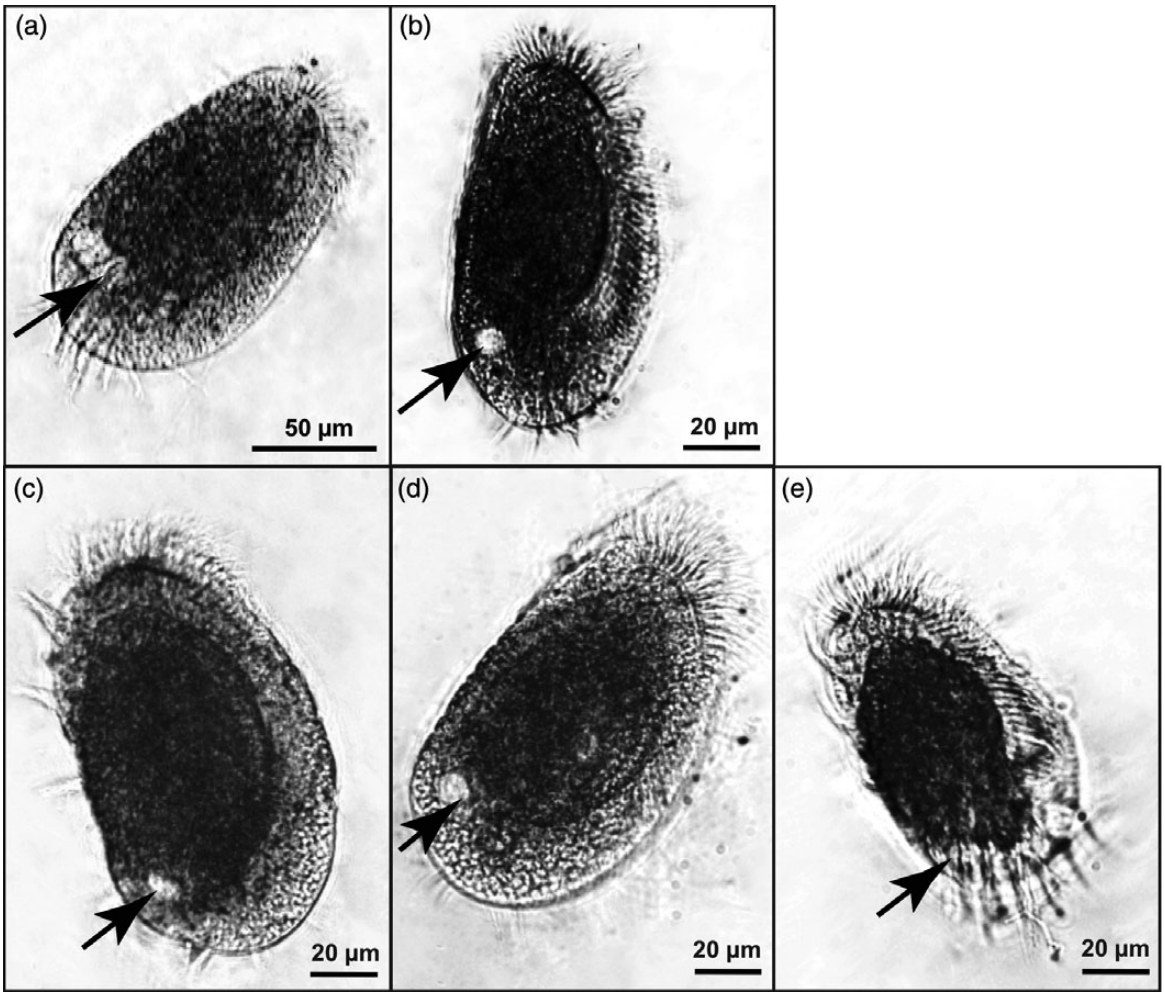

Fig. 6. Contractile vacuoles in the ciliate *Euplotes* sp. at different nutrient treatments: (**a**) N_{Low}, (**b**) P_{Low}, (**c**) N_{Med}, (**d**) P_{Med} and (**e**) NP_{Repl}. For treatment abbreviations see legend Fig. 1. Arrows point to the vacuoles.

their internal element concentration, as indicated by relatively higher homeostasis coefficients. A comparison of two rotifer species indicated differences in stoichiometric regulation strength between species, where *B. plicatilis* appeared to regulate its internal stoichiometry more than *B. calyciflorus*. Intra-specific variation in the ability to cope with elemental imbalance has been shown for a variety of consumer organisms (DeMott and Pape, 2005), suggesting that environmental stoichiometric variation can be an important factor favoring certain species traits in natural populations. Our results further indicate that *Euplotes* sp. regulated their internal N more strongly than their P content, similar to dinoflagellates. These findings are consistent with other studies showing that ciliates engage in compensatory feeding when faced with N limited food resources in order to derive enough N to keep their internal C:N ratio constant, which implies strong homeostatic regulation of internal elemental ratios (Siuda and Dam, 2010). For *B. plicatilis*, regulatory strength of internal N and P content were similar. Both the regulatory pattern and strength of the ciliate and rotifer are comparable with the regulatory strength of copepods found in literature studies. In copepods, C:N ratios are generally more constrained than C:P ratio, which is also consistent with other mesozooplankton (Hessen *et al.*, 2013).

Ecological stoichiometry theory predicts that a mismatch between resource and consumer stoichiometry results in reduced growth and/or fitness of the consumer (Sterner and Elser, 2002; Hessen and Anderson, 2008). Indeed, the ciliate *Euplotes* sp. in our study followed the expected growth trend under nutrient limitation. The population growth rate was highest under replete conditions and decreased under nutrient-limited conditions. Additionally, the organisms were smaller under nutrient limitation. While the growth rate was significantly lower

at N_{Low}, the cell biovolume was smallest at P_{Low}, which indicates that *Euplotes* sp. were more affected by N limitation, which was also evident from the stoichiometric response. One adaptation to P limitation might be a reduction in individual size and hence earlier cell division, while the population growth rate stays relatively high, which has also been observed in other zooplankton (Hessen and Anderson, 2008). A similar trend can be observed in *B. plicatilis* where the population growth rate is not affected by nutrient limitation, but the biovolume was the lowest and hence individuals were the smallest under nutrient limitation. While there was no significant difference in egg diameter, the egg-to-biovolume ratio indicated that the eggs produced under severe nutrient limitation were proportionally larger than under moderate nutrient limitation and replete conditions. This may indicate that the relative investment per offspring may be greater under unfavorable nutrient regimes.

Our results further indicate that ciliates have the capacity to buffer stoichiometric imbalances of primary producers for higher trophic levels. Additionally, these protozoan grazers can also feed on bacteria, which in general are more homeostatic than phytoplankton (Makino *et al.*, 2003). Therefore, if they utilize both bacteria and phytoplankton as a food source, the mismatch between the resource and the consumer can be reduced. Moreover, from a trophic transfer perspective this implies that protozoan grazers feeding both on phytoplankton and bacteria recover carbon fixed in the microbial loop and repackage macromolecules for higher trophic levels in the food web (Sherr and Sherr, 2002). This is consistent with observations showing that heterotrophic dinoflagellates and ciliates comprise a significant part of mesozooplankton diets (Calbet, 2008).

Our results of stoichiometric regulation are relevant in an ecological context, such as trophic transfer and nutrient recycling, and less for physiology given that we cannot exclude the possibility that undigested food left in the consumers is part of the measured values. However, the treatment signal within the consumers should be stronger than any food remains since the grazers were feeding on the manipulated food for over a week. Digestion rates are highly species specific and can vary considerably within taxa. For example, for heterotrophic flagellates digestion rates range between 19 and 28% h^{-1} (Bockstahler and Coats, 1993), and for *O. marina* highly digested material remained up to 24 h (Öpic and Flynn, 1989). For ciliates, digestion rates vary from 1 to 8% h^{-1} (Dolan and Coats, 1991), which suggests for our study that *Euplotes* sp. gut content ranged from completely to 60% emptied after one hour. Nevertheless, our results are applicable to natural conditions, as consumers do not discriminate between the organism consumed and the remains of food in the digestive track. Additionally, our results are comparable with stoichiometric studies of similar species, which show similar trends for heterotrophic dinoflagellates (Malzahn *et al.*, 2010) and it is evident from our study that the ciliate and rotifer have very different body stoichiometry compared with the algal food source. Thus we argue that the remaining food is only of minor importance.

The mechanisms involved in regulating stoichiometric homeostasis vary broadly among organisms, including food selectivity and post-ingestive processes by differential regulation of assimilation and excretion (Meunier *et al.*, 2011; Isari *et al.*, 2013). Post-ingestive differential acquisition of elements could be achieved by adjusting the assimilation efficiency of each element (Frost *et al.*, 2005). It has been suggested that crustacean zooplankton can differentially assimilate C relative to other elements (Anderson *et al.*, 2005; Frost *et al.*, 2005). This infers that herbivores can decrease the efficiency with which they assimilate C-rich compounds during digestion by altering production of digestive enzymes and excrete the excess C, store excess C as lipids, or increase metabolic rates and thus respire excess carbon in the form of CO_2 (Cease and Elser, 2013).

Post-ingestive regulation is also likely in the ciliate *Euplotes* sp. The biovolume of contractile vacuoles as well as the proportional size of the vacuoles compared with the cell size of *Euplotes* sp. increased under severe N and P limitation (for illustration see Fig. 6), which may indicate that ciliates use these vacuoles to excrete excess C, probably in the form of carbohydrates. Another possible explanation for the observed larger vacuoles under nutrient limitation can be related to increased feeding rates, as the contractile vacuoles function as a mechanism to excrete water that was taken up within the food vacuoles during feeding. Therefore, an increased feeding rate would result in an increased amount of water intake that has to be excreted, and hence increases the contractual vacuole size (Kitching, 1934; Patterson, 1980).

Weak homeostasis is likely better under variable environments and for organisms that can store elements when they are available in excess. Plastic organisms are also able to increase their nutrient use efficiency under nutrient imbalance conditions by adding a lower concentration of nutrients to new tissue (Elser *et al.*, 2003). Stoichiometric homeostasis, on the other side, allows organisms to function effectively over a broad range of environmental conditions, with the trade-off of increased costs associated with these physiological mechanisms. Stoichiometric imbalances between primary producer and consumer result in decreased growth, reproduction and survival of the consumer (Cease and Elser, 2013). It is therefore likely that plasticity in terms of stoichiometric

regulation is more advantageous under high environmental fluctuations, while homeostatic regulation is an advantage when environmental conditions are more stable.

In conclusion, this study shows that the strength of stoichiometric regulation in zooplankton increases with increasing from unicellular osmotrophs to mesozooplankton. While heterotrophic protists displayed weak homeostasis, ciliate and rotifer species showed strong homeostasis regulation in terms of their internal stoichiometry. Although homeostasis constrains consumer growth under imbalanced resource supply, our study indicates that these zooplankton species have the potential to trophically upgrade poor autotrophic quality for higher trophic levels. Climate change and eutrophication affect the C: nutrient ratios in aquatic ecosystems in various ways, and consequently the elemental ratio of autotrophs, which may reduce their food quality. Zooplankton may be able to buffer these effects for higher trophic levels to some extent.

ACKNOWLEDGEMENTS

We thank the staff at the Department of Ecology, Environment and Plant Sciences for chemical analysis and Hans H. Jakobsen for providing dinoflagellate cultures. This study has received partial funding from BONUS, the joint Baltic Sea research and development programme (Art 185), funded jointly from the European Union's Seventh Programme for research, technological development and demonstration, and from the Swedish Research Council Formas.

REFERENCES

Ågren, G. I. (2008) Stoichiometry and nutrition of plant growth in natural communities. Annu. Rev. Ecol. Evol. Syst., **39**, 153–170.

Anderson, T. R., Hessen, D. O., Elser, J. J. *et al*. (2005) Metabolic stoichiometry and the fate of excess carbon and nutrients in consumers. *Am. Nat.*, **165**, 1–15.

Bockstahler, K. R. and Coats, D. W. (1993) Grazing of the mixotrophic dinoflagellate Gymnodinium sanguineum on ciliate populations of Chesapeake Bay. *Mar. Biol.*, **116**, 477–487.

Calbet, A. (2008) The trophic roles of microzooplankton in marine systems. *ICES J. Mar. Sci.*, **65**, 325–331.

Cease, A. J. and Elser, J. J. (2013) Biological stoichiometry. *Nat. Educ. Knowl.*, **4**, 15.

DeMott, W. and Pape, B. (2005) Stoichiometry in an ecological context: testing for links between Daphnia P-content, growth rate and habitat preference. *Oecologia*, **142**, 20–27.

Dolan, J. R. and Coats, D. W. (1991) Preliminary prey digestion in a predacious estuarine ciliate and the use of digestion data to estimate ingestion. *Limnol. Oceanogr.*, **36**, 558–565.

Elser, J. J., Acharya, K., Kyle, M. *et al*. (2003) Growth rate-stoichiometry couplings in diverse biota. *Ecol. Lett.*, **6**, 936–943.

Faithfull, C., Huss, M., Vrede, T. *et al*. (2011) Transfer of bacterial production based on labile carbon to higher trophic levels in an oligotrophic pelagic system. *Can. J. Fish. Aquat. Sci.*, **69**, 85–93.

Frost, P. C., Evans-White, M. and Finkel, Z. (2005) Are you what you eat? Physiological constraints on organismal stoichiometry in an elementally imbalanced world. *Oikos*, **1**, 18–28.

Geider, R. J. and La Roche, J. (2002) Redfield revisited: variability of C[ratio]N[ratio]P in marine microalgae and its biochemical basis. *Eur. J. Phycol.*, **37**, 1–17.

Goldman, J., Caron, D. and Dennett, M. (1987) Nutrient cycling in a microflagellate food chain: IV. Phytoplankton-microflagellate interactions. *Mar. Ecol. Prog. Ser.*, **32**, 1239–1252.

Gruber, N. and Galloway, J. (2008) An Earth-system perspective of the global nitrogen cycle. *Nature*, **451**, 293–296.

Guillard, R. R. L. (1975) Culture of phytoplankton for feeding marine invertebrates. In Smith, W. L. and Chanley, M. H. (eds), *Culture of Marine Invertebrate Animals*. Plenum Press, New York, USA. pp 29–60.

Guillard, R. R. L. and Ryther, J. H. (1962) Studies of marine planktonic diatoms: I. *Cyclotella nana* Hustedt, and *Detonula confervacea* (Cleve). *Gran. Can. J. Microbiol.*, **8**, 229–239.

Hantzsche, F. M. and Boersma, M. (2010) Dietary-induced responses in the phagotrophic flagellate *Oxyrrhis marina*. *Mar. Biol.*, **157**, 1641–1651.

Hessen, D. O. and Anderson, T. (2008) Excess carbon in aquatic organisms and ecosystems: physiological, ecological, and evolutionary implications. *Limnol. Oceanogr.*, **53**, 1685–1696.

Hessen, D. O., Elser, J. J., Sterner, R. W. *et al*. (2013) Ecological stoichiometry: an elementary approach using basic principles. *Limnol. Oceanogr.*, **58**, 2219–2236.

Hillebrand, H., Steinert, G., Boersma, M. *et al*. (2013) Goldman revisited: Faster growing phytoplankton has lower N:P and lower stoichiometric flexibility. *Limnol. Oceanogr.*, **58**, 2076–2088.

Isari, S., Antó, M. and Saiz, E. (2013) Copepod foraging on the basis of food nutritional quality: can copepods really choose? *PLoS ONE*, **8**, e84742.

Jensen, T. C., Anderson, T. R., Daufresne, M. *et al*. (2006) Does excess carbon affect respiration of the rotifer *Brachionus calyciflorus* Pallas? *Freshw Biol*, **51**, 2320–2333.

Kennari, A. A., Ahmadifard, N., Kapourchali, M. F. *et al*. (2008) Effect of two microalgae concentrations on body size and egg size of the rotifer *Brachionus calyciflorus*. *Biologia (Bratisl)*, **63**, 407–411.

Kiørboe, T., Moehlenberg, F. and Hamburger, K. (1985) Bioenergetics of the planktonic copepod *Acartia tonsa*: relation between feeding, egg production and respiration, and composition of specific dynamic action. *Mar. Ecol.*, **26**, 85–97.

Kitching, J. (1934) The physiology of contractile vacuoles I. Osmotic relations. *J. Exp. Biol.*, **11**, 364–381.

Landry, M. and Calbet, A. (2004) Microzooplankton production in the oceans. *ICES J. Mar. Sci.*, **61**, 501–507.

Lusk, G. (1924) Animal calorimetry. *J. Biol. Chem.*, **59**, 41–42.

Makino, W., Cotner, J. B., Sterner, R. W. *et al*. (2003) Are bacteria more like plants or animals? Growth rate and resource dependence of bacterial C : N : P stoichiometry. *Funct. Ecol.*, **17**, 121–130.

Malzahn, A., Hantzsche, F. and Schoo, K. (2010) Differential effects of nutrient-limited primary production on primary, secondary or tertiary consumers. *Oecologia*, **162**, 35–48.

Martiny, A., Pham, C. and Primeau, F. (2013) Strong latitudinal patterns in the elemental ratios of marine plankton and organic matter. *Nature*, **6**, 279–283.

McCauley, E. (1984) The estimation of the abundance and biomass of zooplankton in samples. In Downing, J. A. and Rigler, F. H. (eds), A Man. Methods Assess. Second. Product. Fresh Waters, Blackwell Sci. Publ., Oxford. pp 228–265.

Meunier, C. L., Haafke, J., Oppermann, B. *et al.* (2012) Dynamic stoichiometric response to food quality fluctuations in the heterotrophic dinoflagellate *Oxyrrhis marina*. *Mar. Biol.*, **159**, 2241–2248.

Meunier, C. L., Hantzsche, F. M., Cunha-Dupont, A. Ö. *et al.* (2011) Intraspecific selectivity, compensatory feeding and flexible homeostasis in the phagotrophic flagellate *Oxyrrhis marina*: three ways to handle food quality fluctuations. *Hydrobiologia*, **680**, 53–62.

Meunier, C. L., Malzahn, A. and Boersma, M. (2014) A New approach to homeostatic regulation: towards a unified view of physiological and ecological concepts. *PLoS ONE*, **9**, e107737.

Olenina, I., Hajdu, S., Edler, L. *et al.* (2006) Biovolumes and size-classes of phytoplankton in the Baltic Sea. *HELCOM Balt.Sea Environ. Proc.*, **106**, 144.

Öpic, H. and Flynn, K. J. (1989) The digestive process of the dinoflagellate *Oxyrrhis marina* Dujardin, feeding on the chlorophyte, *Dunaliella primolecta* Butcher: a combined study of ultrastructure and free amino acids. *New Phytol.*, **113**, 143–151.

Patterson, D. (1980) Contractile vacuoles and associated structures: their organization and function. *Biol. Rev.*, **55**, 1–46.

Persson, J., Fink, P., Goto, A. *et al.* (2010) To be or not to be what you eat: regulation of stoichiometric homeostasis among autotrophs and heterotrophs. *Oikos*, **119**, 741–751.

Rasband, W. S. ImageJ, U. S. National Institutes of Health, Bethesda, Maryland, USA, http://imagej.nih.gov/ij/, 1997–2014.

R Core Team (2012) *R: A Language and Environment for Statistical Computing*. R Found Stat Comput Vienna, Austria, ISBN 3–900.

Saikia, S. and Nandi, S. (2010) C and P in aquatic food chain: a review on C: P stoichiometry and PUFA regulation. *Knowl. Manag. Aquat. Ecosyst.*, **398**, 03.

Sakami, W. and Harrington, H. (1963) Amino acid metabolism. *Annu. Rev. Biochem.*, **32**, 355–398.

Sherr, E. B. and Sherr, B. F. (2002) Significance of predation by protists in aquatic microbial food webs. *Anton. Leeuw. Int. J. G.*, **81**, 293–308.

Siuda, A. N. S. and Dam, H. G. (2010) Effects of omnivory and predator-prey elemental stoichiometry on planktonic trophic interactions. Limnol. Oceanogr., **55**, 2107–2116.

Sterner, R. (1993) Daphnia *Growth on Varying Quality of* Scenedesmus*: Mineral Limitation of Zooplankton*. Ecology, 74, 2351–2360.

Sterner, R. and Elser, J. (2002) *Ecological Stoichiometry: the Biology of Elements From Molecules to the Biosphere*. Princeton University Press, Princeton, NJ.

Sterner, R., Elser, J. and Hessen, D. (1992) Stoichiometric relationships among producers, consumers and nutrient cycling in pelagic ecosystems. *Biogeochemistry*, **17**, 49–67.

Stoecker, D. and Capuzzo, J. (1990) Predation on protozoa: its importance to zooplankton. *J. Plankton. Res.*, **12**, 891–908.

Taylor, P. and Townsend, A. (2010) Stoichiometric control of organic carbon–nitrate relationships from soils to the sea. *Nature*, **464**, 1178–1181.

Utermöhl, H. (1958) Zur Vervollkommnung der quantitative Phytoplankton-Methodik. *Mitt. int. Ver. theor. angew. Limnol.*, **9**, 1–38.

Weir, J. B. D. B. (1949) New methods for calculating metabolic rate with special reference to protein metabolism. *J. Physiol.*, **109**, 1–9.

Appendix V

Temperature and zooplankton effect on the growth rate of larval and early-juvenile sprat (*Sprattus sprattus*) in the South Baltic Sea

D.P. Fey, L. Szymanek

National Marine Fisheries Research Institute, Gdynia, POLAND

Introduction

Recruitment studies are some of the most important research areas because of the possible link between larval and juvenile fish survival and fish stock size (Houde 1987). Even if spawning stock biomass of a given species is large, the recruitment may be low if high mortality of early life stages occurs as a result of the effect of hydrological factors, feeding conditions or predator pressure. It is therefore essential to evaluate what factors affect the survival of larval and juvenile fish. One of the possible factors influencing survival of larvae and juveniles may be their growth rate - it is assumed that larger and faster growing specimens have higher chance of survival (Anderson 1988). It is because they can easier escape the predators (Hunter 1981), are more efficient in finding food (Blaxter and Staines 1971) and catching the pray (Drost 1987), and have larger resistance to starvation (Houde). Even if in certain circumstances the faster growing specimens may be the ones that die in higher number, the general assumption about better survival of faster growing larvae seems to be valid to high extend. Therefore, monitoring of the growth rate of larvae and evaluation of factors affecting the growth rate should be considered as an important part of the studies related to ecology of larval fish.

The goal of the present work was to describe growth rate of larval sprat in years 2006-2010 and to evaluate the effect of temperature and zooplankton biomass on both the differences among years and the differences between geographical areas (Bornholm Basin and Gdansk Basin). The data presented in this repot represent preliminary results.

Materials and Methods

Larval and juvenile sprat (n=996, L_S range: 9.0-35.0 mm, Mean = 21.5 mm) were collected between June and August 2006-2010 in the area of southern Baltic Sea with MIK 900 um and Bongo 505 um. Then, fish were sorted out on-board and preserved in 95% alcohol. At several stations the zooplankton has been collected with WP2 net, from 2 m above the bottom to surface. After a few months from sampling the sagittal otoliths were extracted from each fish, cleaned in alcohol, dried, and fixed on glass slides in quick-hardening mounting medium Eukitt® (www.sigmaaldrich.com). Standard body length were measured to the nearest 0.1 mm and

corrected for preservation-related shrinkage using formula presented for sprat larvae and juveniles by Fey (1999). Otoliths with unclear patterns (ca. 20%) were prepared for age reading by grinding and polishing according to the method described in Secor et al. (1992). Age was then estimated by counting the daily rings using a compound microscope; this was performed twice by the same person on different occasions. The left or right sagittal was used for age estimation depending on the clarity of the increment pattern. If the ages obtained from the two readings were different by more than 15%, the otolith was re-examined and mean value from the three readings was used. If it was difficult to make a decision about the age, the otolith was excluded. In total, 892 specimens were aged successfully.

The environmental conditions were described with hydrological data – temperature (^{o}C) and salinity (‰), and food availability data – zooplankton biomass (ug/m^3). The mean temperatures and salinity in the research area for May, June, July, and August were calculated for the 0-30 m layer using MIR-PIB database and ICES database. The zooplankton analysis has been conducted at 9 stations. Total biomass of zooplankton organisms within size range up to 89 um body width (size range of zooplankton organisms eatable by sprat larvae and juveniles of up to 35 mm SL).

Fish size at age were described with linear functions separately for specimens collected in different months and different years, and then for all specimens pooled together. The slope and intercept of those two functions were compared with ANCOVA. Those data were also used to calculate residuals of the SL-at-age data so to obtain growth rate index that is not age dependent. All calculations in this work were performed with STATISTICA 6.0 (www.statsoft.com).

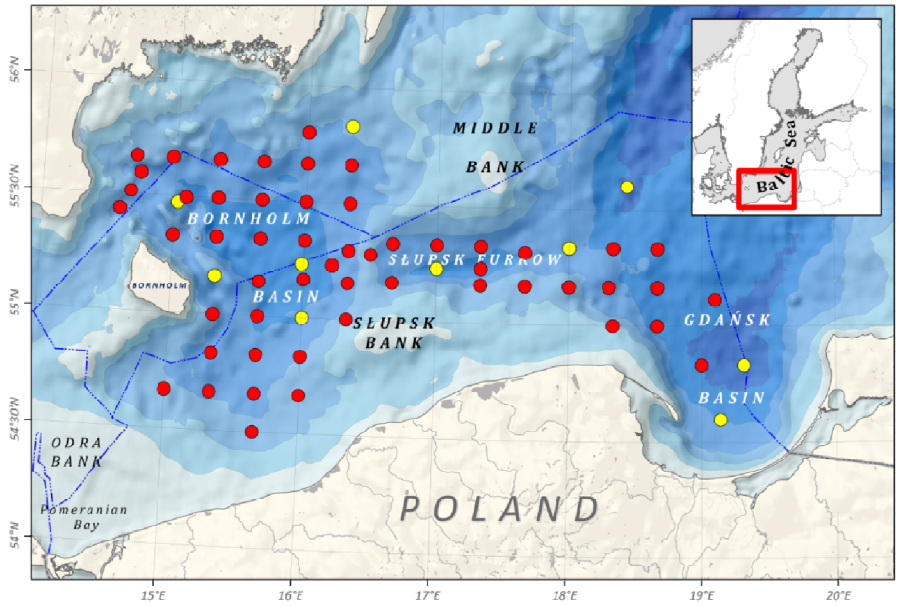

Map 1. Ichthyoplankton (red and yellow) and zooplankton (yellow) stations.

Results

The size at age data pooled from all years and sampling months provide the mean growth rate of 0.54 mm/d (Fig. 1). The high R^2 indicates relatively low variance of the analysed growth rats. Analysing the size-at-age data separately for years and months (Fig. 2) indicate some differences among years when samples from August were compared. The highest growth rate was in 2006 (0.53 mm/d) and 2010 (0.53 mm/d), and the lowest in 2008 (0.42 mm/d) and 2009 (0.39 mm/d). The differences were statistically significant (ANCOVA, $P<0.05$). Similarly, the growth of sprat larvae in June were compared between 2006 (0.63 mm/d) and 2007 (0.59 mm/d) but no statistically significant differences were observed (ANCOVA, $P>0.05$).

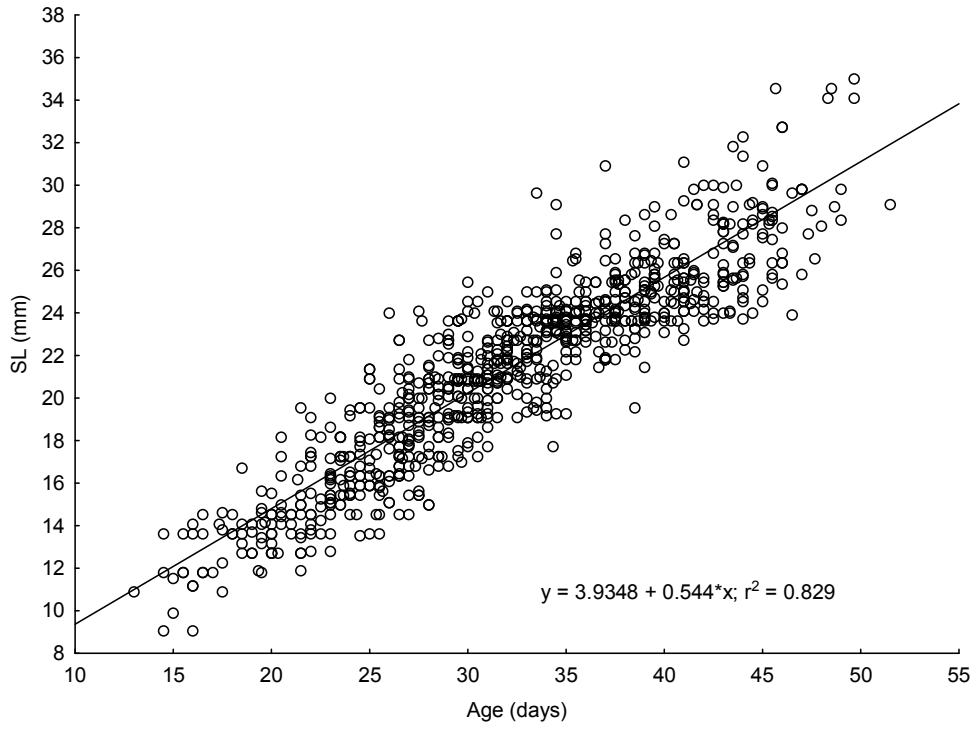

Figure 1. Size at age of larval sprat collected in June-August 2006-2010, described with linear regression.

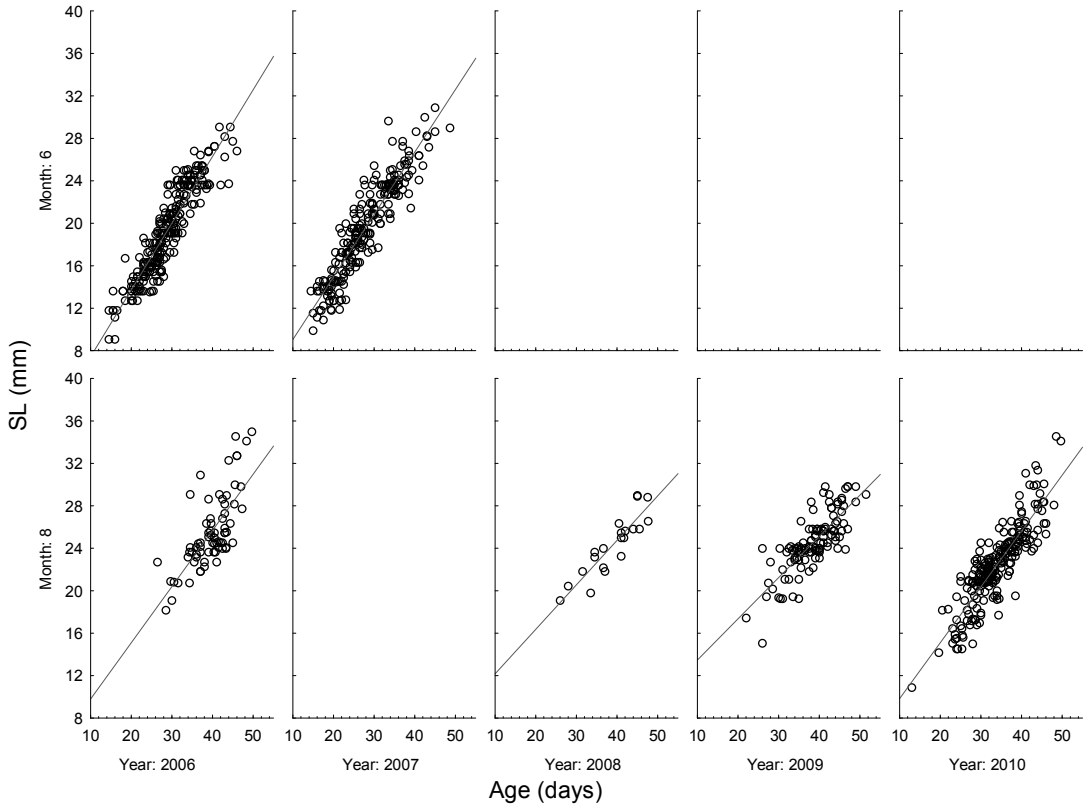

Figure 2. Size at age of larval sprat collected in June-August 2006-2010 presented separately for each cruse (i.e., month-year). Data were described with linear regressions.

The mean growth rates (slope of the linear SL-at-age regression line) of sprat collected in August in different years was negatively correlated with temperature noted during the time the larvae were growing (i.e., in July and August) (Fig. 3) (R^2 for linear regression=0.417). At the same time, the larvae growing in May-June, when the temperature was much lower than in July-August, were characterised by the fastest growth. The differences in growth rate among years can't be explained by zooplankton biomass (Fig. 4) as there was no clear relationship.

The geographical distribution affected the growth rate of larval sprat. In all years and months except June 2006, the same patter has been observed (Fig. 5) – larvae form the Gdansk Basin had the fastest growth, larvae from Slupsk Ferrow were in the middle range and the ones from Bornholm Basin the slowest. More detailed picture of the growth rate distribution among larvae can be observed on the maps (Fig. 6) that confirm the general tendency of growth reduction from west to east. It is, however, much better visible for data collected in August than in June.

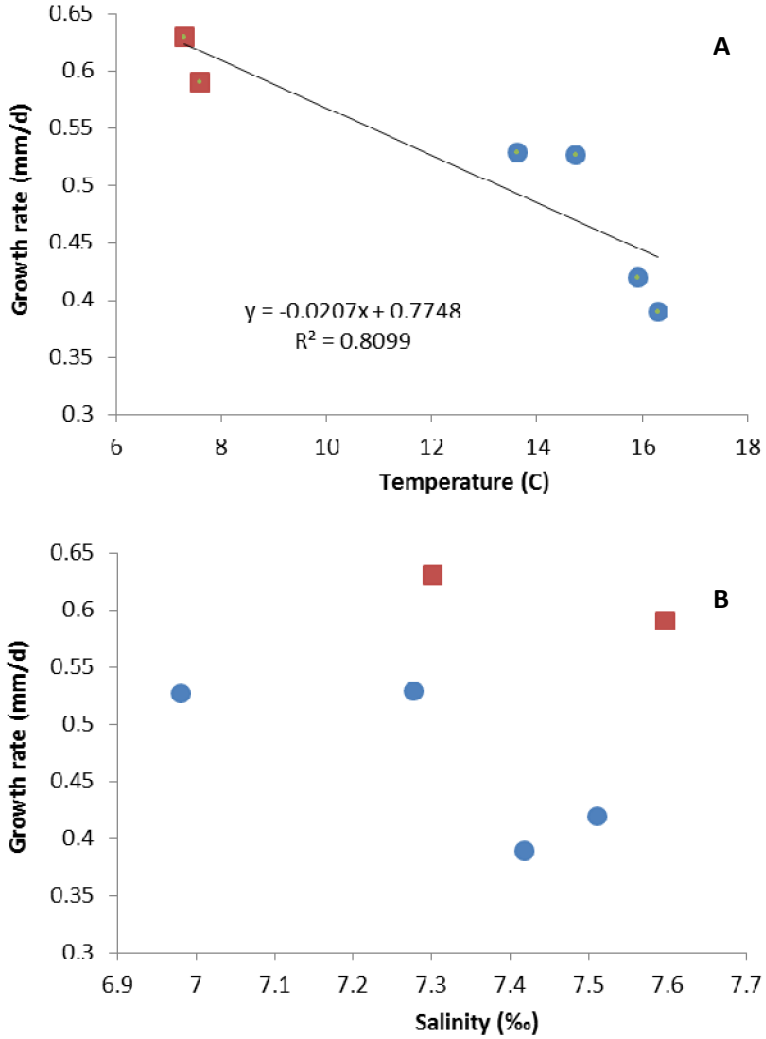

Figure 3. Growth rate of larval sprat (slope of the liner regression describing size at age) dependence on temperature (A) and salinity (B) (mean for two months during which the development of larvae was taking place). Each point represent data for one cruse; squares: larvae collected in June, circles: larvae collected in August.

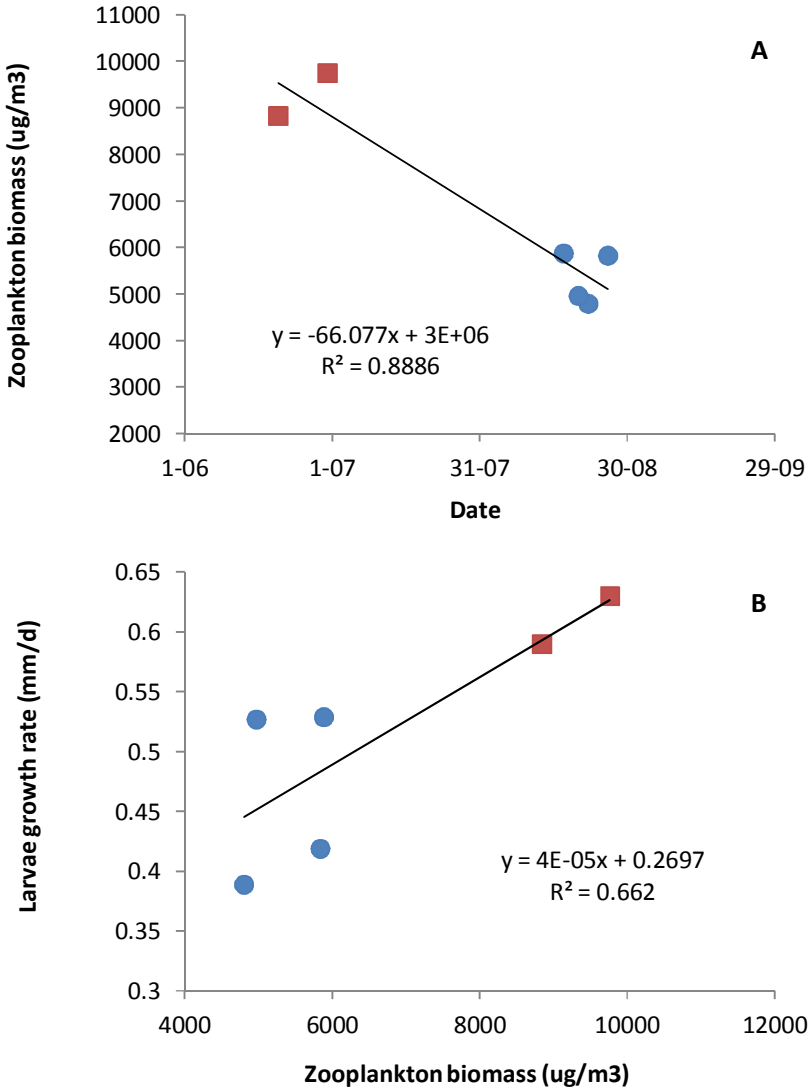

Figure 4. (A) Zooplankton (all organisms in size range 0.1-89 um in width) biomass in the Southern Baltic area during two analysed seasons. (B) Growth rate of larval sprat (slope of the liner regression describing size at age) dependence on zooplankton biomass (all organisms in size range 0.1-89 um in width). Each point represent data for one cruse; squares: larvae collected in June, circles: larvae collected in August.

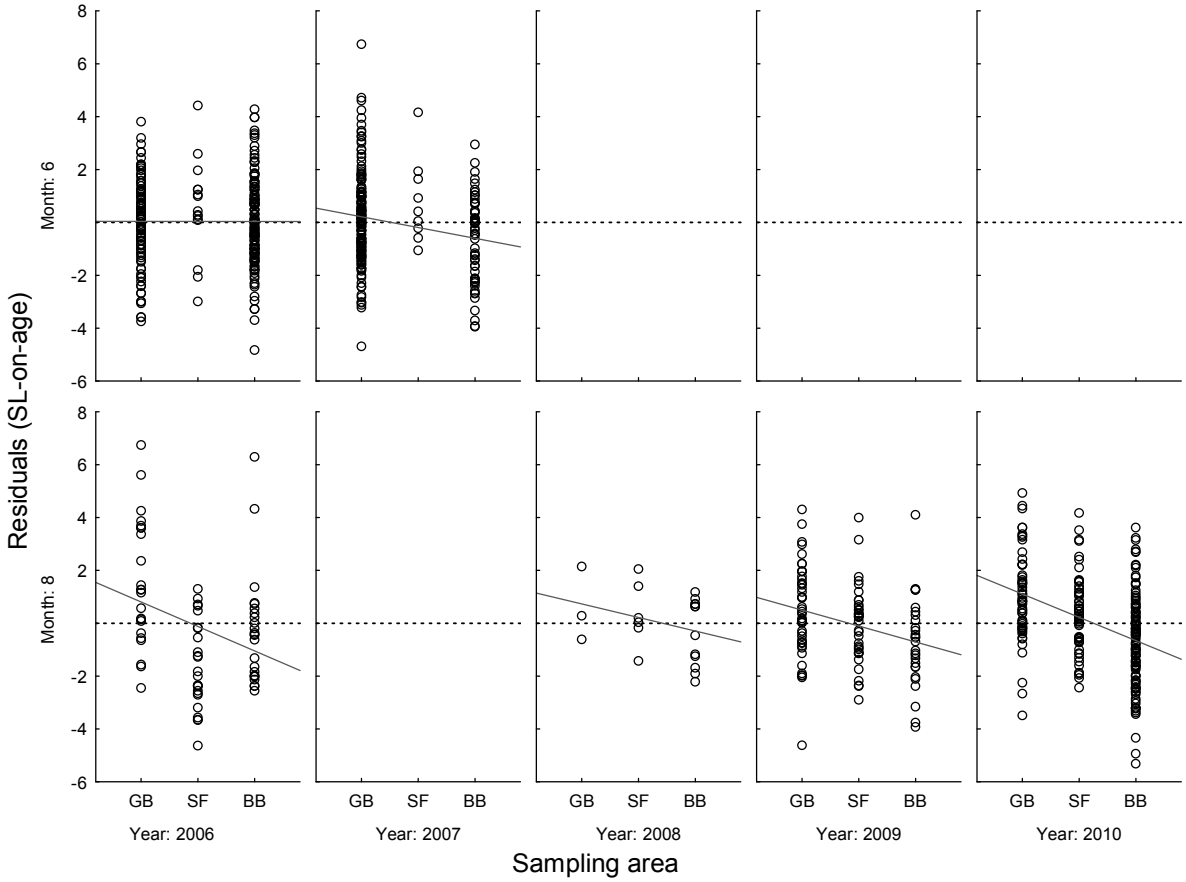

Figure 5. Growth rate of larval sprat (residuals for the linear regressions describing SL at age data, separately for each cruse, i.e. year-month) divided into three groups: for larvae collected in Gdansk Bay (GB), Slupsk Farrow (SF), and Bornholm Basin (BB).

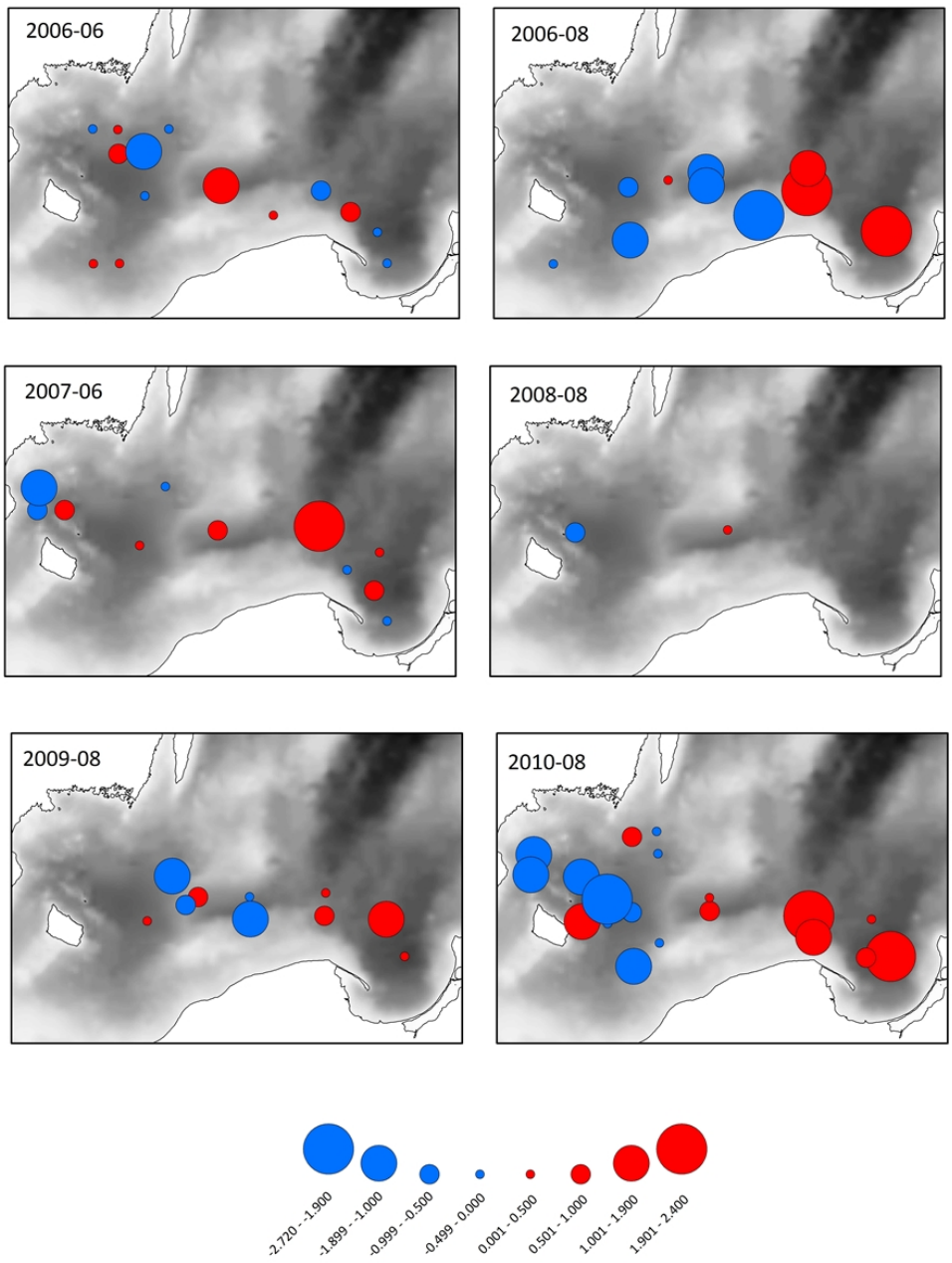

Figure 6. Geographical distribution of the growth rate of larval sprat (residuals for the linear regressions describing SL at age data, separately for each cruse, i.e. year-month). Each point represent mean value for larvae collected at a given station.

The geographical distribution of larval sprat growth rate was related to temperature differences. In July-August (Fig 7B), when the growth rate of larvae was clearly higher in the eastern part of the research area, the temperature differences between west and east were at the level of ca. 1-2°C and the temperature was higher on the east than on the west in all years. In May-Jun (Fig. 7A), the temperature differences between west and east of the research area were relatively large (2°C) and with the same direction as in Jul-Aug (i.e., higher temperature on the east) in 2006. In 2007, the temperature was higher on the west. Because of low number of zooplankton stations, it was not possible to do similar comparison of the possible differences in zooplankton biomass between west and east of the research area.

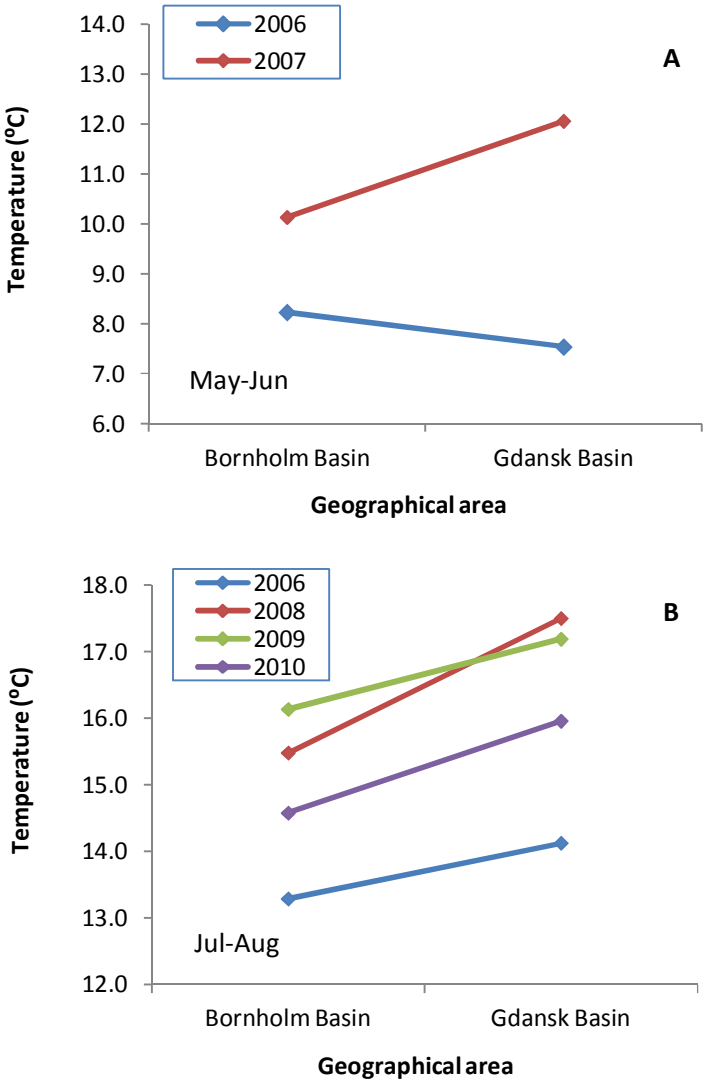

Figure 7. Mean temperature in two geographical areas, Bornholm Basin and Gdansk Basin, in two months during which the development of collected larvae was taking place: May-June (A) and July-August (B).

The growth rates found in this work (ca. 0.53 mm/d) are in accordance with literature data for larval sprat (Baumann 2006, Voss et al. 2008). Although temperature is known for being responsible for growth rate increase of different organisms (Elliott 1975), other factors may be not less or even more important, also for sprat (Voss et al. 2008). Zooplankton biomass was found in the present work to be such a factor for sprat. Temperature was also important, but as an additional factor – affecting the geographical differences in larval growth rates. The importance of analysis including several environmental descriptors which can affect the growth rate different way was underlined for larval sprat by Voss et al. (2008).

Concluding, the growth rate of larval sprat in southern Baltic is higher in May-June than in July August as an result of higher zooplankton biomass, despite much higher temperature in the latest period. The importance of temperature is however observed when geographical differences in growth rate are analysed within the same time period – higher temperature in Gdansk Basis area, comparing to Bornholm Basin area, resulted in faster growth of larvae collected in Gdansk Basin.

References

Anderson, J. T. (1988). A review of size dependent survival during pre-recruit stages of fishes in relation to recruitment. Journal of Northwest Atlantic Fisheries Science 8, 55-66.

Blaxter, J. H. S., Staines, M. (1971). Food searching potential in marine fish larvae. [W]: Fourth European Marine Biological Symposium (Crisp, D. J., red.), pp. 467-485. Cambridge: Cambridge University Press.

Baumann, H., Gröhsler, T., Kornilovs, G., Makarchouk, A., Feldman, V., Temming, A. (2006). Temperature-induced regional and temporal growth differences in Baltic young-of-the-year sprat, Sprattus sprattus. Marine Ecology Progress Series 317, 225-23.

Drost, M. R. (1987). Relation between aiming and catch success in larval fishes. Canadian Journal of Fisheries and Aquatic Sciences 44, 304-315.

Elliot, J. M. (1982). The effects of temperature and ration size on the growth and energetics of salmonids in captivity. Comparative Biochemistry and Physiology 73B, 81-91.

Fey, D. P. (1999). Effects of preservation technique on the length of larval fish: methods of correcting estimates and their implication for studying growth rates. Archive of Fishery and Marine Research 47, 17-29.

Houde, E. D. (1987). Fish early life dynamics recruitment variability. American Fisheries Society Symposium 2, 17-29.

Hunter, J. R. (1981). Feeding ecology and predation of marine fish larvae. [W]: Marine fish larvae, morphology, ecology and relation to fisheries (Lasker, R., red.), 131 p. University Washington Press, Seattle.

Secor, D. H., Dean, J. M., Laban, E. H. (1992). Otolith removal and preparation for microstructural examination. [W]: Otolith microstructure examination and analysis (Stevenson, D. K. i Campana S. E., red.), pp. 19-57. Canadian Special Publication of Fisheries and Aquatic Science 117.

Voss, R, Dickmann, M., Hinrichsen, H.-H., Floeter, J. (2008). Environmental factors influencing larval sprat *Sprattus sprattus* feeding during spawning time in the Baltic Sea.

Appendix VI

Testing of the zooplankton mean size and total abundance (MSTS) indicator calculated based on the Polish monitoring data from the southern Baltic Sea.

Piotr Margonski & Joanna Calkiewicz
National Marine Fisheries Research Institute, Gdynia, POLAND

The indicator concept

This core HELCOM indicator is primarily relevant for food webs (EU Marine Strategy Framework Directive (MSFD) criterion 4.3: *abundance/distribution of key trophic groups/species*) and its secondary link is to biodiversity (EU MSFD criterion 1.6: *habitat condition*). The zooplankton mean size and total abundance (MSTS) trends indicate that the investigated pelagic food web structure is or is not optimal for energy transfer from primary producers (phytoplankton) to fish.

Pivotal position of zooplankton organisms in the pelagic food web is indicative of both fish feeding conditions (and to some extent the predatory pressure of small pelagic fish on zooplankton) as well as grazing pressure of zooplankton on phytoplankton (HELCOM 2015). MSTS is strongly linked to two anthropogenic pressures listed in the MSFD Annex III, Table 2: selective extraction of species and nutrient and organic matter enrichment.

As described by Elena Gorokhova (HELCOM 2015), this core indicator employs zooplankton mean size (MS) and total stock (TS) to evaluate pelagic food web structure, with particular focus on lower levels. MSTS evaluates good environmental status (GES) using two GES boundaries, one for mean size and one for total standing stock (abundance or biomass) of zooplankton. The mean zooplankter size is presented as a ratio between the total zooplankton abundance (TZA) and total biomass (TZB). This metrics is complemented with an absolute measure of total zooplankton stock, TZA or TZB, to provide MSTS. Thus, MSTS is a two-dimensional or multimetric indicator representing a synthetic descriptor of zooplankton community structure (Figure 1).

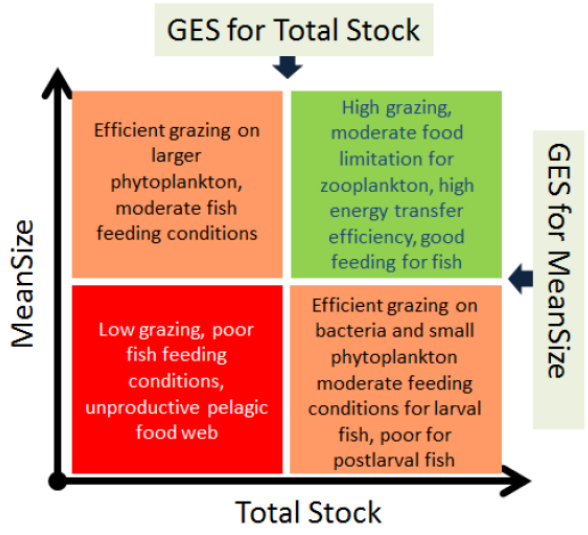

Figure 1. The MSTS concept. The green area represents GES condition, yellow areas represent sub-GES conditions where only one of the two parameters is adequate and the red area represents sub-GES conditions where both parameters failed (HELCOM 2015).

HELCOM (2015) states the GES boundaries are set using a reference period within existing time series that defines a status when the food web structure was not measurably affected by eutrophication and represents good fish feeding conditions. This indicator evaluates the structural- and functional integrity of the foodweb. Thus, on a conceptual level GES is achieved when:

- there is a high proportion of large-sized individuals (mostly copepods) in the zooplankton community that efficiently graze on phytoplankton and provide good-quality food for zooplanktivorous fish, and
- the abundance (biomass) of zooplankton is at an adequate level to support fish growth and exert control over phytoplankton production.

The reference periods for MSTS should reflect a time period when effects of eutrophication, defined as 'acceptable' chlorophyll-a concentration, are low, whereas nutrition of zooplanktivorous fish is adequate for optimal growth. Hence, these are the periods when eutrophication- and overfishing-related food web changes are negligible. Target setting is based on actual data from the reference period within existing monitoring data series for the respective areas.

Material and Methods

Data that are the Polish contribution to the HELCOM COMBINE Programme were used. The longest data series (since 1979) were collected at deepwater stations in the Polish EEZ whereas those taken at more coastal ones started within the last twenty years (Fig. 2). In most of the cases, samples were taken 5 times per year using the WP-2 net.

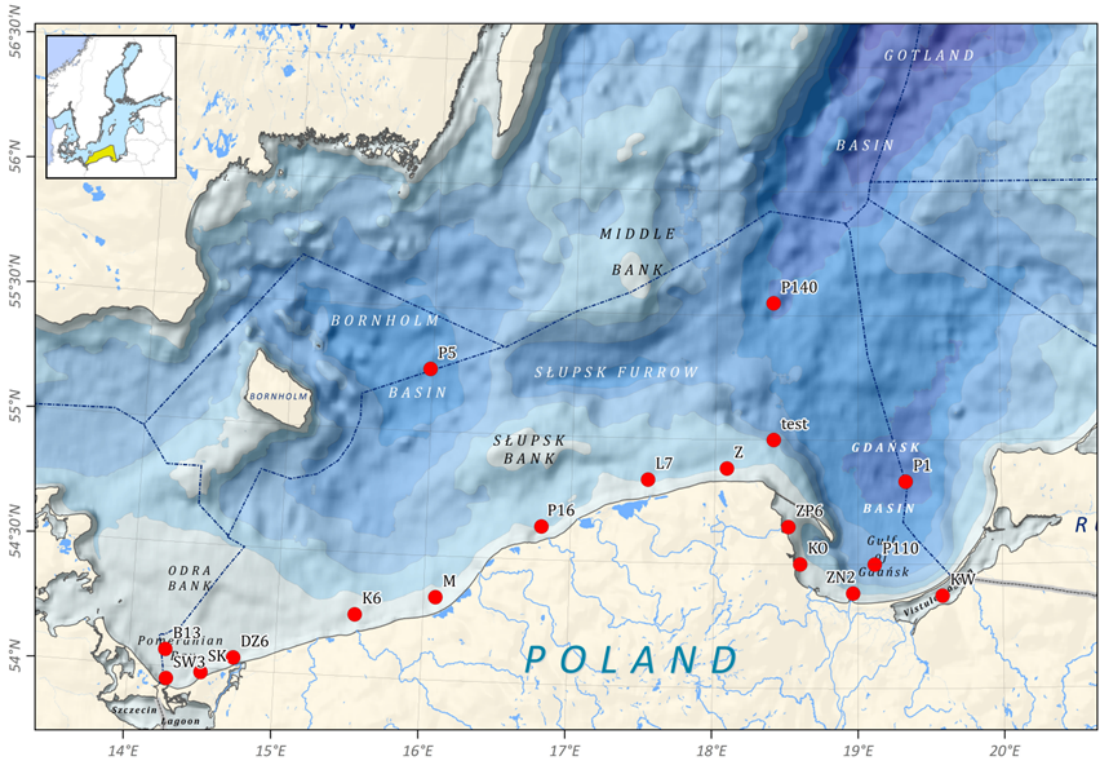

Fig. 2. Location of the zooplankton monitoring station sampled within the HELCOM COMBINE Programme in the Polish EEZ.

For the purpose of this pilot analysis, data from the deep-water station located at the southern slope of the Gotland Basin (P140), were selected. As the MSTS evaluation is currently restricted to the zooplankton communities during June-September period only (HELCOM 2015), P140 station data were checked if the sampling frequency during summer time was equally balanced over the entire period. As it was not balanced we followed the procedure described in Table 1. Using this method we were able to "create" the August data series with 26 data points.

Table 1. Frequency of sampling during June-September period at the 140 station. When in August of the given year sample was not taken, we were checking in samples during July of September were collected close enough (late July or in the beginning of September) to be representative for the August conditions. The same approach was applied for the June time series. Data highlighted in red were removed from further analyses.

	June	July	August	September
1979			1	
1980	1			1
1981	1			1
1982	1			1
1983			1	
1984			1	
1985			1	
1986	1		1	1
1987	1		1	1
1988	1			
1989	1		1	1
1990	1		1	1
1991	1		1	1
1992			1	1
1993	1		1	
1994	1		1	
1995			1	
1996			1	1
1997	1			
1999	1		1	
2002	1		1	
2003				1
2004	1		1	1
2005	1		1	1
2006			1	1
2007	1		1	1
2008	1		1	1
2009	1		1	1
2010	1		1	1
2011	1		1	1
2012	1		1	1
2013	1		1	1
times sampled	**23**	**0**	**26**	**21**

To identify the reference periods when zooplankton community was sufficient to efficiently transfer primary production to secondary consumers, we were using chlorophyll *a* EQR in the eastern part of the Gotland Basin (HELCOM 2009) and mean weight in the catch and in the stock of sprat in SD 22-32 (ICES 2015) (Fig. 3).

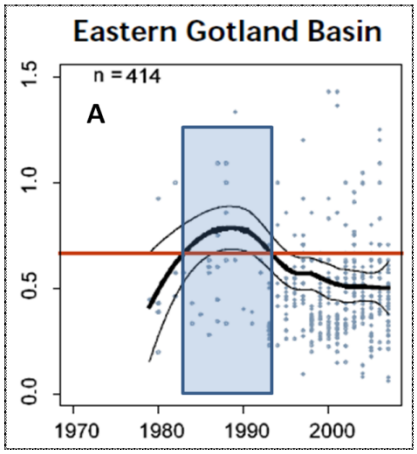

Figure 3. Long-term variability in chlorophyll-a expressed as EQR in the eastern Gotland Basin, based on HELCOM 2009 (panel A) and mean weight in the stock (WEST) of sprat in ICES Subdivisions 22-32 (ICES 2015) (panel B) used to identify time period (shaded area) when zooplankton community was sufficient to efficiently transfer primary production to secondary consumers.

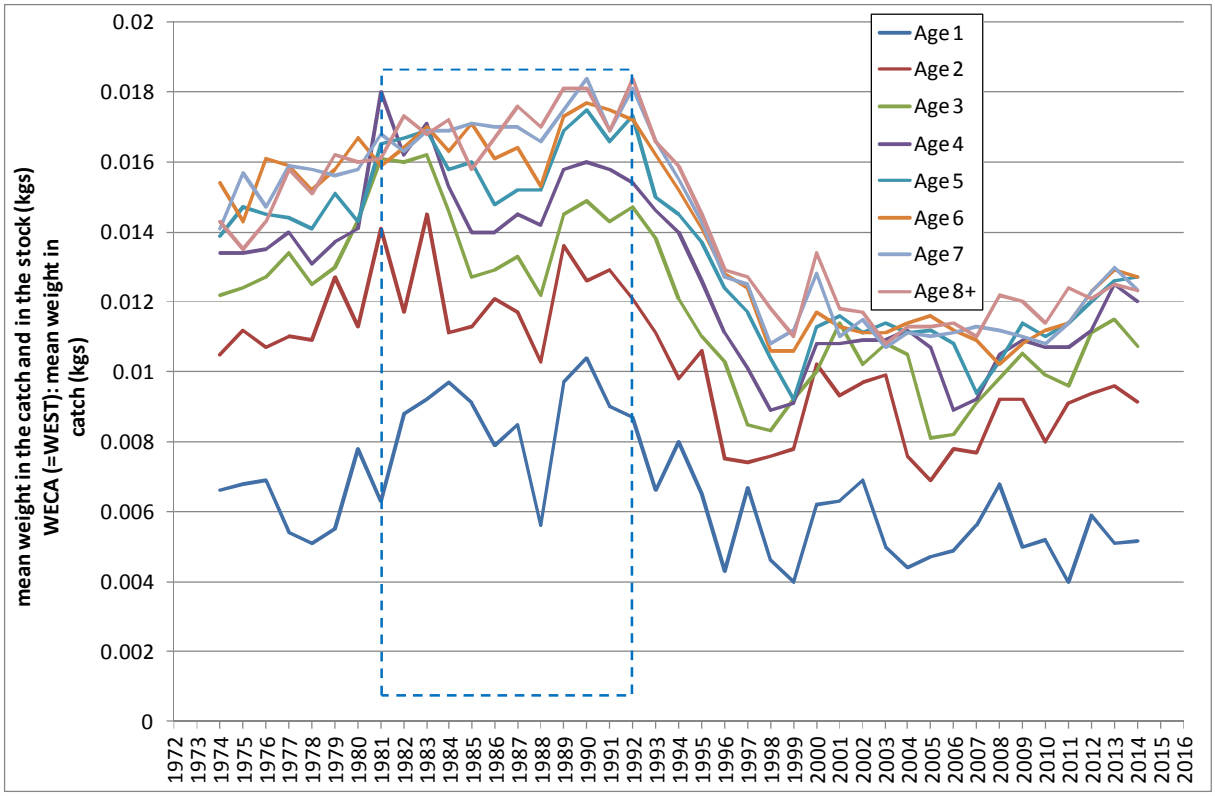

In the further steps (normality tests and transformations) we were strictly following methods described in HELCOM (2015) document. The mean value and standard deviation was assessed based on the selected reference period(s) to determine the baseline against which GES evaluation was tested and subsequently indicator values for the entire data series were standardized to z-scores.

Results

Results for total zooplankton biomass are presented in Fig. 4.

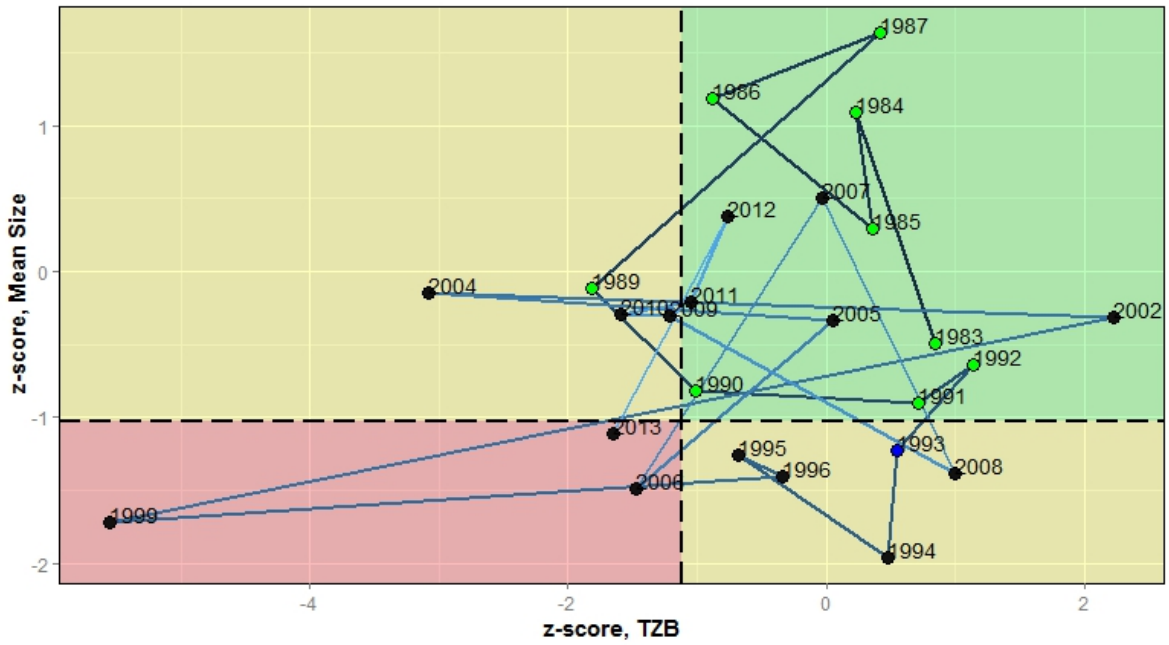

Fig. 4. Mean size (MS) and the total zooplankton biomass (TZB) as observed at the P140 station (southern slope of the Gotland Basin). The green area represents GES condition, yellow areas represent sub-GES conditions where only one of the two parameters is adequate and the red area represents sub-GES conditions where both parameters failed. Data were analysed with respect to ReConChl (horizontal dashed line) and RefConFish (vertical dashed line), both defined as the lower bound of the 99%-CI for the respective mean values calculated for zooplankton time series during the reference time period, indicating GES boundaries. Consequently, only years located in the right upper quadrant, (green area) can be considered to be in GES. The data are presented as z-scores calculated using mean and SD for the reference periods.

To investigate trends in accumulated small changes for the zooplankton mean size and total stock over long time-periods, the CuSum charts are constructed presenting the recursively accumulating negative deviations (one-sided lower CuSum). Results for P140 station analysis are presented in Figs. 5 and 6.

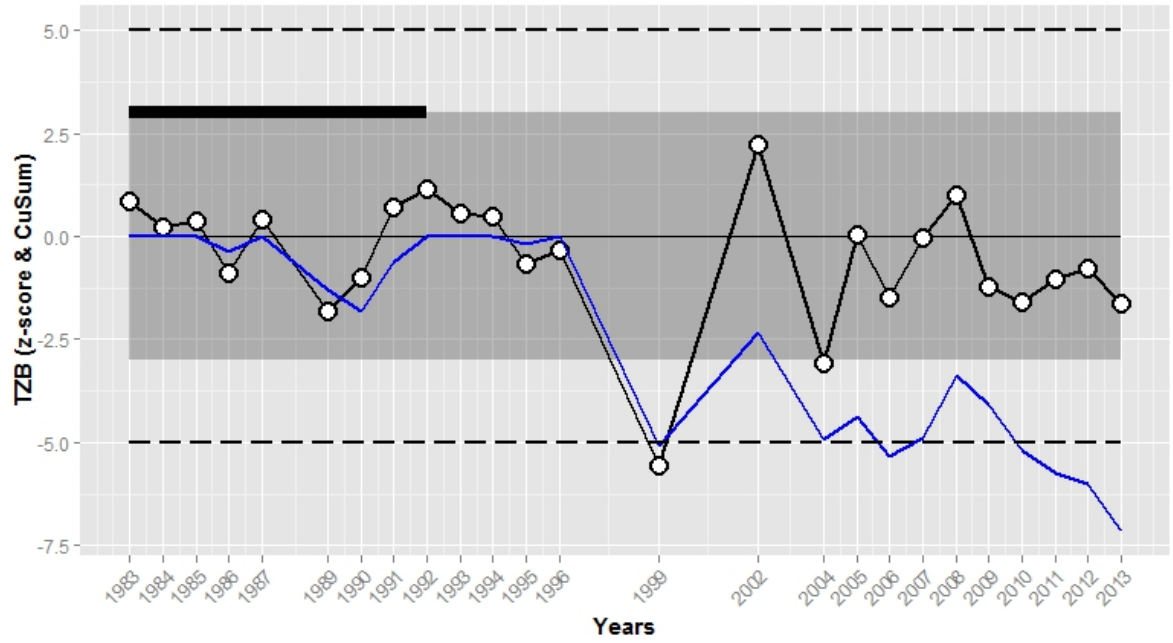

Fig. 5. CuSum analysis of total zooplankton biomass (TZB) at the P140 station. The data were normalized to z-scores (open symbols). Grey area indicates +/-3σ from the mean for the reference period; where σ is a standard deviation. The GES boundaries are shown as dashed lines (-5σ from the mean for the reference period) and the reference period (years) is indicated as a black bar on the top. The lower CuSum (solid blue line) indicates accumulated changes in TZB. The lower CuSum line is "approaching" to GES boundaries several times starting in late 1990s and finally crossing it in 2010.

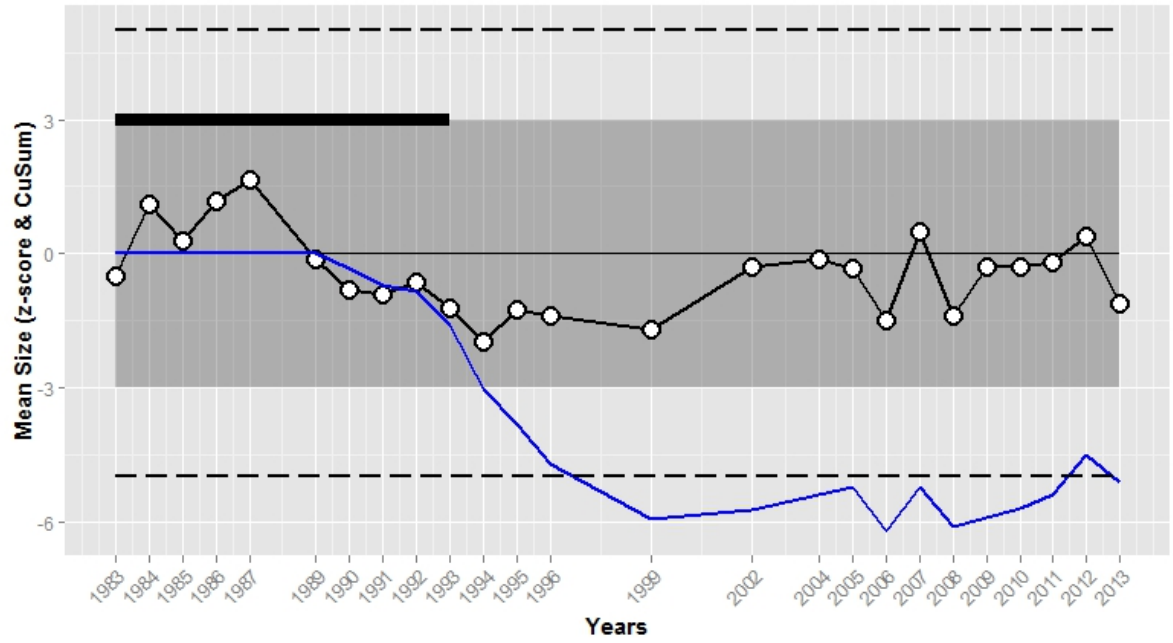

Fig. 6. CuSum analysis of mean size (MS) at the P140 station. The lower CuSum line crossed the respective GES boundary in 1997 (pattern of the blue line was interpolated between 1996 and 1999 data points). For the symbol and pattern description see the Fig. 5.

For TZB, z-scored data were crossing the -3σ border line only twice: in 1999 and 2004, however in the current century, in majority of the cases, they negatively deviated from the long-term mean. The mean size data started to be lower than the long-term mean in 1989 and stayed on the negative side to the present moment, thus considering the cumulative effect of those negative anomalies, Fig. 6 indicates losing the GES status much earlier than in the case of TZB. Considering this more conservative approach and the 'one-out-all-out'-principle (OOAO), staring from 1997, MSTS indicates the sub-GES conditions at the P140 station.

Further steps

Several issues were identified at the current stage of the MSTS indicator development:

1. As discussed at the HELCOM Zooplankton Expert Network (ZEN) Workshop (30 Nov – 1 Dec 2015), the major problem is the unification of the biomass calculation methods over the entire Baltic Sea area. At the moment, biomass estimates provided by different national experts are not comparable in many cases as they are based on different methods. This has to be solved before results are finally analysed and the indicator is fully operational.
2. Reference conditions for chlorophyll *a* EQR and sprat condition should be identified based on the sub-regional (i.e. regionally disaggregated) data to reflect the spatial dynamics at the local scale. In the case of presented analyses it was not possible, thus our results has to be treated with caution.

When problems listed above are solved further steps will include (HELCOM 2015):

1. Coastal vs. offshore areas comparison.
2. Testing methods on how to combine results derived from several data series located in the same assessment unit.
3. Different aspects of confidence variability.

Conclusions

The MSTS indicator appears to be a promising tool to test the condition and the spatio-temporal dynamics of the pelagic food web with the special emphasis on the bottom-up impact(s) at lower food web levels. It is, however, still "work-in-progress".

References

HELCOM 2015. Zooplankton Mean Size and Total Stock (MSTS). HELCOM core indicator report. Online. Document viewed on 2015-12-05, http://www.helcom.fi/Core%20Indicators/Zooplankon%20mean%20size%20and%20total%20stock-HELCOM%20core%20indicator%20report%202015-extended%20version.pdf

ICES 2015. Report of the Baltic Fisheries Assessment Working Group (WGBFAS). ICES CM 2015/ACOM:10, 826 p. http://www.ices.dk/sites/pub/Publication%20Reports/Expert%20Group%20Report/acom/2015/WGBFAS/01%20WGBFAS%20Report%202015.pdf

Acknowledgments
Polish zooplankton data were collected within the National Monitoring Programme and permission to demonstrate them was granted by the Chief Inspector of Environmental Protection (http://www.gios.gov.pl/).

APPENDIX VII

Phenology and nutritional condition of larval and adult fish

GEOMAR, DTU Aqua, University Hamburg

METHODS:

Nutritional condition and growth analyses on larval Baltic cod

Nutritional condition and growth were investigated by determining the RNA–DNA ratio of individual Baltic cod larvae. The RNA/DNA ratio is a biochemical indicator which reflects the nutritional condition and the growth potential of an organism. A higher RNA/DNA ratio reflects a better nutritional condition due to a higher number of ribosomes being present allowing for a better protein biosynthesis capacity. Besides analyzing the RNA/DNA ratio, growth was determined by converting RNA/DNA ratio to specific growth rates. For comparison with other published results and to allow for calculation of specific growth rates (SGR) using the model by Buckley et al. (2008) RNA/DNA ratios were standardized to sRD ratios according to Caldarone et al. (2006). The percentages of cod larvae with a positive growth were determined by calculating the number of larvae with a specific growth rate > 0% as a proportion of the total number of all analysed larvae (all size classes included).

Cod larvae were collected in the Bornholm Basin of the Baltic Sea during cruises with the research vessel 'ALKOR' in March, June, August 2011 and the research vessel 'DANA' in November 2011. Additional larvae from Alkor cruises in June, July, August 2006 were available for analyses. Double oblique hauls with a Bongo net (60 cm mouth diameter, mesh size 335 and 500 µm) were conducted on a station grid with approximately 10 nautical miles spacing to map the horizontal distribution of larvae. A vertically resolving Multinet (Hydro-Bios, Kiel, Germany, Type MAXI, aperture 71* 71 cm = 0.5 m^2, mesh size 335 µm) was towed at a speed of three knots for approximately 3 min in each 5-m depth interval in July 2006 and August 2011 to analyse the vertical distribution of larval cod in relation to vertical profiles of the ambient hydrographic conditions (salinity, temperature, oxygen concentration) recorded with a CTD. Sampling was conducted over a 24-h period at intervals of ca. 4 h, resulting in 6 complete vertical profiles at each station.

Cod larvae were immediately sorted from the samples under a stereomicroscope and placed into ice-cooled Petri dishes with sea water. Each larva was placed on a glass object slide with engraved scale bar and a picture was taken with a digital camera mounted on a dissecting microscope for subsequent length measurements. Thereafter, larvae were quickly transferred individually into labelled Eppendorf vials filled with sea water and frozen at -80 °C. All samples were frozen within 30 min. after capture. RNA/DANA ratios were determined as described by Huwer et al. 2011.

Food for larval cod – zooplankton abundance

For the evaluation of match/mismatch scenarios between zooplankton prey fields and larval fish condition 150µm Baby-Bongo (0.12 m^2 mouth opening) samples were taken on representative stations in the Bornholm basin parallel to the Bongo and Multinet fish larvae samples. Aim was to first determine the "biovolume" of the total zooplankton from the Bongo net (335µm mesh) by measuring the volume of the fixed sample without any further taxonomic differentiation. Additionally 150 µm Baby-Bongo samples were analysed with regards to species composition and developmental stages. In the laboratory, the taxonomic composition was analyzed with a compound microscope. The sample size was adjusted to provide at least 150 counts of *Pseudocalanus spp*. Individuals were identified to nauplii, 5 copepodite stages (C1 to C5) and adult females and males. (nauplii stages, copepodids C1 – CV and adult stages, differentiated into males and females). The abundance of copepodite stages C1 to C6 (no. ind. m^{-3}) was estimated from the integrated Bongo net catches with zooplankton counts and filtered volumes derived from flow meter readings. Cod larvae stomach content analyses by Voss et al. (2003) revealed that cod larvae in the size classes 4-6mm feed predominantly on nauplii throughout the year with a complete avoidance for all copepodite stages of Acartia spp and actively selecting for *Pseudocalanus spp*. Therefore only *Pseudocalanus spp* was in focus for the analyses of the relationships between larval cod growth, condition and zooplankton abundance. Although nauplli are the most important food item, the data analyses concentrated on using C1 stages, since these are better represented in the 150µm net catches (nauplii cannot be quantitatively sampled with 150µm meshes). It has to be kept in mind that a high abundance of copepodite C1 stages can only occur, if a high abundance of nauplii was present before, therefore the phenology of the C1 stages also reflects the phenology of the nauplii.

RESULTS:

Seasonal patterns in larval cod condition

Seasonal patterns in larval cod condition for the years 2006 and 2011 were analysed by determining the RNA/DNA ratios. Highest RNA/DNA ratios in 2006 were observed in June for the size classes 4.5 -6mm showing a declining trend over the season (Fig. 1). There was no significant difference in the mean nutritional condition between the sampling months for the size classes larger 6mm (Fig. 1). In 2011 highest RNA/DNA ratios were observed in August in the size range 4.5- 6mm with similar RNA/DNA values as observed in June 2006. Cod larvae larger 6mm showed similar condition when comparing June, August and November 2011 (Fig. 2).

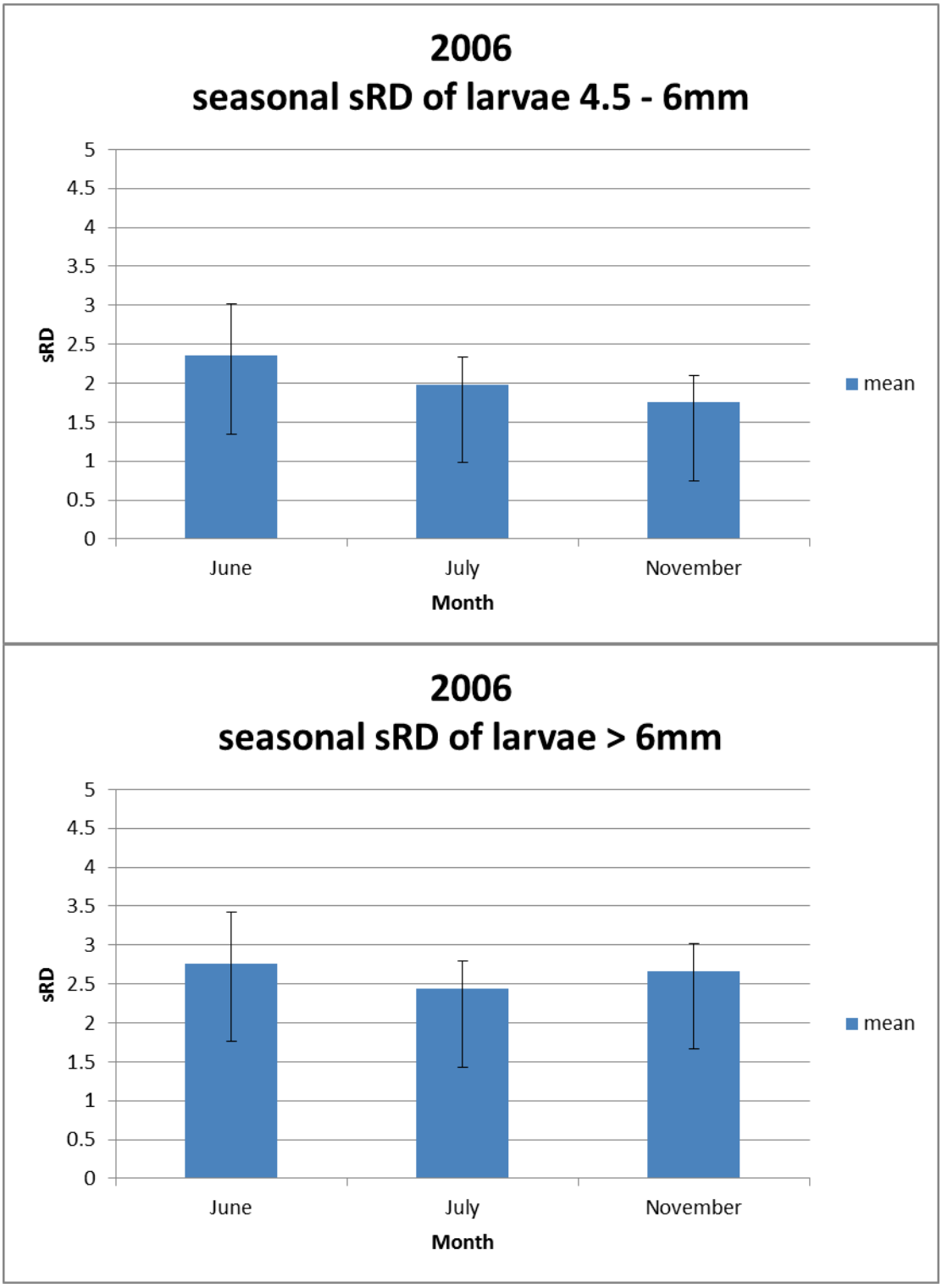

Fig. 1: Mean and standard deviation of the standardized RNA/DNA ratios of all cod larvae caught in the Bornholm basin in 2006 in June, July and November. (Upper panel) RNA/DNA ratios from size classes 4.5 -6mm, N= 23 for June, N=36 for July and N=4 for November. (Lower panel) RNA/DNA ratios from size classes >6mm, N=24 for June, N=45 for July and N=26 for November.

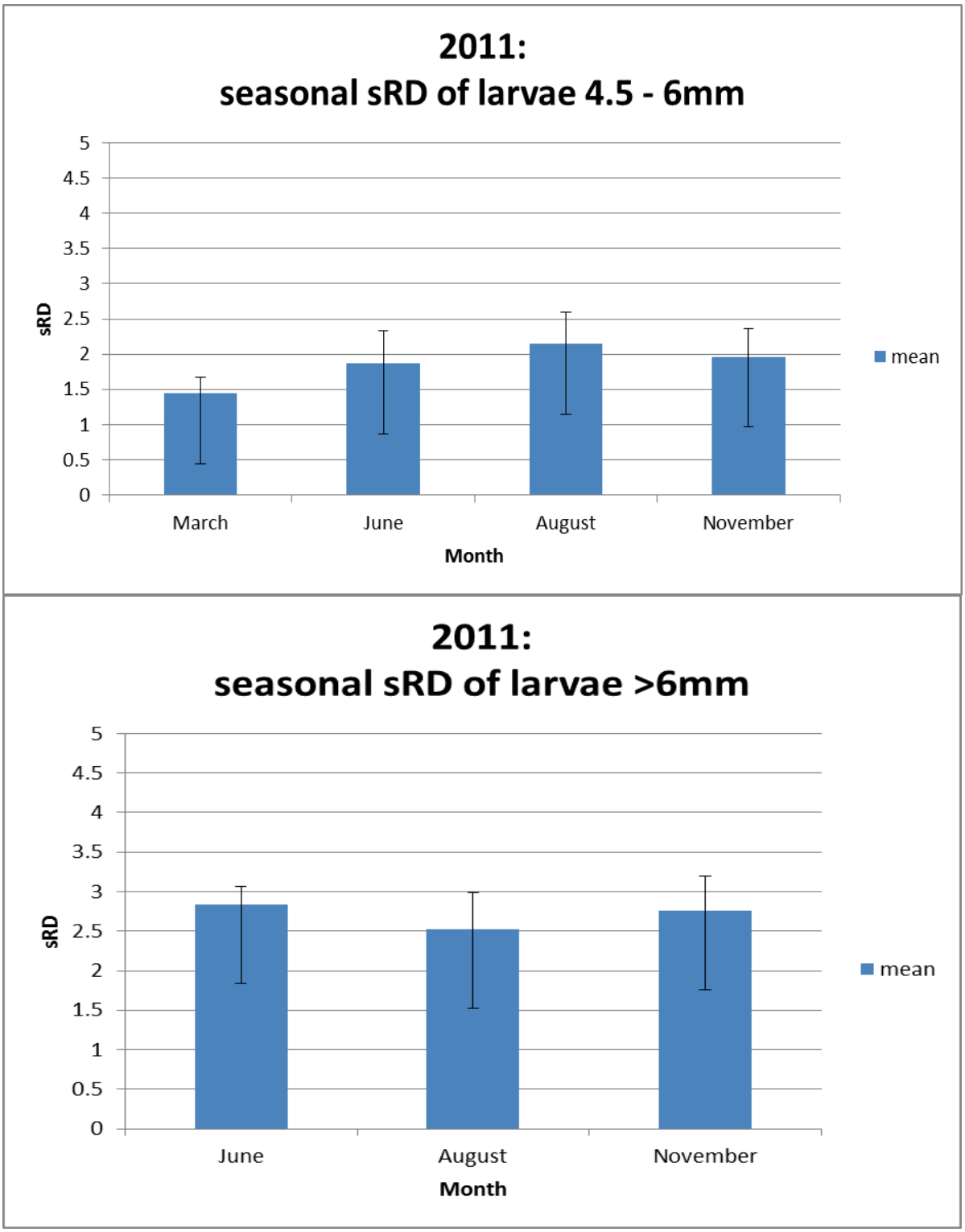

Fig. 2: Mean and standard deviation of the standardized RNA/DNA ratios of all cod larvae caught in the Bornholm basin in 2011 in March, June, August and November. (Upper panel) RNA/DNA ratios from size classes 4.5 -6mm, N=8 for March, N=70 for June, N=293 for August and N=18 for November. (Lower panel) RNA/DNA ratios from size classes >6mm, N=27 for June, N=316 for August and N=25 for November.

Larval condition and recruitment

To evaluate whether "recruitment at age 2" could be affected by the growth rate of the larvae, RNA/DNA data for the different sampling months were converted to specific growth rates based on the multispecies growth model by Buckley et al. (2008) taking environmental temperature experienced by the larvae into account. Assuming that only larvae experiencing a positive growth rate have a chance to survive, the numbers of larvae with positive growth rates were related to the total number of larvae and defined as % positively growing larvae. The results are shown in Fig. 3 indicating "highest survival potential" in August 2007 and August 2011 compared to intermediate survival potential in 2006, whereas only very poor survival potential was indicated by the results from 1994 & 1995.

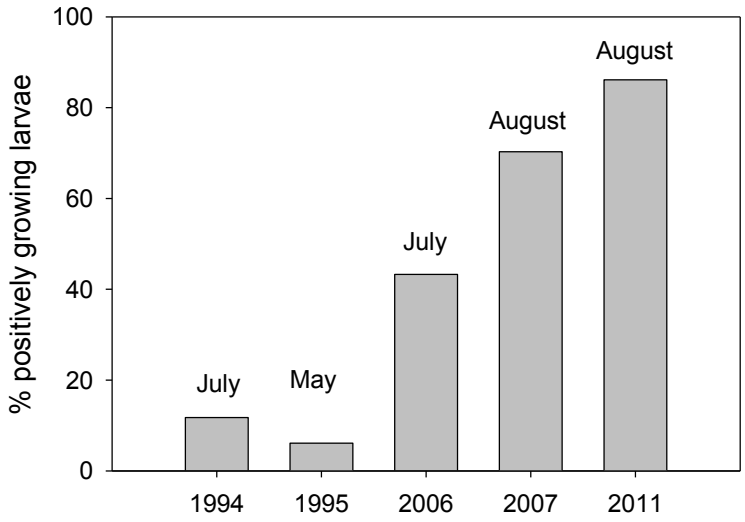

Fig 3. Comparison of percentages of larvae showing positive growth (derived from RNA/DNA ratios) for the different sampling months and years (based on all size classes in the samples).

When the percentage of positively growing larvae was analysed in relation to numbers of recruits of the different age groups, positive correlations between the numbers of growing larvae and the numbers of recruits could be shown. Fig. 4 shows that the number of age 2 recruits (ICES, 2013) increased with the number of larvae experiencing positive growth and explained 74 % of the variability in the model. The positive relationship between recruits and the percentage of larvae showing positive growth rates also carried over to age class 3 (Fig.5) and age class 4 (Fig.6).

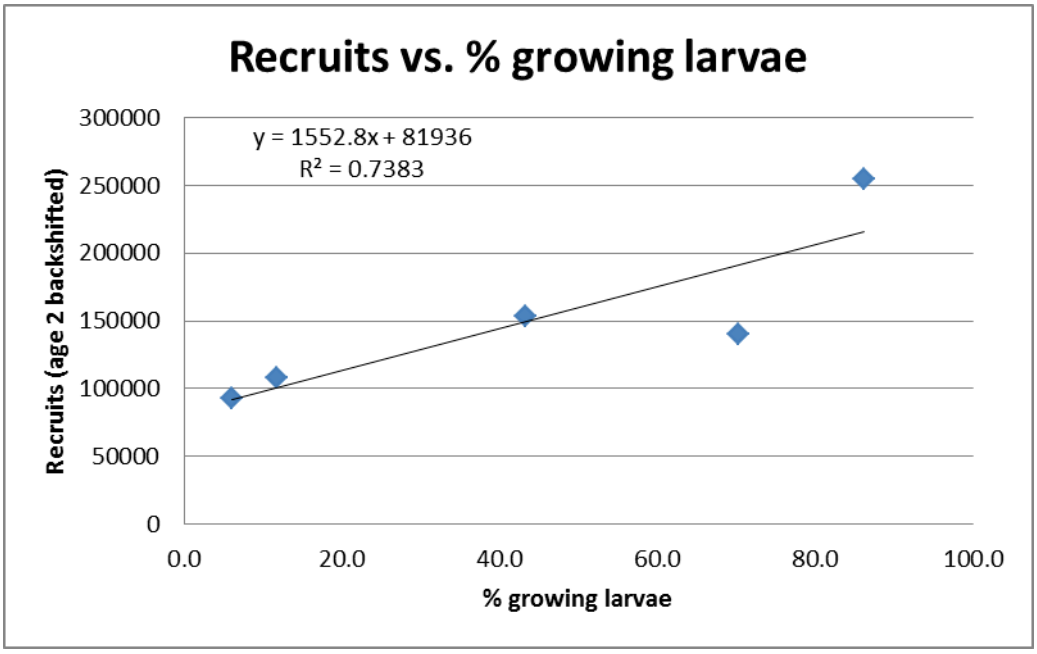

Fig.4: Relation between number of recruits (ICES, 2013) and percentage of cod larvae showing positive growth rates (derived via RNA/DNA ratios). Data points represent the years 1994, 1995, 2006, 2007 and 2011 presenting the months, when high larval abundances were found.

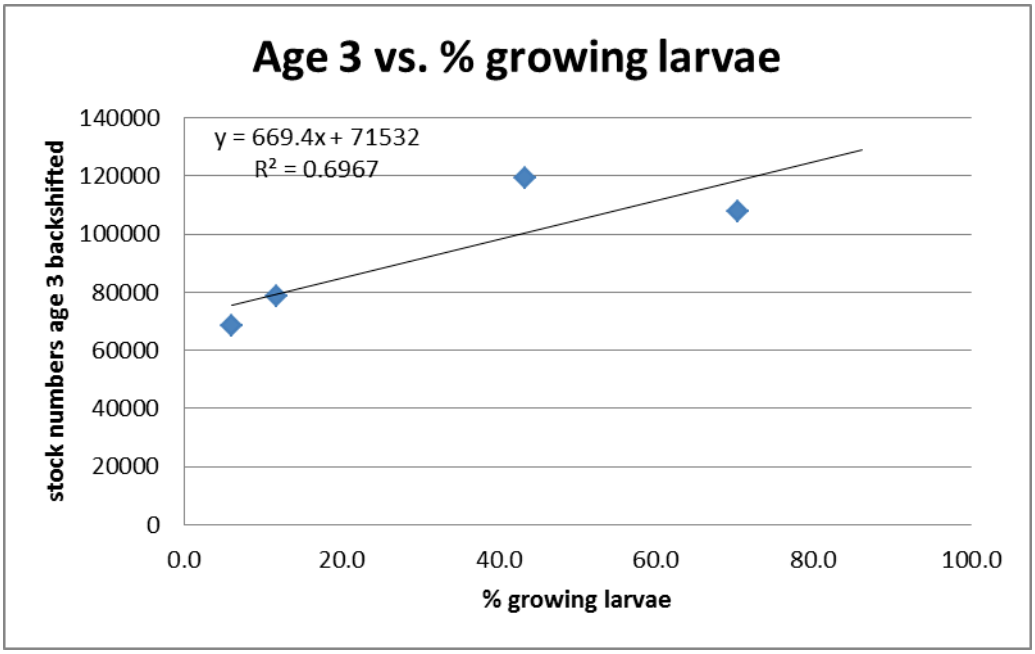

Fig. 5: Relation between stock numbers at age 3 (ICES, 2013) and percentage of cod larvae showing positive growth rates (derived via RNA/DNA ratios). Data points represent the years 1994, 1995, 2006, and 2007 presenting the months, when high larval abundances were found.

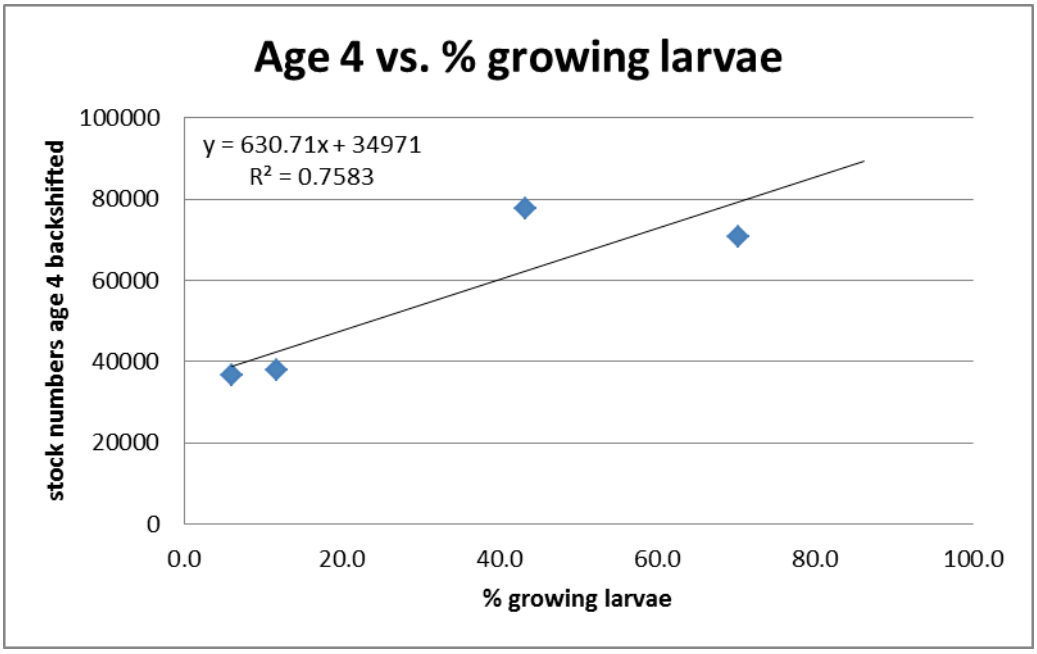

Fig. 6: Relation between stock numbers at age 4 (ICES, 2013) and percentage of cod larvae showing positive growth rates (derived via RNA/DNA ratios). Data points represent the years 1994, 1995, 2006, and 2007 presenting the months, when high larval abundances were found.

Larval condition and zooplankton

To be able to compare the percentages of larvae with positive growth from the years 1994, 1995, 2006 and 2007 in relation to prey availability zooplankton biovolumes were used, since detailed zooplankton and prey field abundance data are not available for comparison with cod larvae data from 1994 and 1995. The percentage of larvae with positive growth significantly increased with an increase in average biovolume indicating the importance of an adequate prey field for cod larval growth (Fig. 7).

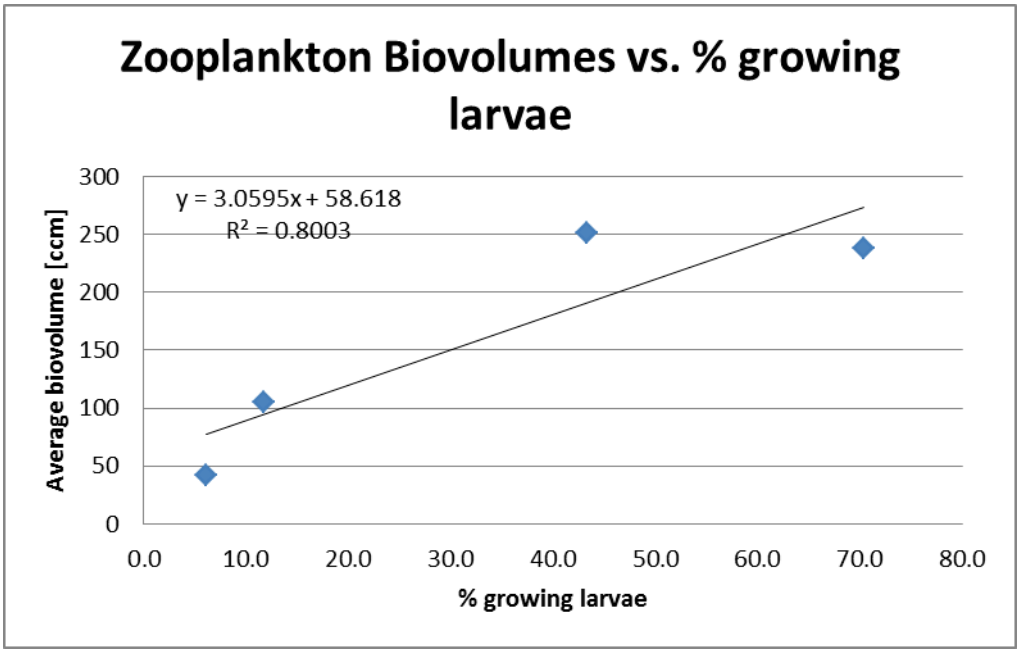

Fig.7: Relation between average biovolume (ccm) of zooplankton in 150µm baby bongo samples and percentage of cod larvae showing positive growth rates (derived via RNA/DNA ratios). Data points represent the years 1994, 1995, 2006, and 2007 presenting the months, when high larval abundances were found.

The phenology in the abundance of *Pseudocalanus spp*, representative of the most important food item for cod larvae in the years 2006 and 2011 is given in Fig. 8. Larval cod condition and abundance of the copepodites C1 stages were significantly correlated and showed an increase of larval condition with increase in prey availability for the size classes 4-5mm and >6 mm (Fig. 9).

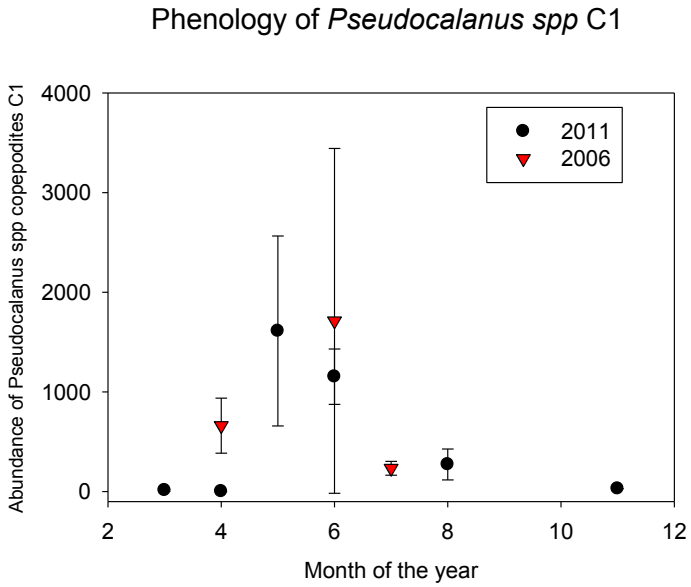

Fig. 8: mean and standard deviation in the abundance of *Pseudocalanus spp* copepodite C1 stages in the years 2006 and 2011.

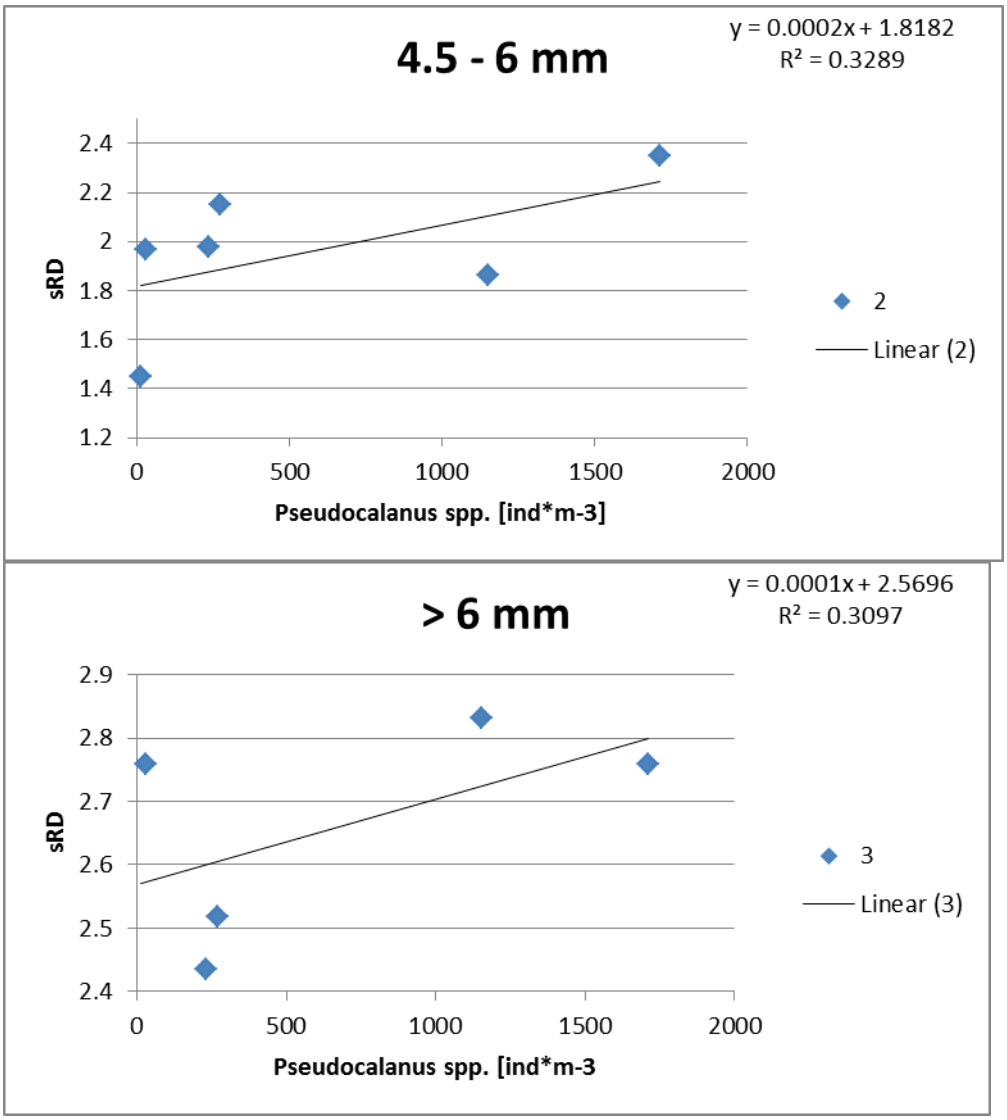

Fig. 9: Relation between the mean nutritional condition (standardized RNA/DNA ratios) of cod larvae sampled in 2006 and 2011 and the mean abundance of *Pseudocalanus spp.* C1 copepodites determined from zooplankton samples in the same months. Upper panel gives the relationship for cod larvae between 4.5 and 6 mm. Lower panel shows the relationship for cod larvae larger 6mm.

Zooplankton phenology

The zooplankton composition and biomass showed a considerable inter-annual variability in the years 2006 and 2011-2014 (Figs. 10, 11). The timing of the spring increase and the maxima in total abundance varied from May to August which is largely related to the abundance and occurrence of cladocera and rotifers in the area. In years with high rotifer abundance (2012, 2014), the vernal zooplankton increase started in April-May; in years of their absence (2006, 2011, 2013) the abundance peaked later in the year due to mass development of cladocera during summer. Cladocera were also responsible for the large

inter-annual variation in total zooplankton abundance and biomass of 62.000 to 143.000 Ind. m^{-3} and 88-190 mg C m^{-3}.The year 2011 and 2012 were characterized by an exceptional low cladoceran abundance and biomass. In contrast to rotifers and cladocera, total copepods were remarkable stable in timing and abundance despite a pronounced variation in the composition of species.

The total abundance and biomass of the different stages of *Pseudocalanus* spp. varied generally little between the years with 8.400-14.400 Ind. m^{-3} and 20.0 – 36.6 mg mg C m^{-3} (Figs. 12, 13). However, the timing of the occurrence of the most important stages C1-C2 varied considerable. In 2006, 2011 and 2013 C1 stages occurred relatively early in the year, which coincides with a relatively high abundance of C1 and C2 during summer. The abundance of these stages was higher in 2011 and 2013 than 2006. In contrast to these years, the occurrence of C1 was late in 2012 and 2014 and the stocks of early juveniles were low.

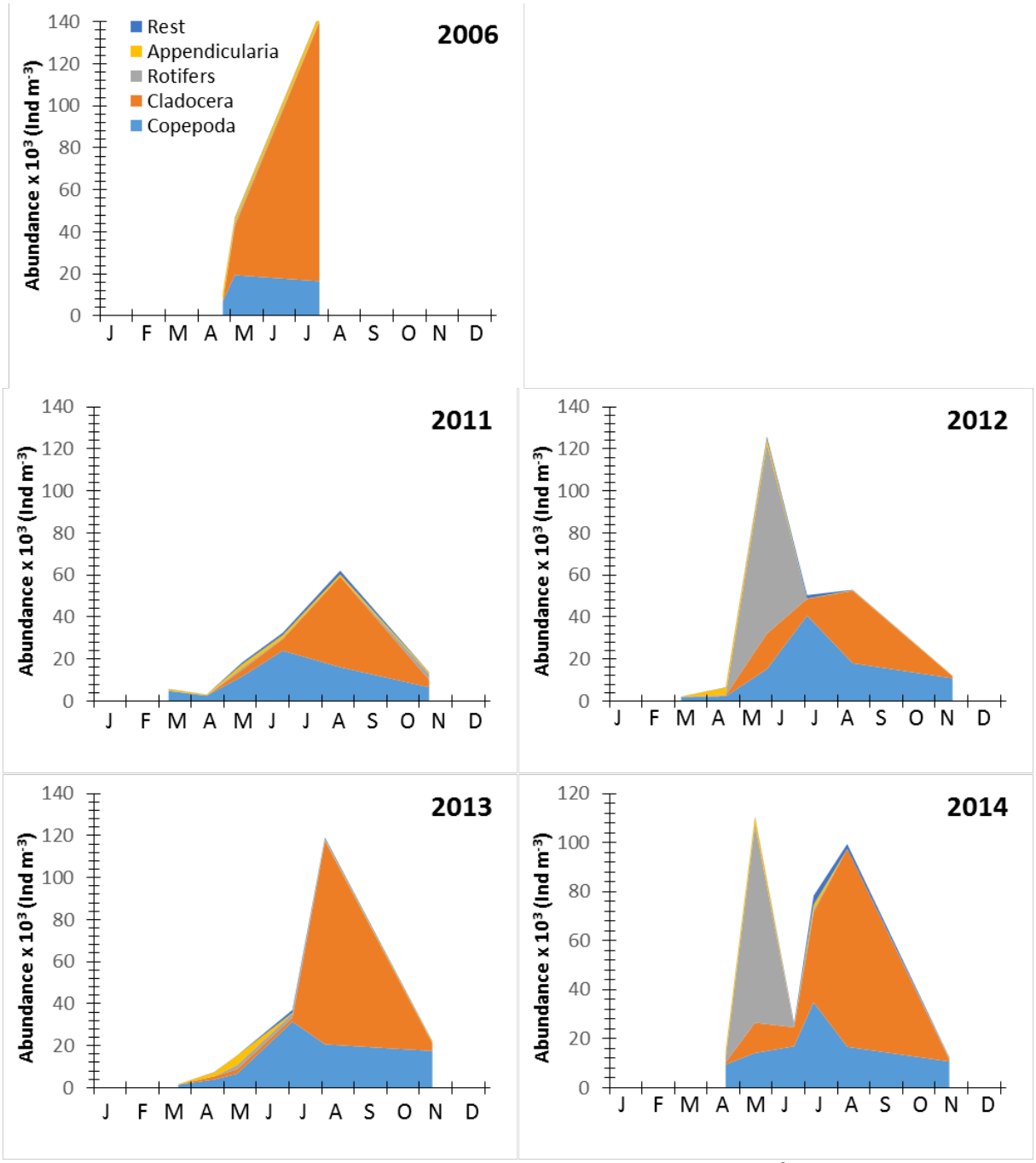

Figure 10: Seasonal variation of total zooplankton abundance (Ind. m^{-3}) and the contribution of major taxonomic groups to total stocks (shown as cumulative abundance).

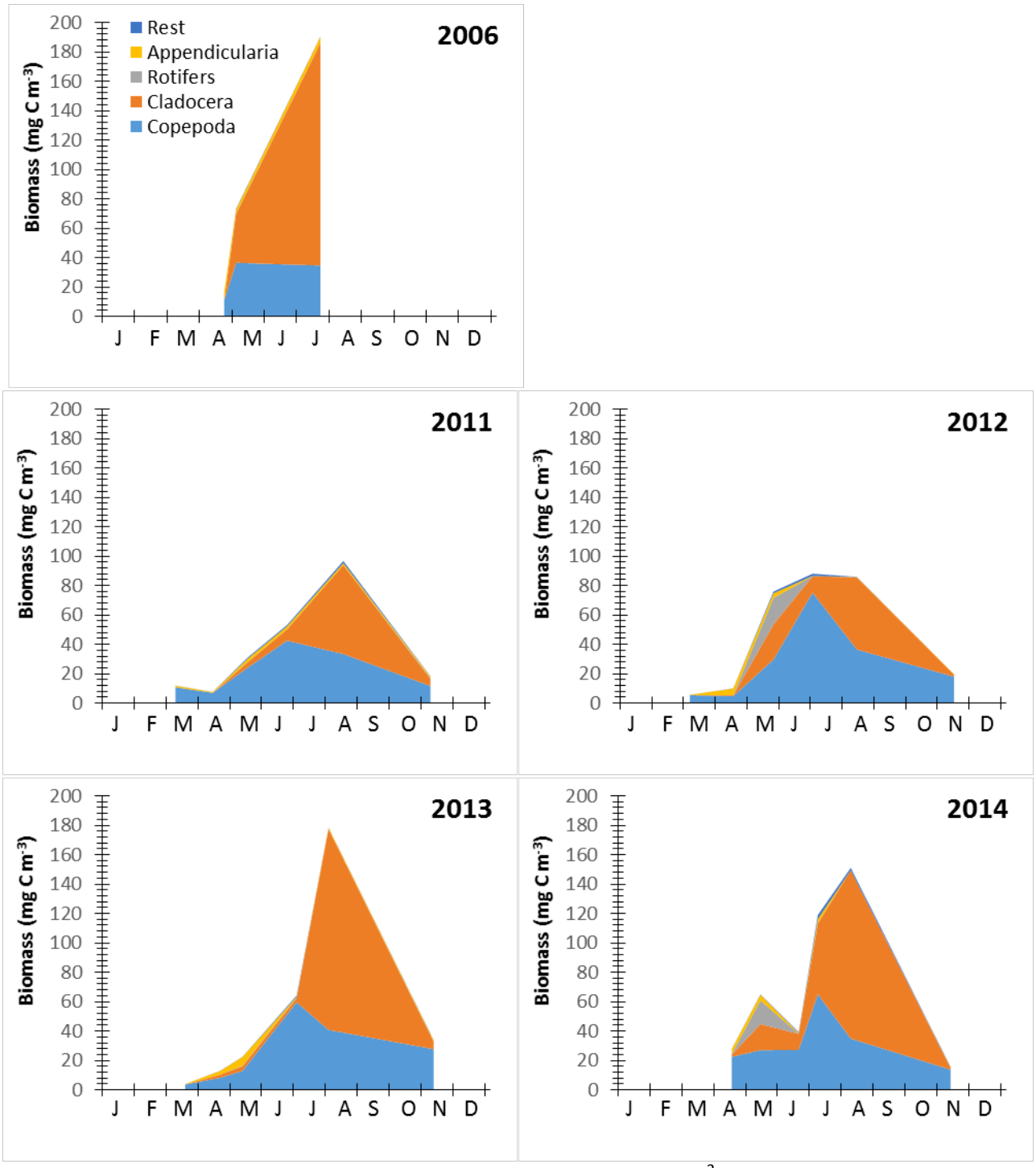

Figure 11: Seasonal variation of total zooplankton biomass (Ind. m^{-3}) and the contribution of major taxonomic groups to total stocks (shown as cumulative biomass).

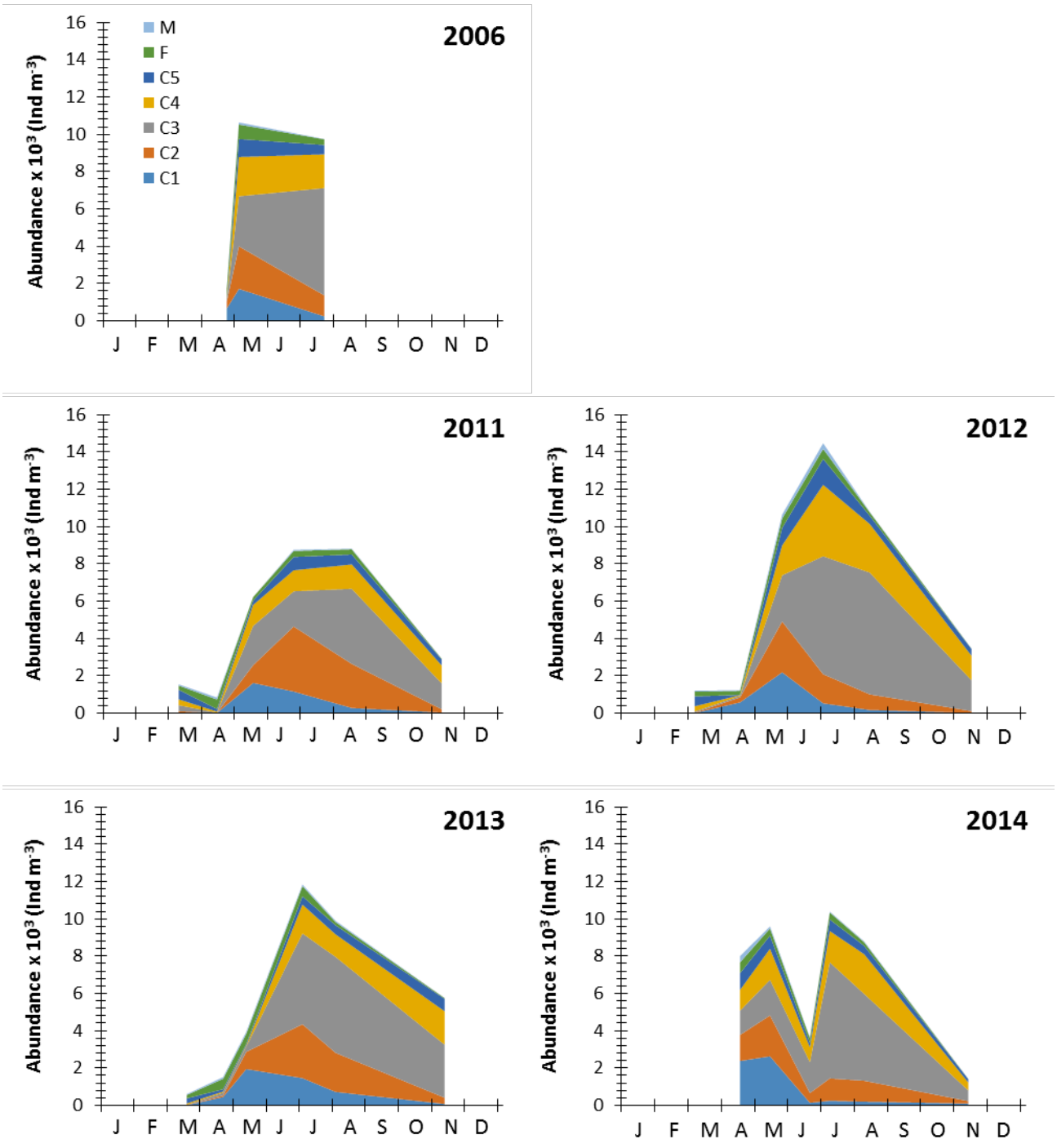

Figure 12: Seasonal variation of total abundance of *Pseudocalanus* spp. (Ind. m^{-3}) and the cumulative contribution of the various copepodite stages (C_1-C_5, F=female, M=male) to the stock.

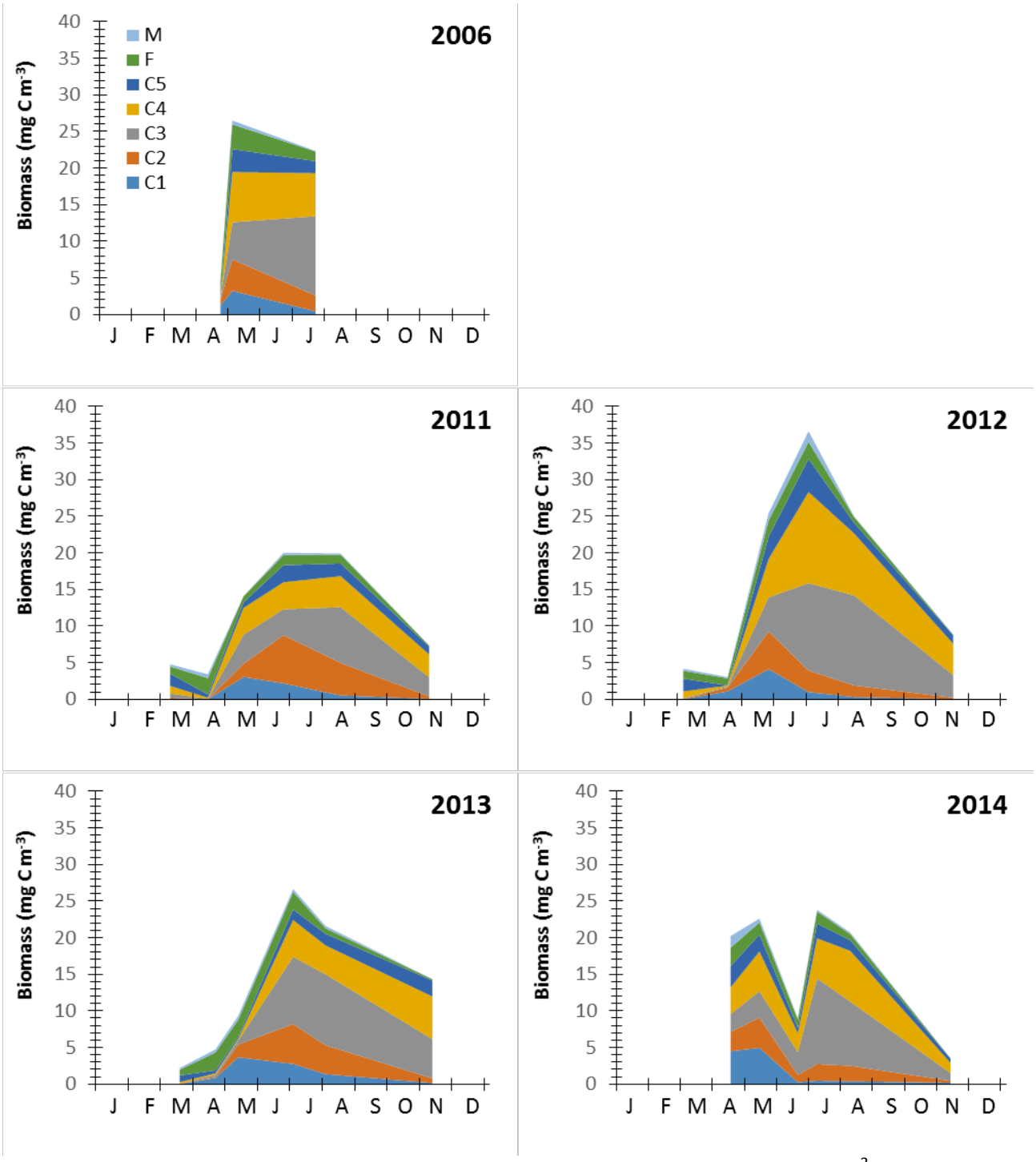

Figure 13: Seasonal variation of total biomass of *Pseudocalanus* spp. (mg C m^{-3}) and the cumulative contribution of the various copepodite stages (C_1-C_5, F=female, M=male) to the stock.

A summary of the results in relation to stock recruitment is given in Figure 14 where the differences in spawning stock biomass, numbers of cod eggs from different stages, larval abundance data, larval growth and recruitment at age 2 are compared between 5 years indicating the bottle necks and the variability between the years studied.

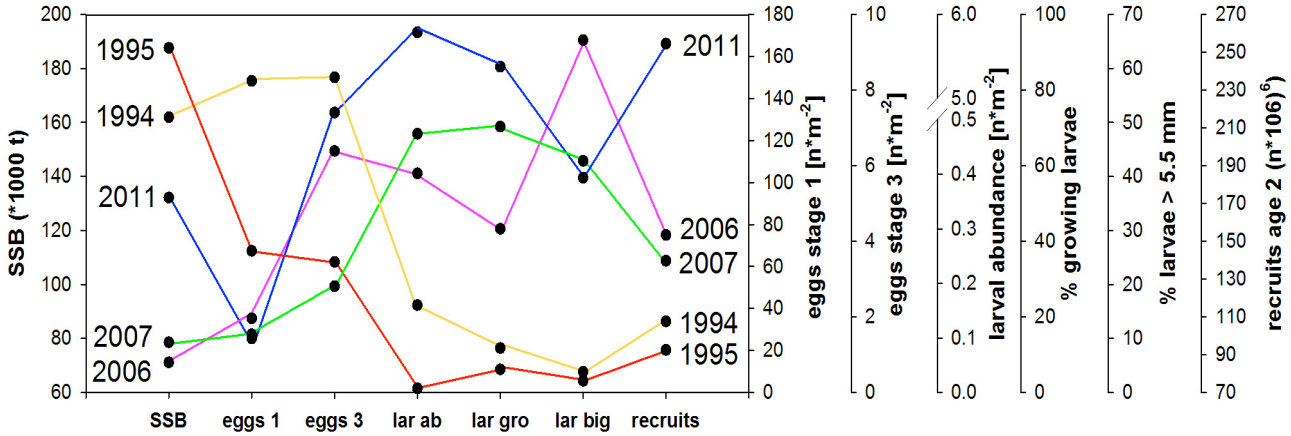

Fig. 14. Development from spawning stock to recruits in 1994, 1995, 2006, 2007 and 2011 (SSB = spawning stock biomass, eggs 1 = stage 1 eggs, eggs 3 = stage 3 eggs, lar ab = average larval abundance, lar gro = ratio (%) of larvae showing positive growth, lar big = ratio (%) of larvae > 5.5.mm of all sampled larvae, recruits = recruits at age 2). Shift from high SSB to low recruitment and vice versa are occurring between the late egg stage and the ratio of larvae in growing condition. Values are for July 1994, May 1995, July 2006, August 2007 and August 2011. Estimates of SSB and age 2 recruits from ICES (2013), abundance data of eggs and larvae from an ichthyoplankton database. (Note: ‘‘lar gro’’ & “lar big”, these data refer to ratios, whereas all other data refer to abundances). (Modified and complimented after Huwer et al. 2011)

Adult cod condition analyses

Results show a significant decline in nutritional condition over time both calculated as K and HSI. The former is illustrated in Figure 15 for the two BITS surveys (March and November in SD 25).

These data were reported to the Benchmark Workshop on Baltic Cod Stocks (WKBALTCOD) and the Baltic Fisheries Assessment Working Group in spring 2015, and the condition data were used to provide data to calculate natural mortality in recent years for use in the assessment. Related data for the availability of herring and sprat in catches are available for modelling.

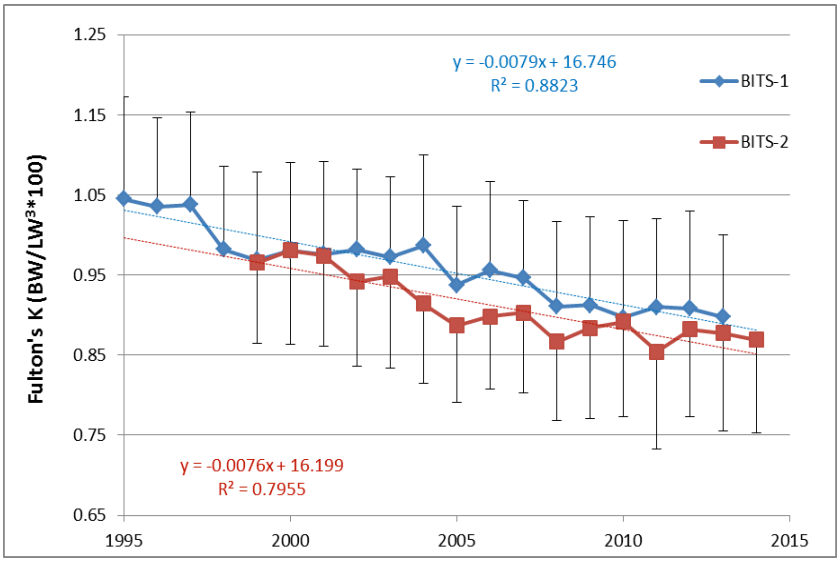

Figure 15. Fulton's condition factor, K, (BW/L^3*100) ± STD of cod caught during BITS 1 and 2 cruises 1995-2014.

The trends were similar for female and male cod, which was unexpected, as most published data reports differences in growth and energy allocation between sexes (Fig. 16) In contract, we found differences in the decline of condition among different size groups 15-29 cm, 30-49 cm and > 50 cm.
The decline in L was more pronounced in the two larger groups than in the smaller. There was no significant difference in the trend among Sub-divisions 24, 25, 26 and 28 in these survey data.

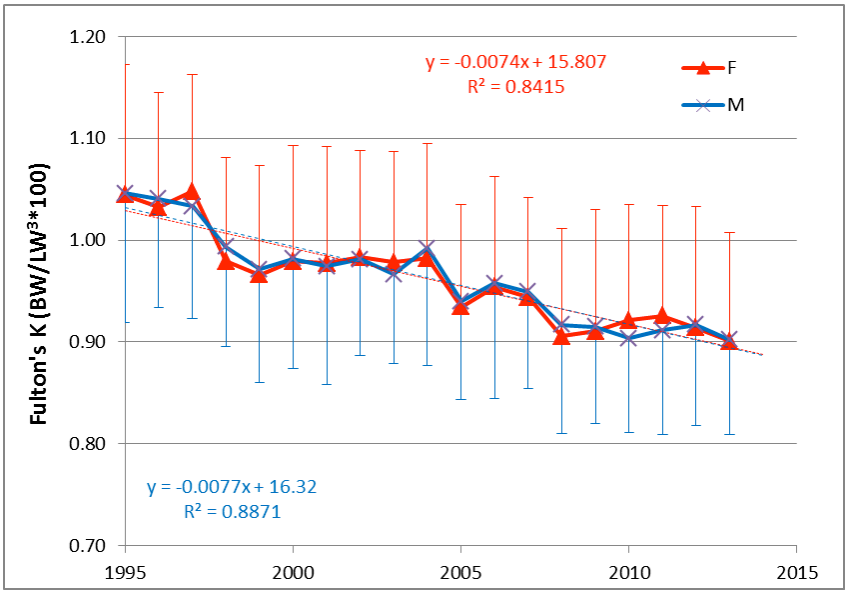

Figure 16. Fulton's condition factor, K, (BW/L^3*100) for female and male cod during BITS 1 and 2 cruises 1995-2014.

The analyses included also an analysis of the maturity, where the L50 over time (50 % maturing) was calculated. The L50 declined significantly over time and was negatively correlated with the decrease in condition, i.e. the cod mature earlier at a poorer condition.

Observed stomach contents were roughly separated in the two groups (i) fish and (ii) benthic invertebrates. For each group, the mass of consumed wet weight was estimated per individual stomach, as well as the energy that has been consumed, and then averaged for each 1-cm TL group (Fig 17).

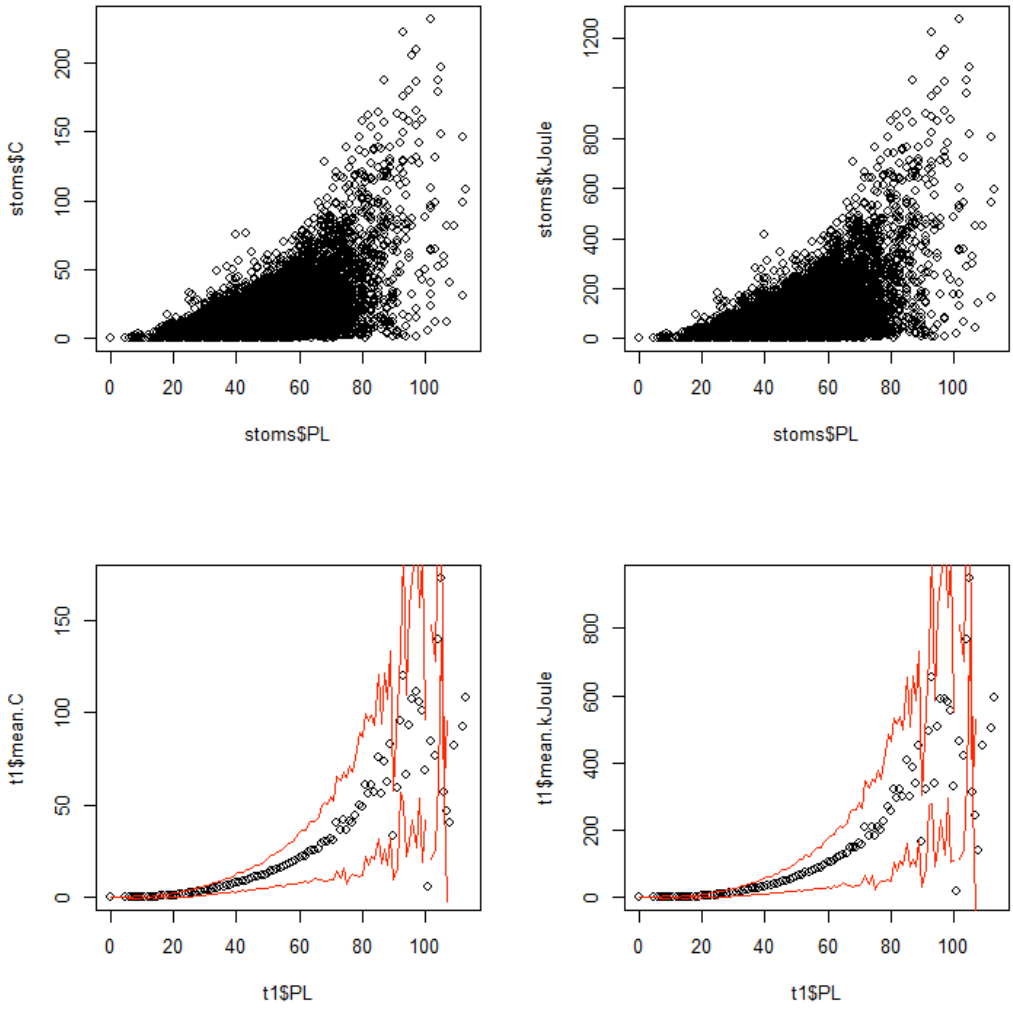

Figure 17: Wet mass and energy consumed for the individual stomachs (top left and right) and averages with one standard deviation (lower left and right)

Several exploratory analyses have been conducted in order to identify, if there is a trend over time in total consumption, and if yes, for which length groups this trend may be considered consistent. The most general signal was visible, when cod <40 cm were compared to cod >40 cm. Cod from 15-40 cm total length showed a decreasing trend in total consumption and energy intake starting in the mid 1980s, whereas cod > 40 did not show this tendency (Fig. 18). Focusing on cod 15-40 cm, the ratio between benthic and pelagic food decreased simultaneously (Fig. 19).

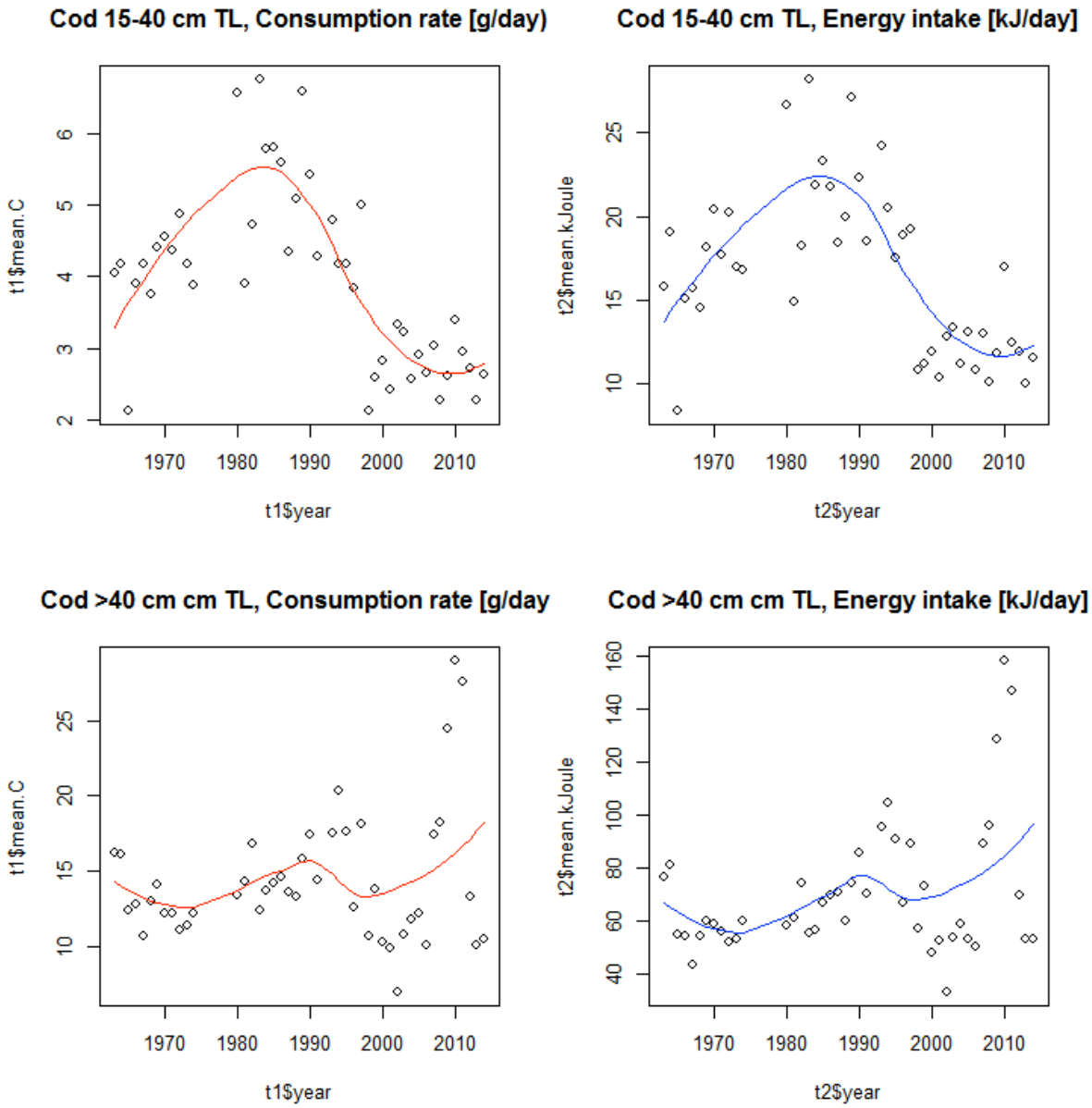

Figure 18: Consumption and energy intake for cod 15-40 cm, and > 40 cm total length over time.

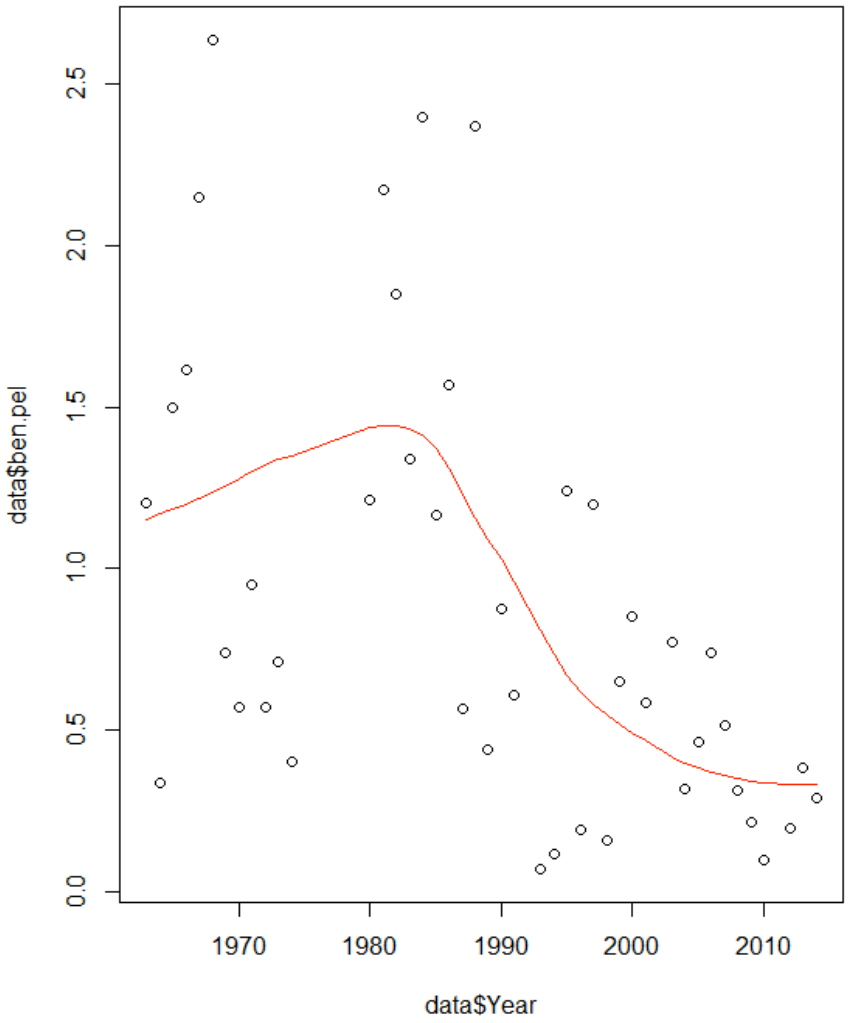

Figure 19: Ratio between consumed benthic and pelagic food for cod 15-40 cm total length over time.

REFERENCES

Buckley, L.J., Caldarone, E.M., Clemmesen, C. (2008) Multi-species larval fish growth model based on temperature and fluorometrically derived RNA/DNA ratios: results from a meta-analysis. Marine Ecology Progress Series 371, 221-232

Caldarone, E.M., Clemmesen, C.M., Berdalet, E., Miller, T.J., Folkvord, A., Holt, G.J., Olivar, M.P., Suthers, I.M. (2006) Intercalibration of four spectrofluorometric protocols for measuring RNA/DNA ratios in larval and juvenile fish. Limnology and Oceanography: Methods 4, 153-163

Huwer B., Clemmesen C., Grønkjær P., Köster F.W. (2011) Vertical distribution and growth performance of Baltic cod larvae - Field evidence for starvation-induced recruitment regulation during the larval stage? Progress in Oceanography 91(4): 382-396

ICES (2013) Report of the Baltic Fisheries Assessment Working Group (WGBFAS), 10 - 17 April 2013, ICES Headquarters, Copenhagen. ICES CM 2013/ACOM:10. 747 pp.

Voss, R., Koester, F.W., Dickmann, M. (2003) Comparing the feeding habits of co-occurring sprat (*Sprattus sprattus*) and cod (*Gadus morhua*) larvae in the Bornholm Basin, Baltic Sea. Fisheries Research 63, 97-111

Appendix VIII

Fish distribution and cod condition with respect to environmental changes in the Bornholm Basin including Cruise Report of FRV Clupea Cruise Number 281 & 291 with Metadata

Daniel Oesterwind[1],Vincent Siebert[1,2]
[1]Thünen-Institute of Baltic Sea Fisheries
[2]University of Rostock

Within the Bonus project two research cruises with FRV Clupea were conducted in 2014 and 2015 for about 2 weeks (see cruise reports). The cruises were divided into two parts:
The objective of the first part was to observe the abundance and distribution of fish species in the Bornholm Sea and the condition of adult cod. In detail, we recorded hydroacoustic data with a scientific echosounder (SIMRAD EK60) to analyse the abundance, vertical and horizontal distribution of herring, sprat and cod. In addition fishery hauls were performed with a pelagic trawl (PSN 388/Krake, 20 mm stretched meshes in the codend) and hydrological data were documented with a Seabird CTD. Haul composition of fishery stations were noticed and fish were weighted for each species. A subsample of individual weights and lengths of fish were recorded for each species and subsamples of cod, herring and sprat stomachs were stored and delivered to DTU Aqua. For cod additional data to estimate the gonatosomatic and heptosomatic index as well as Fulton's conditions factor were sampled and analysed.
Within the framework of the first part of the cruises fishery distribution and cod condition were analysed with respect to changing environmental conditions. For this purpose, data from previous cruises at the Bornholm Basin performed with the same standards could be included.
The objective of the second cruise leg was to determine the density and abundance of phytoplankton, zooplankton, ichthyoplankton and gelatinous plankton in the Bornholm Sea in order to analyse their dependence on local hydrographic features in the area, including seawater salinity, temperature and oxygen saturation. Therefore a grid with plankton stations were performed with a Bongo-plankton-gear with different mesh sizes. The main focus was to increase the knowledge on growth condition of early life stages of cod and of other important fish species in the central Baltic Sea.

Federal Research Institute for Rural Areas,

Forestry and Fisheries

Thünen-Institute of Baltic Sea Fisheries

Alter Hafen Süd 2, 18069 Rostock Telefon 0381 8116138 Telefax 0381 8116-199 Datum 14.08.20144 E-Mail: daniel.oesterwind@ti.bund.de

Cruise report

FRV Clupea, Cruise 281

01.07. to 15.07.2014

Ichthyoplankton and fish in the central Baltic

Person in charge: Dr. Daniel Oesterwind

Cruise leaders: Dr. Daniel Oesterwind (part 1), Paul Kotterba (part 2)

Background

The objective of the first leg of the cruise was to observe the abundance and distribution of fish species in the Bornholm Sea and Gdansk Deep. In detail we focused on the abundance, vertical and horizontal distribution and feeding ecology of herring, sprat and especially cod. In parallel data about hydrography were recorded.
The objective of the second cruise leg was to determine the density and abundance of phytoplankton, zooplankton, ichthyoplankton and gelatinous plankton in the Bornholm Sea in order to analyse their dependence on local hydrographic features in the area, including seawater salinity, temperature and oxygen saturation. The study was the third cruise of FFS Clupea following this specific design of a survey, which was set up to fundamentally increase the knowledge on growth condition of early life stages of cod and of other important fish species in the central Baltic Sea.

Summary

Part 1
The first part of the cruise started on the 1st of July in Rostock port Marienehe and ended on the 6th of July at Rügen port Sassnitz. Except for one blustering day, weather conditions were good and the trip was realized as planned. A total of 44 hydrography stations were conducted and a total of 14 fishing trawls were performed (Table A1).
1.460 kg of fish were caught and measured. In detail, we measured the length of 4502 clupeids, measured and sampled individual parameters (e.g. length, weight, gonad weight, sex maturity,

stomach fullness, stomachs, otholits) of 525 individuals of cod and took 514 stomach samples of clupeids.

Part 2
Due to changing wind and weather conditions, only selected stations had been sampled during the second leg. An increasing wind speed during the night between the 8th and 9th of July and expectations of worsening wind conditions for the following days lead to the decision to skip the remaining stations and return to Rostock-Marienehe on Wednesday, July 9th.
Nevertheless, 17 of the 45 stations had been sampled; including a focus station (No. 23) in the centre of the Bornholm Basin (see figure 2). In total, 17 oblique hauls with a Bongonet (335/500µm mesh size) – Baby-Bongonet (150µm mesh size)-combination had been conducted, each of them being accompanied by the recording of a CTD-profile. At station 23, additional samples for the study of phytoplankton- and zooplankton biodiversity and abundance were taken by vertical tows of a WP-2 net (100 µm) and by stratified water sampling with Niskin bottles from various depths (Table A2).

Cruise schedule and preliminary results

Part 1
FRV Clupea left the port of Marienehe on the 1st of July to steam eastwards to Bornholm. The first transect (T2) were reached in the morning of the 2nd of July and acoustic records started immediately. We performed 11 CTD stations and 3 OTM trawls. After the completion of transect 2 (T2) RV Clupea sailed in eastern direction to the Deep of Gdansk to the next transect (TG) which was started in the morning of the 3th of July. In parallel to acoustic recordings we conducted 11 CTD stations and 3 OTM trawls. From the Deep of Gdansk we shipped back to Bornholm and continued our acoustic records on transect 3 (T3) in the morning of the 4th of July. During the day we performed 12 CTD stations and 3 fishing hauls. During the following night Clupea sailed in western direction to continue the acoustic records on transect 1 (T1) on the 5th of July. On this transect we performed 11 CTD stations and 4 OTM trawls.
The catch composition for the whole trip is shown in table 1.
Besides of the wet weights and individual parameters, we sampled a total of 294 herring, 220 sprat and 272 cod stomachs and 257 tissue samples for genetic analysis.

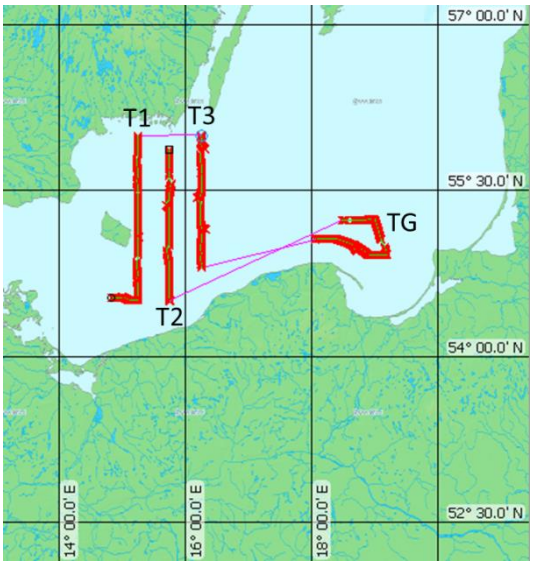

Figure 1: Transects and acoustic records (red) during first cruise leg.

Table 1. Fished wet weight by species.

Species	wet weight (kg)
Cod	198,7
Herring	1088,0
Garfish	22,5
Salmon	0,7
Lumpsucker	1,2
Saithe	0,8
Sprat	127,8
Sticklebacks	18,6
Whiting	3,0
total	**1461,3**

Part 2

On July 7th, 5 p.m. (local time) FRV Clupea left the port of Sassnitz directly heading towards the Bornholm Basin, where the first station was sampled at 10 p.m. On the morning of July 8th, the focus station 23 in the centre of the Bornholm Basin was sampled while the easterly winds increased during the course of the day. During the night to July 9th, the wind reached a strength of about 7 Bft and the scientific programme had to be interrupted. With regard to bad wind forecasts for the following days and after consultation with the ship's command it was decided to cancel the remaining sampling stations and to return to Rostock.

In total, 17 oblique Bongo Net hauls had been taken and samples were fixed for later detailed analysis of the taxonomic composition, abundance and size distribution of the zooplankton. Another important objective was to determine the frequency of fish larvae within the catches. While numerous pelagic fish eggs could be observed during the cruise, the number of fish larvae within the samples remained relatively small. Those larvae were dominated by clupeid and gobiid species particularly close to the island of Bornholm, while only a few cod larvae had been observed. Initially, several fish larvae were collected and immediately frozen at -80°C for later biochemical analyses. The increasing wind strength, however, impaired the working conditions and made the continuation of the isolation of fish larvae for these purpose impossible. At station 23, the additional sampling included 3 hauls, each with 2 vertical plankton nets (Apstein 55µm mesh size; WP-2 100µm mesh size), water samples for the analysis of phytoplankton density and the determination of oxygen saturation and salinity from different depths (0, 5, 10, 20, 30, 40, 50, 60 and 80 metres).

The catch frequency of gelatinous plankton at the different stations was nearly 100%. The jellyfish were dominated by the genera *Aurelia* and *Cyanea*, while ctenophores like *Mnemiopsis* could not be observed within the samples.

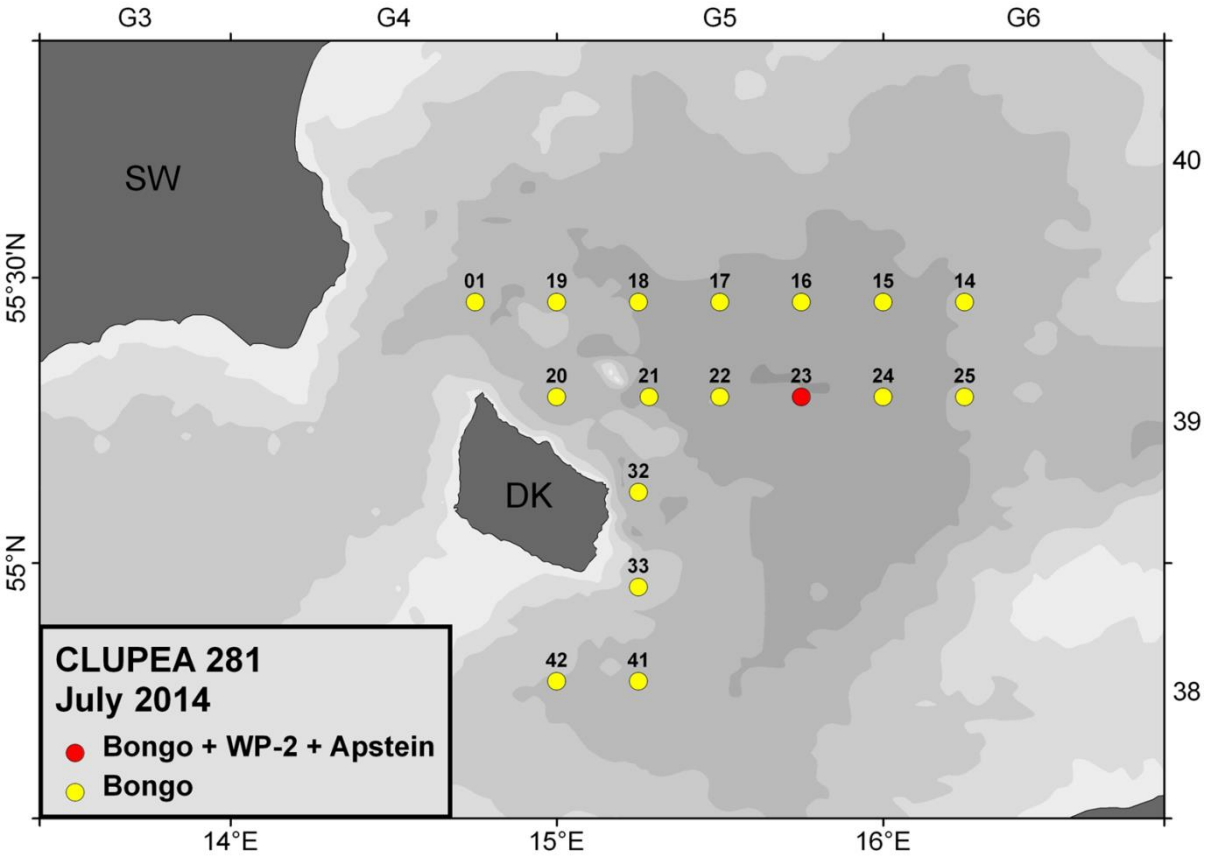

Figure 2. Stations sampled during the second leg of CLU 281.

Cruise participants

1.	leg	Dr. Daniel Oesterwind	Senior Scientist	(TI-OF)
		Dr. Daniel Stepputtis	Senior Scientist	(TI-OF)
2.	leg	Paul Kotterba	PhD student	(TI-OF)
		Dr. Jörg Dutz	Senior Scientist	(IOW)

I hereby thank all participants, the captain and the crew of FRV Clupea for their cooperation and support.

Rostock, 14.08.2014

Dr. Daniel Oesterwind

(Scientist in charge)

Table A1. Cruise stations FRV Clupea Cruise number 281 Part 1.

Cruise station	vessel station	device	date	starting time	starting position	
1	4191	CTD SBE19+	02.07.14	04:02:15	55°52,132N	015°44,970E
2	4192	CTD SBE19+	02.07.14	05:22:53	55°40,005N	015°44,927E
3	4193	OTM PSN388 Krake	02.07.14	05:48:04	55°37,275N	015°45,044E
4	4194	CTD SBE19+	02.07.14	07:10:22	55°33,887N	015°46,758E
5	4195	CTD SBE19+	02.07.14	07:48:20	55°30,066N	015°45,206E
6	4196	OTM PSN388 Krake	02.07.14	08:33:43	55°24,861N	015°45,059E
7	4197	CTD SBE19+	02.07.14	09:53:54	55°22,301N	015°41,706E
8	4198	CTD SBE19+	02.07.14	10:19:10	55°20,091N	015°44,776E
9	4199	CTD SBE19+	02.07.14	11:31:32	55°09,883N	015°44,763E
10	4200	CTD SBE19+	02.07.14	12:42:42	55°00,173N	015°44,686E
11	4201	OTM PSN388 Krake	02.07.14	12:52:58	55°00,173N	015°44,724E
12	4202	CTD SBE19+	02.07.14	14:52:31	54°50,019N	015°44,876E
13	4203	CTD SBE19+	02.07.14	16:02:40	54°40,165N	015°45,125E
14	4204	CTD SBE19+	02.07.14	17:12:57	54°30,134N	015°44,962E
15	4205	CTD SBE19+	03.07.14	03:32:44	55°13,872N	018°28,212E
16	4206	OTM PSN388 Krake	03.07.14	03:59:16	55°13,817N	018°33,571E
17	4207	CTD SBE19+	03.07.14	05:08:06	55°13,536N	018°39,318E
18	4208	CTD SBE19+	03.07.14	05:38:28	55°13,959N	018°45,390E
19	4209	CTD SBE19+	03.07.14	06:39:17	55°14,111N	019°00,016E
20	4210	CTD SBE19+	03.07.14	07:52:51	55°04,430N	019°05,105E
21	4211	OTM PSN388 Krake	03.07.14	08:14:58	55°02,736N	019°06,340E
22	4212	CTD SBE19+	03.07.14	09:29:52	54°59,622N	019°09,036E
23	4213	CTD SBE19+	03.07.14	10:11:39	54°54,927N	019°11,531E
24	4214	CTD SBE19+	03.07.14	11:30:47	54°54,973N	018°54,084E
25	4215	CTD SBE19+	03.07.14	12:54:46	55°00,495N	018°40,044E
26	4216	OTM PSN388 Krake	03.07.14	13:05:41	55°00,286N	018°40,508E
27	4217	CTD SBE19+	03.07.14	16:12:35	55°03,957N	018°21,586E
28	4218	CTD SBE19+	03.07.14	17:23:58	55°04,020N	018°05,766E
29	4219	CTD SBE19+	04.07.14	02:57:15	54°45,290N	016°15,249E
30	4220	CTD SBE19+	04.07.14	03:33:13	54°49,935N	016°15,111E
31	4221	CTD SBE19+	04.07.14	04:42:11	55°00,057N	016°15,061E
32	4222	OTM PSN388 Krake	04.07.14	04:52:16	55°00,042N	016°15,148E
33	4223	OTM PSN388 Krake	04.07.14	06:52:22	55°06,393N	016°15,165E
34	4223	CTD SBE19+	04.07.14	08:03:35	55°08,698N	016°19,747E
35	4225	CTD SBE19+	04.07.14	08:29:18	55°10,021N	016°15,071E
36	4226	CTD SBE19+	04.07.14	09:36:27	55°20,041N	016°14,863E
37	4227	OTM PSN388 Krake	04.07.14	10:17:28	55°23,783N	016°14,330E
38	4228	CTD SBE19+	04.07.14	11:18:15	55°25,614N	016°10,991E
39	4229	CTD SBE19+	04.07.14	11:57:30	55°30,111N	016°15,124E
40	4230	CTD SBE19+	04.07.14	13:02:18	55°39,958N	016°15,049E
41	4231	CTD SBE19+	04.07.14	14:13:26	55°49,921N	016°14,883E
42	4232	OTM PSN388 Krake	04.07.14	14:19:07	55°50,009N	016°14,897E

Cruise station	vessel station	device	date	starting time	starting position	
43	4233	CTD SBE19+	04.07.14	16:21:34	56°00,069N	016°14,988E
44	4234	CTD SBE19+	05.07.14	02:45:14	56°00,075N	015°15,110E
45	4235	CTD SBE19+	05.07.14	03:51:50	55°50,057N	015°15,071E
46	4236	OTM PSN388 Krake	05.07.14	04:04:27	55°49,328N	015°14,921E
47	4237	CTD SBE19+	05.07.14	05:11:57	55°46,878N	015°14,226E
48	4238	CTD SBE19+	05.07.14	06:03:08	55°40,079N	015°14,980E
49	4239	CTD SBE19+	05.07.14	07:18:37	55°30,046N	015°15,177E
50	4240	OTM PSN388 Krake	05.07.14	07:27:09	55°29,998N	015°15,157E
51	4241	CTD SBE19+	05.07.14	09:05:26	55°21,561N	015°15,040E
52	4242	CTD SBE19+	05.07.14	10:24:30	55°10,095N	015°15,025E
53	4243	OTM PSN388 Krake	05.07.14	11:25:40	55°01,829N	015°15,023E
54	4244	CTD SBE19+	05.07.14	12:57:45	55°02,962N	015°15,347E
55	4245	OTM PSN388 Krake	05.07.14	13:56:59	54°54,536N	015°15,004E
56	4246	CTD SBE19+	05.07.14	15:02:41	54°51,984N	015°14,301E
57	4247	CTD SBE19+	05.07.14	16:43:14	54°40,004N	015°14,929E
58	4248	Plankton Multinetz	05.07.14	17:00:43	54°39,944N	015°14,509E
59	4249	CTD SBE19+	05.07.14	18:20:06	54°30,212N	015°15,141E

Table A2. Cruise stations FRV Clupea Cruise number 281 Part 2.

Cruise station	vessel station	device	date	starting time	Starting position	
60	4250	Bongo net	07.07.14	19:57:34	54°47,574N	014°59,679E
60	4250	CTD SBE19+	07.07.14	20:16:08	54°46,810N	014°59,698E
61	4251	Bongo net	07.07.14	21:19:18	54°47,447N	015°15,046E
61	4251	CTD SBE19+	07.07.14	21:34:59	54°46,681N	015°15,204E
62	4252	Bongo net	07.07.14	22:46:58	54°57,385N	015°14,970E
62	4252	CTD SBE19+	07.07.14	22:56:45	54°57,826N	015°14,966E
63	4253	Bongo net	08.07.14	00:00:09	55°07,442N	015°15,001E
63	4253	CTD SBE19+	08.07.14	00:14:53	55°07,884N	015°15,782E
64	4254	Bongo net	08.07.14	01:35:29	55°17,221N	015°00,547E
64	4254	CTD SBE19+	08.07.14	01:51:09	55°17,829N	014°59,921E
65	4255	Bongo net	08.07.14	02:54:56	55°17,259N	015°16,211E
65	4255	CTD SBE19+	08.07.14	03:11:33	55°17,655N	015°17,287E
66	4256	Bongo net	08.07.14	04:04:00	55°17,571N	015°29,935E
66	4256	CTD SBE19+	08.07.14	04:19:15	55°18,062N	015°29,894E
67	4257	WP 2	08.07.14	05:22:23	55°17,504N	015°45,019E
67	4257	WP 2	08.07.14	05:34:30	55°17,523N	015°44,882E
67	4257	WP 2	08.07.14	05:46:39	55°17,536N	015°44,674E
67	4257	WP 2	08.07.14	05:57:23	55°17,543N	015°44,546E
67	4257	WP 2	08.07.14	06:08:59	55°17,523N	015°44,349E
67	4257	WP 2	08.07.14	06:19:21	55°17,494N	015°44,192E
67	4257	WP 2	08.07.14	06:29:59	55°17,451N	015°44,052E
67	4257	CTD SBE19+	08.07.14	06:42:34	55°17,371N	015°43,860E
67	4257	CTD SBE19+	08.07.14	06:52:57	55°17,319N	015°43,728E
67	4257	CTD SBE19+	08.07.14	06:58:15	55°17,295N	015°43,652E
67	4257	CTD SBE19+	08.07.14	07:02:21	55°17,270N	015°43,599E
67	4257	CTD SBE19+	08.07.14	07:09:41	55°17,238N	015°43,489E
67	4257	CTD SBE19+	08.07.14	07:14:47	55°17,216N	015°43,399E
67	4257	CTD SBE19+	08.07.14	07:23:58	55°17,171N	015°43,255E
67	4257	CTD SBE19+	08.07.14	07:29:31	55°17,144N	015°43,171E
67	4257	CTD SBE19+	08.07.14	07:36:09	55°17,108N	015°43,068E
67	4257	CTD	08.07.14	07:43:20	55°17,077N	015°42,929E

Cruise station	vessel station	device	date	starting time	Starting position	
		SBE19+				
67	4257	Bongo net	08.07.14	07:58:48	55°17,535N	015°44,926E
68	4258	Bongo net	08.07.14	09:10:08	55°17,602N	015°59,805E
68	4258	CTD SBE19+	08.07.14	09:24:45	55°17,914N	015°59,949E
69	4259	Bongo net	08.07.14	10:26:47	55°17,466N	016°14,779E
69	4259	CTD SBE19+	08.07.14	10:41:02	55°17,847N	016°14,771E
70	4260	Bongo net	08.07.14	11:46:29	55°27,418N	016°15,015E
70	4260	CTD SBE19+	08.07.14	11:59:20	55°27,701N	016°14,966E
71	4261	Bongo net	08.07.14	12:55:28	55°27,433N	016°00,028E
71	4261	CTD SBE19+	08.07.14	13:08:13	55°27,610N	016°00,016E
72	4262	Bongo net	08.07.14	14:05:23	55°27,520N	015°45,035E
72	4262	CTD SBE19+	08.07.14	14:19:06	55°27,814N	015°44,871E
73	4263	Bongo net	08.07.14	15:16:36	55°27,539N	015°29,997E
73	4263	CTD SBE19+	08.07.14	15:30:37	55°27,951N	015°29,760E
74	4264	Bongo net	08.07.14	16:27:54	55°27,507N	015°15,165E
74	4264	CTD SBE19+	08.07.14	16:45:03	55°28,162N	015°14,522E
75	4265	Bongo net	08.07.14	17:40:59	55°27,373N	015°00,143E
75	4265	CTD SBE19+	08.07.14	17:51:57	55°27,782N	014°59,668E
76	4266	Bongo net	08.07.14	18:49:11	55°27,521N	014°45,677E
76	4266	CTD SBE19+	08.07.14	19:01:10	55°27,969N	014°45,277E

Federal Research Institute for Rural Areas,

Forestry and Fisheries

THÜNEN

Thünen-Institute of Baltic Sea Fisheries

Alter Hafen Süd 2, 18069 Rostock Telefon 0381 8116138 Telefax 0381 8116-199 Datum 04.12.2015 E-Mail: daniel.oesterwind@ti.bund.de

Cruise report

FRV Clupea, Cruise 291

01.07. to 15.07.2015

Ichthyoplankton and fish in the central Baltic

Person in charge: Dr. Daniel Oesterwind

Cruise leaders: Dr. Daniel Stepputtis (part 1), Paul Kotterba (part 2)

Background

The objective of the first leg of the cruise was to observe the abundance and distribution of fish species in the Bornholm Sea and Gdansk Deep. In detail we focused on the abundance, vertical and horizontal distribution and feeding ecology of herring, sprat and especially cod. In parallel data about hydrography were recorded.
The objective of the second cruise leg was to determine the density and abundance of phytoplankton, zooplankton, ichthyoplankton and gelatinous plankton in the Bornholm Sea in order to analyse their dependence on local hydrographic features in the area, including seawater salinity, temperature and oxygen saturation. The study was the third cruise of FFS Clupea following this specific design of a survey, which was set up to fundamentally increase the knowledge on growth condition of early life stages of cod and of other important fish species in the central Baltic Sea and is since 2014 a part of the BONUS financed Bio-C^3 Project.

Part 1

Cruise schedule and preliminary results

The first part of the cruise started on the 30th of June with the calibration of the hydro-acoustic system. After calibration FRV shipped to the Bornholm Basin, where the first station was performed in the morning of the 2nd July. Last station was performed on the 7th of July before FRV Clupea arrived in port Sassnitz in the morning of the 8th of July to prepare the second leg of

the cruise (Figure 1). Between the stations, FRV Clupea had a break for two days (4th and 5th of July to store freshwater and food in Sassnitz).

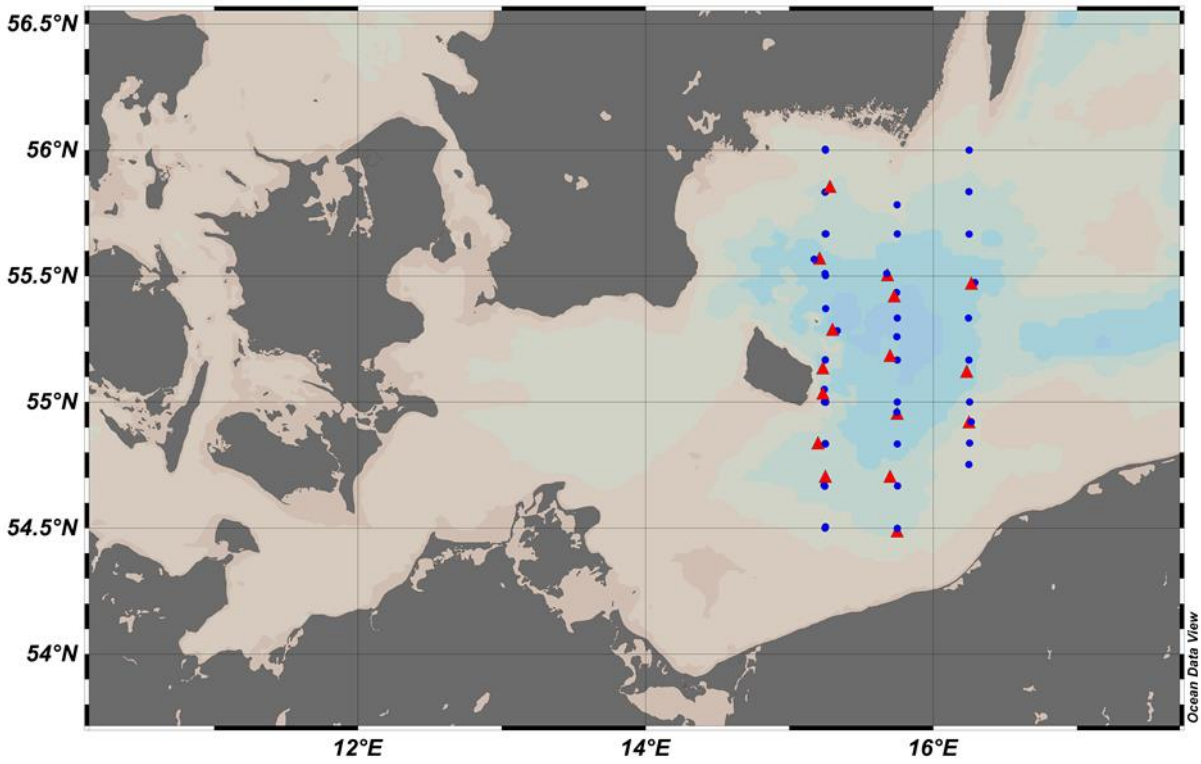

Figure 2. Shipped transects with conducted fishery stations (red triangle) and performed CTD stations (blue circle).

A total of 44 hydrography stations were conducted and a total of 15 fishing trawls were performed (Table A1). All in all a total of around 1750 kg fish and eight different species were caught (Table 1).

Tabelle 1. Catch weight in kg by species for the different fishery hauls.

	Haul															
Species	**1**	**2**	**3**	**4**	**5**	**6**	**7**	**8**	**9**	**10**	**11**	**12**	**13**	**14**	**15**	**total**
Gadus morhua		111,22	10,68	25,98	0,38		8,22	1,52	0,25	3,76	6,24	0,19	22,66	5,46		196,55
Gasterosteus aculeatus													0,00	0,01		0,01
Clupea harengus	123,72	55,72	45,66	6,92	61,00	3,26	73,42	39,94	0,12	96,16	37,70	12,54	45,84	35,02	310,68	947,70
Scomber scombrus									1,25							1,25
Ammodytes ssp.						0,01										0,01
Cyclopterus lumpus					0,77	0,23	0,57	0,84			0,15	0,65	0,63			3,83
Sprattus sprattus	41,54	1,20	37,55	12,06	101,48		67,40	52,58	87,42	0,82	7,86	8,88	63,16	2,20	105,40	589,55
Merlangius merlangus							0,09			0,16	0,27					0,53
total	**165,26**	**168,14**	**93,89**	**44,96**	**163,62**	**3,50**	**149,71**	**94,88**	**89,03**	**100,90**	**52,22**	**22,25**	**132,29**	**42,69**	**416,08**	**1739,42**

Preliminary results show, that compared to the former years the hydrological data indicate a higher salinity (up to 18 psu) and higher oxygen concentration in the deeper water layer in the Bornholm Basin. This increase was probably caused by a Major Baltic Inflow (MBI) at the end of the year 2014. In addition the estimated Fulton's condition index for cod reveals a better fitness of cod compared to 2013. The sampled stomachs have been transferred to the collaborating institute DTU Aqua, Copenhagen for further analyses.

Part 2

Cruise schedule and preliminary results

The scientific crew boarded the vessel on the afternoon of the 10th of July at the port of Sassnitz, Rügen. Due to bad weather conditions, the departure was delayed until the morning of the 11th of July. We arrived at the Bornholm Basin at the late morning and immediately started the sampling. For further information on the succession of station sampled and measurements/catches conducted see figure 2 and Table A2. Calm sea conditions during the following days enabled a continuous sampling and the accomplishment of all intended investigations until the evening of July, 13th and a subsequent return towards the home port Rostock-Marienehe. On route to Rostock, additional hydrological measurements and phytoplankton sampling were conducted for the Leibnitz Institute for Baltic Sea Research. The cruise ended in the afternoon of July 14th at the port of Rostock-Marienehe, the equipment was removed from the ship and transferred to the institute on the following day.

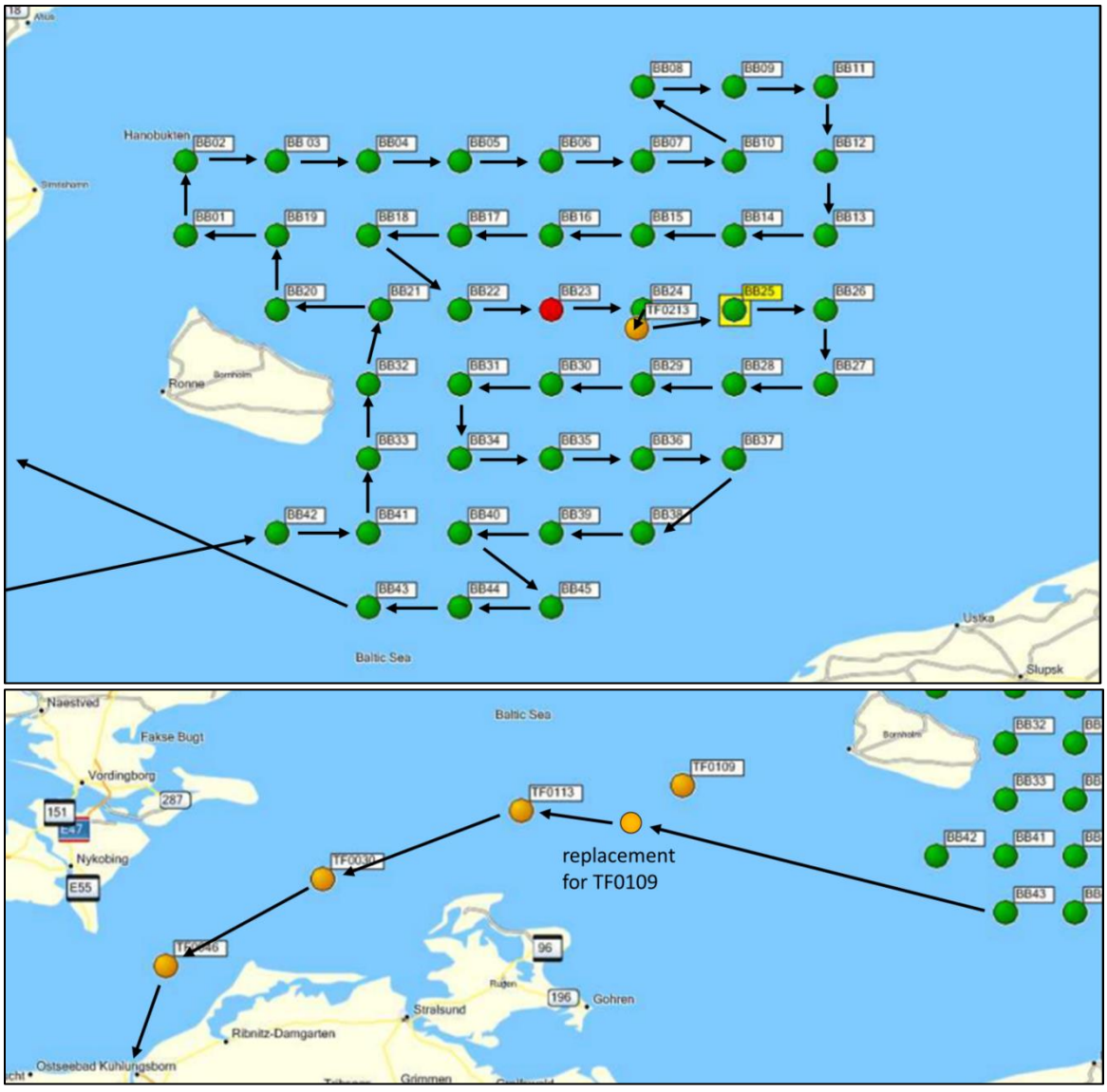

Figure 2. Maps of the southern Baltic Sea including the station sampled during the second part of CLU291. upper panel shows the sampled stations and the cruise track in the Bornholm Basin, lower panel shows the additional stations that have been sampled on the way back to the port of Rostock.

While a small amount of clupeid larvae was observed at most of the stations sampled, nearly no cod larvae were found. Furthermore, only single individuals of *Mnemiopsis leidyi* have been recognized and sampled during the cruise.
The Plankton samples taken during the cruise have been transferred to the collaborating institutes (DTU Aqua, Copenhagen and IOW, Warnemünde) for further analyses.

Cruise participants

1. leg	Vincent Siebert	Masterstudent	(TI-OF, University of Rostock)
	Dr. Daniel Stepputtis	Senior Scientist	(TI-OF)
2. leg	Paul Kotterba	PhD student	(TI-OF)
	Svend-Erik Levinsky	Technician	(DTU-Aqua)

I hereby thank all participants, the captain and the crew of FRV Clupea for their cooperation and support.

Rostock, 04.12.2015

Dr. Daniel Oesterwind
(Scientist in charge)

Table A1. Cruise stations FRV Clupea Cruise number 291 Part 1.

Cruise station	year station	device	date	Starting time	starting position	
1	6495	CTD SBE19+	02.07.15	03:56:34	54°29,961N	015°45,054E
2	6496	CTD SBE19+	02.07.15	05:08:05	54°40,046N	015°45,076E
3	6497	OTM PSN388 Krake	02.07.15	05:37:08	54°41,294N	015°44,702E
4	6498	CTD SBE19+	02.07.15	07:12:55	54°50,005N	015°45,040E
5	6499	OTM PSN388 Krake	02.07.15	07:52:18	54°54,857N	015°45,059E
6	6500	CTD SBE19+	02.07.15	08:54:10	54°57,596N	015°44,837E
7	6501	CTD SBE19+	02.07.15	09:17:14	55°00,024N	015°44,976E
8	6502	CTD SBE19+	02.07.15	10:24:58	55°10,035N	015°44,997E
9	6503	OTM PSN388 Krake	02.07.15	10:38:04	55°10,259N	015°44,534E
10	6504	CTD SBE19+	02.07.15	12:05:49	55°15,551N	015°44,860E
11	6505	CTD SBE19+	02.07.15	12:42:31	55°20,019N	015°44,987E
12	6506	OTM PSN388 Krake	02.07.15	13:12:50	55°23,077N	015°44,960E
13	6507	CTD SBE19+	02.07.15	14:19:15	55°26,085N	015°44,762E
14	6508	OTM PSN388 Krake	02.07.15	14:51:28	55°29,970N	015°45,035E
15	6509	CTD SBE19+	02.07.15	15:54:55	55°30,611N	015°40,556E
16	6510	CTD SBE19+	02.07.15	17:09:20	55°40,065N	015°45,051E
17	6511	CTD SBE19+	02.07.15	18:00:26	55°46,976N	015°44,870E
18	6512	CTD SBE19+	03.07.15	03:52:40	56°00,172N	015°14,935E
19	6513	CTD SBE19+	03.07.15	05:06:38	55°49,987N	015°14,851E
20	6514	OTM PSN388 Krake	03.07.15	05:33:25	55°52,974N	015°15,170E
21	6515	CTD SBE19+	03.07.15	07:41:38	55°40,025N	015°14,913E
22	6516	OTM PSN388 Krake	03.07.15	08:16:47	55°35,996N	015°14,163E
23	6517	CTD SBE19+	03.07.15	09:30:27	55°33,983N	015°10,349E
24	6518	CTD SBE19+	03.07.15	10:12:10	55°30,088N	015°15,022E
25	6519	CTD SBE19+	03.07.15	11:11:16	55°22,260N	015°15,095E
26	6520	CTD SBE19+	03.07.15	12:39:17	55°10,070N	015°14,906E
27	6521	OTM PSN388 Krake	03.07.15	13:06:04	55°10,157N	015°14,507E
28	6522	OTM PSN388 Krake	03.07.15	15:08:33	55°00,907N	015°14,947E
29	6523	CTD SBE19+	03.07.15	16:09:49	55°03,057N	015°14,574E
30	6524	CTD SBE19+	03.07.15	16:42:26	55°00,040N	015°14,693E
31	6525	CTD SBE19+	03.07.15	17:52:07	54°50,125N	015°14,979E
32	6526	CTD SBE19+	03.07.15	19:06:53	54°40,185N	015°14,499E
33	6527	CTD SBE19+	03.07.15	20:19:13	54°29,991N	015°14,869E
34	6528	CTD SBE19+	06.07.15	03:58:25	54°30,316N	015°15,001E
35	6529	CTD SBE19+	06.07.15	05:04:45	54°39,999N	015°14,779E
36	6530	OTM PSN388 Krake	06.07.15	05:14:10	54°40,066N	015°14,903E
37	6531	CTD SBE19+	06.07.15	07:05:25	54°50,027N	015°15,022E
38	6532	OTM PSN388 Krake	06.07.15	07:15:34	54°49,978N	015°15,349E
39	6533	CTD SBE19+	06.07.15	09:16:41	54°59,972N	015°15,137E
40	6534	CTD SBE19+	06.07.15	10:30:04	55°10,019N	015°14,925E
41	6535	OTM PSN388 Krake	06.07.15	11:21:47	55°16,269N	015°15,388E
42	6536	CTD SBE19+	06.07.15	12:26:54	55°16,981N	015°19,922E

Cruise station	year station	device	date	Starting time	starting position	
43	6537	CTD SBE19+	06.07.15	14:14:13	55°30,617N	015°14,839E
44	6538	CTD SBE19+	06.07.15	15:26:07	55°40,025N	015°15,193E
45	6539	CTD SBE19+	06.07.15	16:39:33	55°49,992N	015°14,926E
46	6540	CTD SBE19+	06.07.15	17:50:33	55°59,964N	015°15,015E
47	6541	CTD SBE19+	07.07.15	03:50:38	55°59,997N	016°14,966E
48	6542	CTD SBE19+	07.07.15	05:03:25	55°50,066N	016°14,932E
49	6543	CTD SBE19+	07.07.15	06:12:09	55°39,992N	016°15,016E
50	6544	OTM PSN388 Krake	07.07.15	07:13:05	55°31,273N	016°14,978E
51	6545	CTD SBE19+	07.07.15	08:23:05	55°28,441N	016°17,391E
52	6546	CTD SBE19+	07.07.15	09:22:14	55°19,985N	016°14,725E
53	6547	CTD SBE19+	07.07.15	10:31:03	55°09,993N	016°14,892E
54	6548	OTM PSN388 Krake	07.07.15	10:38:32	55°09,904N	016°14,899E
55	6549	CTD SBE19+	07.07.15	12:25:02	55°00,016N	016°15,199E
56	6550	OTM PSN388 Krake	07.07.15	12:45:49	54°57,712N	016°15,133E
57	6551	CTD SBE19+	07.07.15	13:52:45	54°55,298N	016°15,851E
58	6552	CTD SBE19+	07.07.15	15:26:14	54°50,247N	016°15,138E
59	6553	CTD SBE19+	07.07.15	16:10:08	54°45,122N	016°14,924E

Table A2. Cruise stations FRV Clupea Cruise number 291 Part 2.

Cruise station	year station	device	date	Starting time	starting position	
60	6554	Bongo net	11.07.15	10:56:10	54°47,522N	014°59,989E
61	6555	CTD SBE19+	11.07.15	11:08:10	54°47,708N	015°00,762E
62	6556	CTD SBE19+	11.07.15	12:04:44	54°47,366N	015°15,037E
63	6557	Bongo net	11.07.15	12:12:37	54°47,316N	015°15,303E
64	6558	CTD SBE19+	11.07.15	13:35:26	54°57,521N	015°14,948E
65	6559	Bongo net	11.07.15	13:44:48	54°57,422N	015°15,296E
66	6560	CTD SBE19+	11.07.15	14:57:56	55°07,524N	015°14,828E
67	6561	Bongo net	11.07.15	15:03:41	55°07,524N	015°14,879E
68	6562	CTD SBE19+	11.07.15	16:21:01	55°17,471N	015°17,057E
69	6563	Bongo net	11.07.15	16:31:05	55°17,468N	015°17,146E
70	6564	CTD SBE19+	11.07.15	17:46:29	55°17,545N	015°00,092E
71	6565	Bongo net	11.07.15	17:54:33	55°17,521N	015°00,237E
72	6566	CTD SBE19+	11.07.15	19:07:50	55°27,496N	014°59,870E
73	6567	Bongo net	11.07.15	19:15:59	55°27,471N	014°59,916E
74	6568	CTD SBE19+	11.07.15	20:18:54	55°27,543N	014°45,076E
75	6569	Bongo net	11.07.15	20:26:59	55°27,584N	014°45,332E
76	6570	CTD SBE19+	11.07.15	21:40:28	55°37,386N	014°44,979E
77	6571	Bongo net	11.07.15	21:48:07	55°37,336N	014°45,112E
78	6572	CTD SBE19+	11.07.15	22:50:28	55°37,420N	014°59,871E
79	6573	Bongo net	11.07.15	22:58:05	55°37,391N	015°00,006E
80	6574	CTD SBE19+	12.07.15	00:01:43	55°37,435N	015°15,005E
81	6575	Bongo net	12.07.15	00:09:02	55°37,384N	015°15,145E
82	6576	CTD SBE19+	12.07.15	01:10:29	55°37,351N	015°29,932E
83	6577	Bongo net	12.07.15	01:17:08	55°37,308N	015°30,104E
84	6578	CTD SBE19+	12.07.15	02:17:42	55°37,504N	015°45,047E
85	6579	Bongo net	12.07.15	02:24:32	55°37,463N	015°45,157E
86	6580	CTD SBE19+	12.07.15	03:22:35	55°37,523N	015°59,936E
87	6581	Bongo net	12.07.15	03:29:52	55°37,517N	016°00,182E
88	6582	CTD SBE19+	12.07.15	04:27:32	55°37,566N	016°15,054E
89	6583	Bongo net	12.07.15	04:34:42	55°37,608N	016°15,208E
90	6584	CTD SBE19+	12.07.15	06:09:16	55°47,408N	016°00,154E
91	6585	Bongo net	12.07.15	06:15:53	55°47,403N	016°00,162E
92	6586	CTD SBE19+	12.07.15	07:18:14	55°47,574N	016°15,179E
93	6587	Bongo net	12.07.15	07:24:11	55°47,613N	016°15,284E
94	6588	CTD SBE19+	12.07.15	08:22:55	55°47,563N	016°30,025E
95	6589	Bongo net	12.07.15	08:27:29	55°47,549N	016°30,102E
96	6590	CTD SBE19+	12.07.15	09:37:44	55°37,617N	016°30,049E
97	6591	Bongo net	12.07.15	09:42:45	55°37,600N	016°30,134E
98	6592	CTD SBE19+	12.07.15	10:54:04	55°27,454N	016°30,060E
99	6593	Bongo net	12.07.15	10:59:22	55°27,408N	016°30,120E
100	6594	CTD SBE19+	12.07.15	12:01:44	55°27,507N	016°14,954E
101	6595	Bongo net	12.07.15	12:07:48	55°27,495N	016°15,052E

Cruise station	year station	device	date	Starting time	starting position	
102	6596	CTD SBE19+	12.07.15	13:12:59	55°27,547N	015°59,851E
103	6597	Bongo net	12.07.15	13:19:47	55°27,583N	015°59,902E
104	6598	CTD SBE19+	12.07.15	14:24:47	55°27,508N	015°45,114E
105	6599	CTD SBE19+	12.07.15	14:33:00	55°27,628N	015°45,185E
106	6600	Bongo net	12.07.15	14:40:02	55°27,723N	015°45,319E
107	6601	CTD SBE19+	12.07.15	15:48:07	55°27,492N	015°29,889E
108	6602	Bongo net	12.07.15	15:55:07	55°27,595N	015°29,964E
109	6603	CTD SBE19+	12.07.15	17:01:30	55°27,444N	015°15,283E
110	6604	Bongo net	12.07.15	17:09:44	55°27,452N	015°15,474E
111	6605	CTD SBE19+	12.07.15	18:34:17	55°17,812N	015°29,734E
112	6606	Bongo net	12.07.15	18:42:02	55°17,844N	015°29,897E
113	6607	CTD SBE19+	12.07.15	19:40:33	55°17,464N	015°44,627E
114	6608	CTD SBE19+	12.07.15	19:56:27	55°17,505N	015°44,947E
115	6609	CTD SBE19+	12.07.15	20:02:10	55°17,528N	015°45,052E
116	6610	CTD SBE19+	12.07.15	20:07:47	55°17,550N	015°45,151E
117	6611	CTD SBE19+	12.07.15	20:12:58	55°17,572N	015°45,235E
118	6612	CTD SBE19+	12.07.15	20:18:45	55°17,592N	015°45,328E
119	6613	CTD SBE19+	12.07.15	20:24:54	55°17,613N	015°45,421E
120	6614	CTD SBE19+	12.07.15	20:31:50	55°17,631N	015°45,528E
121	6615	Apstein	12.07.15	20:45:05	55°17,636N	015°44,801E
122	6616	Apstein	12.07.15	21:00:35	55°17,664N	015°45,002E
123	6617	Apstein	12.07.15	21:14:04	55°17,701N	015°45,186E
124	6618	WP 2	12.07.15	21:29:25	55°17,733N	015°45,368E
125	6619	WP 2	12.07.15	21:38:53	55°17,750N	015°45,471E
126	6620	WP 2	12.07.15	21:48:34	55°17,762N	015°45,571E
127	6621	Bongo net	12.07.15	21:59:25	55°17,707N	015°45,682E
128	6622	CTD SBE19+	12.07.15	23:08:41	55°17,408N	015°59,971E
129	6623	Bongo net	12.07.15	23:17:20	55°17,339N	016°00,090E
130	6624	CTD SBE19+	13.07.15	00:21:00	55°17,351N	016°14,991E
131	6625	Bongo net	13.07.15	00:28:27	55°17,273N	016°15,135E
132	6626	CTD SBE19+	13.07.15	01:28:42	55°17,344N	016°29,901E
133	6627	Bongo net	13.07.15	01:34:49	55°17,281N	016°29,959E
134	6628	CTD SBE19+	13.07.15	02:38:50	55°07,589N	016°29,632E
135	6629	Bongo net	13.07.15	02:44:16	55°07,550N	016°29,659E
136	6630	CTD SBE19+	13.07.15	03:41:01	55°07,479N	016°15,222E
137	6631	Bongo net	13.07.15	03:47:23	55°07,441N	016°15,310E
138	6632	CTD SBE19+	13.07.15	04:48:46	55°07,464N	015°59,992E
139	6633	Bongo net	13.07.15	04:56:45	55°07,400N	016°00,072E
140	6634	CTD SBE19+	13.07.15	05:59:41	55°07,515N	015°44,942E
141	6635	Bongo net	13.07.15	06:06:49	55°07,484N	015°45,022E
142	6636	CTD SBE19+	13.07.15	07:08:39	55°07,612N	015°30,086E
143	6637	Bongo net	13.07.15	07:14:45	55°07,594N	015°30,152E
144	6638	CTD SBE19+	13.07.15	08:26:58	54°57,491N	015°29,942E
145	6639	Bongo net	13.07.15	08:33:06	54°57,484N	015°30,124E

Cruise station	year station	device	date	Starting time	starting position	
146	6640	CTD SBE19+	13.07.15	09:34:22	54°57,551N	015°45,169E
147	6641	Bongo net	13.07.15	09:41:33	54°57,502N	015°45,396E
148	6642	CTD SBE19+	13.07.15	10:41:23	54°57,491N	016°00,062E
149	6643	Bongo net	13.07.15	10:48:10	54°57,491N	016°00,250E
150	6644	CTD SBE19+	13.07.15	11:45:18	54°57,509N	016°15,076E
151	6645	Bongo net	13.07.15	11:50:05	54°57,512N	016°15,206E
152	6646	CTD SBE19+	13.07.15	13:21:34	54°47,434N	016°00,020E
153	6647	Bongo net	13.07.15	13:26:57	54°47,399N	016°00,113E
154	6648	CTD SBE19+	13.07.15	14:27:59	54°47,496N	015°45,001E
155	6649	Bongo net	13.07.15	14:34:53	54°47,438N	015°45,086E
156	6650	CTD SBE19+	13.07.15	15:36:54	54°47,555N	015°29,947E
157	6651	Bongo net	13.07.15	15:43:07	54°47,509N	015°30,106E
158	6652	CTD SBE19+	13.07.15	17:08:45	54°37,516N	015°44,540E
159	6653	Bongo net	13.07.15	17:15:05	54°37,479N	015°44,572E
160	6654	CTD SBE19+	13.07.15	18:14:15	54°37,489N	015°29,843E
161	6655	Bongo net	13.07.15	18:20:21	54°37,454N	015°29,906E
162	6656	CTD SBE19+	13.07.15	19:20:25	54°37,583N	015°15,071E
163	6657	Bongo net	13.07.15	19:26:42	54°37,539N	015°15,057E
164	6658	CTD SBE19+	14.07.15	00:20:26	54°55,980N	014°00,236E
165	6659	WP 2	14.07.15	00:25:28	54°55,955N	014°00,331E
166	6660	WP 2	14.07.15	00:30:44	54°55,941N	014°00,444E
167	6661	WP 2	14.07.15	00:35:27	54°55,930N	014°00,545E
168	6662	CTD SBE19+	14.07.15	02:28:43	54°55,022N	013°30,229E
169	6663	WP 2	14.07.15	02:33:22	54°55,001N	013°30,274E
170	6664	WP 2	14.07.15	02:37:56	54°55,002N	013°30,343E
171	6665	WP 2	14.07.15	02:42:35	54°55,009N	013°30,420E
172	6666	CTD SBE19+	14.07.15	05:35:05	54°43,425N	012°46,989E
173	6667	CTD SBE19+	14.07.15	08:18:26	54°28,023N	012°13,026E